Aiming for illusions: The perception of size and its influence on motor control

Hester Knol

Aix-Marseille Université

Ecole Doctorale Sciences du Mouvement Humain

Aiming for illusions:
The perception of size and its influence on motor control

Hester Knol

Thèse en vue d'obtenir le grade de docteur d'Aix-Marseille Université

Specialité : Contrôle Perceptivo-Moteur et Apprentissage

Soutenance le 14 décembre 2016 devant le jury composé de:

Patrick Haggard	University College London	Examinateur
Raoul Huys	Université de Toulouse	Co-directeur
Viktor Jirsa	Aix-Marseille Université	Directeur de Thèse
Jean-Christophe Sarrazin	ONERA, Salon de Provence	Co-encadrant
Jeroen Smeets	Vrije Universiteit Amsterdam	Rapporteur
Frank Zaal	Rijksuniversiteit Groningen	Rapporteur

UMR 1106 – Institut de Neurosciences des Systèmes INS
Faculté de Médecine de la Timone – 27 Bd Jean Moulin – 13385 Marseille Cedex 5, France

Aan waat'ren der rust.

Foar oma

To my grandmother Gré (in memoriam)

Abstract

The influential two-visual streams hypothesis ascribes specific functional roles to the ventral and the dorsal network of the visual system. The ventral system has been hypothesized to process information for conscious perception (vision-for-perception), whereas the dorsal stream processes information for action (vision-for-action). The idea of two separate visual networks in the human brain inspired an enormous amount of research over the past 20 or so years. The results are conflicting and divisive about the idea, causing a seemingly insurmountable gap between supporters and opponents. This thesis aims to unravel a part of the jigsaw puzzle of how perception and action are functioning.

The Ebbinghaus figure consists of an object embedded in a specific context (e.g., centre circle surrounded by smaller or bigger circles). The perceived object size often deviates from its physical size, which is the so-called Ebbinghaus illusion. The Ebbinghaus figure has been used to distinguish vision-for-perception that is susceptible to visual illusions (i.e., relative size) from vision-for-action that remain unaffected by perceptions of relative sizes (i.e., absolute physical size). Albeit several papers report that the Ebbinghaus illusion affects solely perception, a growing number of studies demonstrate that action is similarly affected by this illusion. A rule to control the size perception of the centre object in the Ebbinghaus figure to 'appear smaller' or to 'appear bigger' does not exist so that predicting illusion magnitudes remains guesswork. Therefore, it remains also questionable whether all Ebbinghaus figures evoke an illusion, and which factors are key for illusion effects. We quantified the Ebbinghaus figure based on its geometry and systematically assessed its size illusion. One third of all Ebbinghaus configurations did not result in significant illusion effects. For the other part, the illusion effects were due to all geometrical parameters of the Ebbinghaus figure.

After the quantification of Ebbinghaus figures, a visuomotor task was implemented in which precision and speed of the voluntary movement were investigated. The visuomotor behaviour was quantitatively and qualitatively described for discrete

and reciprocal sliding movements in terms of kinematics and the underlying dynamics. The description of the visuomotor task and of the perception of Ebbinghaus figures lead to combine both visuomotor task and Ebbinghaus figures. The latter study demonstrates that the Ebbinghaus figure influences the movement. The Ebbinghaus factors that affected perception, however, did not all appear to significantly influence the movement.

Due to its systematic approach and the methodological contributions, this work can serve as a basis for future studies on the perception and action mechanisms. This dissertation demonstrated that the ventral stream and dorsal stream are not strictly functionally distinct, and that potentially different informational variables are used for 'vision for perception' and 'vision for action' irrespective of whether certain variables cause (perceptual) illusions.

Résumé

L'hypothèse bien connue des deux voies visuelles attribue des rôles fonctionnels spécifiques aux réseaux cérébraux ventral et dorsal du système visuel. Ce modèle émet l'hypothèse selon laquelle la voie ventrale sous-tend le traitement de l'information pour la perception consciente (vision-for-perception), alors que la voie dorsale est impliquée dans le traitement de l'information pour l'action (vision-for-action). L'idée de deux réseaux visuels distincts dans le cerveau humain a fait l'objet de très nombreux travaux de recherche au cours des 20 dernières années. Mais les résultats apparaissent contradictoires et divisent de façon catégorique la communauté scientifique entre les partisans d'une spécification anatomique pour le traitement de l'information visuelle et les adversaires. Cette thèse vise à éclaircir une partie du mystère de la façon dont la perception et l'action s'articulent.

La figure d'Ebbinghaus se compose d'un objet incorporé dans un contexte spécifique (par exemple, un cercle central entouré par des cercles plus petits ou plus grands). Dans cette situation, la taille de l'objet perçu diffère généralement de sa taille physique, un phénomène bien connu sous le nom d'Illusion Ebbinghaus. La figure Ebbinghaus a été utilisée pour distinguer la fonction d'une vision pour la perception (consciente), sensible aux illusions visuelles (taille relative), de la fonction d'une

vision pour l'action affectée par les propriétés physiques de l'objet (taille physique). Alors que les publications rapportent que l'illusion d'Ebbinghaus affecte exclusivement la perception, un nombre croissant d'études démontrent que l'action est impactée de façon similaire par cette illusion. Actuellement, il n'existe pas de règle qui permet de contrôler la perception de la taille de l'objet cible (apparaissant comme plus grand ou plus petit) dans l'Illusion d'Ebbinghaus et à partir de laquelle on puisse prédire son amplitude. Par conséquent, on peut se demander si la figure d'Ebbinghaus évoque systématiquement une illusion et quels sont les facteurs qui déterminent les effets observés. Dans une première étude, nous avons ainsi cherché à quantifier la figure d'Ebbinghaus à partir de ses propriétés géométriques et évalué de façon systématique les effets sur la taille perçue. Les résultats montrent qu'un tiers des configurations Ebbinghaus n'ont pas révélé d'effet significatif d'illusion. Pour l'autre partie des configurations Ebbinghaus en revanche, les effets d'illusion étaient dus à l'ensemble des paramètres géométriques manipulés.

Après quantification des configurations Ebbinghaus, une démarche comparable de caractérisation des mouvements visuomoteurs a été implémentée sous la forme d'une tâche visuomotrice dans laquelle les mouvements volontaires étaient étudiés sous des contraintes de précision et de vitesse. Pour des mouvements d'atteinte discrets et continus, le comportement était décrit quantitativement et qualitativement en termes de cinématiques et dynamiques sous-jacentes. La caractérisation des mouvements visuomoteurs et la quantification de la perception des configurations Ebbinghaus ont ensuite permis de concevoir une tâche visuomotrice dont les cibles étaient des figures d'Ebbinghaus. Les résultats de cette dernière étude révèlent que les figures d'Ebbinghaus influencent le mouvement. Mais, les facteurs géométriques manipulés pour affecter la perception n'influencent pas tous le mouvement.

Grâce à son approche systématique et à ses développements méthodologiques, les travaux de cette thèse pourront servir de référence pour de nouvelles études sur les mécanismes de perception et d'action. Cette thèse a également démontré que les voies ventrale et dorsale ne sont pas strictement distinctes *fonctionnellement*, et que différentes variables informationnelles sont potentiellement utilisées pour 'la vision pour la perception' et 'la vision pour l'action' indépendamment du fait que certaines variables causent des illusions.

Publications

This document summarizes the research conducted during my PhD. Some ideas and figures have appeared previously in the following:

1. Knol H, Huys R, Sarrazin JC, Jirsa VK (2015) Quantifying the Ebbinghaus figure effect: target size, context size, and target-context distance determine the presence and direction of the illusion. *Front. Psychol.* 6:1679. doi: 10.3389/fpsyg.2015.01679.
2. Huys R, Knol H, Sleimen-Malkoun R, Temprado JJ, Jirsa VK (2015) Does changing Fitts' index of difficulty evoke transitions in movement dynamics? *EPJ Nonlinear Biomed. Phys.* 3: 8. doi: 10.1140/epjnbp/s40366-015-0022-4.
3. Knol H, Sarrazin JC, Spiegler A, Huys R, Jirsa VK. Ebbinghaus figures that deceive the eye do not necessarily deceive the hand. *Under review.*
4. Knol H, Spiegler A, Huys R, Jirsa VK. Dynamical perception and action mechanisms under illusionary conditions using Bayesian statistics. *In preparation.*

Acknowledgments

The choice to do a PhD, and to do this PhD in Marseille was a good and difficult one. I appreciate the support of many people that have been somehow important for me as a beginning scientist, for me as a colleague, for me as friend, for me as a daughter and sister.

Dank je wel Raoul Huys. Thank you for sharing your knowledge and supporting me during these years. Thank you for your honesty, your trust, and advice in science and life. It was a pleasure working and learning with you. Oh, and thank you for your lovely humour, especially early in the morning before having had breakfast. You can cut your wild hairs, but please, never loose them.

Thank you Viktor Jirsa. Thank you for trust in me. Thank you for giving me the opportunity to start my PhD in your lab. Thank you for showing me around in science. Your time-to-time guidance and friendly human encounters in the lab, in the pub, and at home has made a difference.

Merci Jean-Christophe Sarrazin. Thank you for your endless motivation, and the gift to make others enthusiastic for the work we are doing. Thank you for your help with the French administrative system that is most of the time difficult for me to understand.

I would like to acknowledge the jury members: Jeroen Smeets, Frank Zaal and Patrick Haggard. Thank you for your time and interest in my work.

Thank you INS-members for sharing ideas, cakes, food, and drinks.

Thank you ONERA DCSD in Salon de Provence for welcoming me even though I was hardly ever around. Merci Francine, Christelle, Bruno, Sami, Kevin, Laurent.

Thank you Pascale and Véro for being my friends, for taking care of me when it was necessary, and most of all for making me feel home.

Thank you Christophe for bringing music and bad words in my life that made me survive in Marseille (and its traffic).

Merci Lisbeth, Isabelle, Fabienne for doing beautiful music projects, having wonderful rehearsals with aperos in the pool, and thank you for being friends. Also thank you Thierry, Daniele, Jean-Claude and Anne-Marie for sharing the joy of music and our wonderful rehearsals! Merci Henri, for your support and for welcoming me/us at your beautiful place.

Thank you Galina Mal-IEIE-va, ma chérie (chérie lady), for being my friend through good and bad days.

Thank you Paula for being a beautiful, creative, nerdy, loving, helpful, and understanding friend that made me feel welcome in a time where everything was new.

Thank you Tim Proix for hosting me and helping me out when I arrived in Marseille, and for all the good times outside the lab.

Thank you friends that reminded me of the beautiful, and sometimes challenging life outside of the lab and being a bit of family to me: Isabelle, Caro, Antoine, Paolo, Rohit, Ana, Javi, Seb, Carlijn, Niek, Solveig, Kasia, Spase, Claude, Svetlana, Piotr, Rita, Richard, Luka, Marisa, Tim Kunze, Martin, Marta, Jorge, Mathieu, Stefania, Domagoj, Huifang.

Thank you Marmaduke for your technical support, and thanks you for sharing some of your ideas about how to make this world a good/better place.

Thank you Mireille, for sharing your ideas about science.

Thank you Irene and Julie, and previously Adam, Francesca, Marcel, and Emmanuel for being my office buddies to share cookies, weekend-stories, and work-stuff with.

Foar myn leaven. To my friends that I left (spatially) at home, but that remained my deepest friends and support and will remain connected to me wherever I go on this planet.

I want to thank my grandparents pake Tseard and beppe Tryntsje, and my lovely, big family. Especially I owe a big 'thank you' to my parents and Dolon, for loving me and supporting me always, for assuring me to take risks, and to go for nothing else but everything. Ik hâld fan jim.

No word will catch my gratitude for you with the right tone and feeling, Andreas. Thank you, for sharing life with me.

Contents

Abbreviations:

PCA	Principal Component Analysis
TVSH	Two Visual Streams Hypothesis
ID	Index of Difficulty
CV	Coefficient of Variation
SD	Standard Deviation
DST	Dynamical Systems Theory
RD-model	Rayleigh damping and Duffing oscillator model
MT	Movement Time
AT	Acceleration Time
DT	Deceleration Time
PV	Peak Velocity

Chapter 1 | General introduction

"Experience is not a thing that happens to people, but a thing that people do."
- O'Regan

1.1 Preliminaries

Visual perception is a crucial part of a functioning human being. Since ancient times, scientists have been fascinated by the way human beings perceive the world. Perception can hardly exist without movement of one-self or its' surrounding. Think of, for example, eye movements. Even when we think we are not moving, our eyes are making little rapid movements (so called saccades) that allow building an understanding of our visual environment. Thus perception and action are crucially linked. But how perception and action are functionally coupled and coordinated remains a puzzle. As a logical consequence, numerous studies have investigated how our body deals with visual perception, goal-directed movements, and how perception and movements are coupled.

One influential hypothesis that gained much attention in the last decades is the two visual streams hypothesis (TVSH). This hypothesis proposes that visual information for perception is processed relatively independently from the visual information for action. Visual illusions have been used as a tool to make a distinction between the ventral stream that processes 'vision for perception' and the dorsal stream that processes 'vision for action'. The ventral stream is found to be sensitive to the relative size of objects and therefore sensitive to size-illusions, whereas the dorsal stream is processing the absolute, physical size information of objects and thus remains unaffected by size-illusions. The hypothesis has been widely endorsed, but

also met much criticism. The experimental results of the last 20 years are contradictory and inconclusive.

In the work that is presented in this thesis we study the perception of size illusions on perception and action. We aim to quantify the perception of a size illusion in order to answer the question whether perception is always sensitive to size illusions. Subsequently, the question whether size illusions will influence movements, and if so, if these effects depend on the movement type, can be answered.

In order to gain a deeper understanding in the nature of the theoretical debate, the following sections will provide a short overview of the background of the two visual systems hypothesis and the results from psychophysical experiments. This section will be followed by an overview of the influence of visual illusions on movements in the framework of the dynamical systems theory.

1.2 Dichotomy of the visual system

By focusing on the neural areas and connections involved in (cognitive) processes, neuroscientists raised one important dichotomy of the visual perception system in the 1980s. The first discussion of an anatomical dichotomy of the visual system concerned the distinction of 'vision of object identity' and 'vision of space' that were localized in the subcortical geniculostriate and tectofugal systems, respectively (Trevarthen, 1968). In 1982 Ungerleider and Mishkin found that macaques with lesions in the inferotemporal cortex were unable to identify objects, but maintained the ability to locate objects. The macaques with lesions in the posterior parietal cortex showed the inverse pattern. Subsequently, the geniculostriate-tectofugal dichotomy was replaced by a cortical dichotomy of the visual system with corticocortical connections originating in the striate area that are mediating both vision of object identity and of space (Ungerleider and Mishkin, 1982). They referred to the distinct cortical visual systems as the 'what' and the 'where' system.

1.2.1 The two-visual systems hypothesis

Following the influential work of Ungerleider and Mishkin (1982), a hypothesis was forwarded in which two visual processing systems were not identified as 'what' and 'where, but as 'vision for perception' and 'vision for action' (Goodale and Milner, 1992; Milner and Goodale, 1995). The two visual systems hypothesis (TVSH) was established after studies with patient D.F. Patient D.F. suffers from visual agnosia as a result of accidental monoxide poisoning that damaged the ventral stream of the visual system (e.g., Murphy et al., 1998). The ventral pathway is projecting from the primary occipital cortex to the inferotemporal cortex. Damage to the ventral pathway can lead to visual agnostic patients that are unable to identify or recognize objects but are successful in performing motor tasks with these objects. For example, a letter would not be recognized as being a letter, but could nevertheless be successfully put in a mailbox. Damage to the dorsal cortical pathway that projects from the primary occipital cortex to the posterior parietal cortex, can result in optic ataxic patients. Optic ataxic patients are unable to reach accurately to objects, although they can recognize the object (e.g., Perenin and Vighetto, 1988). This led scientists to functionally dissociate the visual system into a ventral and dorsal stream. The ventral stream processes visual information for *conscious perception*, whereas the direct visual guidance of *action* is the exclusive avocation of the dorsal stream (Milner and Goodale, 1995).

1.2.2 Visual illusions as a tool to study the dichotomy of the visual system

Visual illusions[1] that can make objects or representations look smaller or bigger than they are have been applied to study the extent to which the ventral and dorsal stream are functionally distinct. Examples of contextual illusions are the Müller-Lyer figure and the Ebbinghaus figure (also called Titchener circles; see figure 1.1). The logic behind the visual illusion application is that the perception of object size operates within the allocentric frame of reference. Encoding target position, as well as planning the arm trajectory towards it, can be influenced by the spatial relationships that the target has with environmental cues (Conti and Beaubaton, 1980; Foley, 1975;

[1]In philosophy it is debated what visual illusions are, whether they exist, or even, whether everything we perceive is necessarily an illusion. I acknowledge the debate, but in the rest of this thesis I will adopt the nomenclature as is commonly used in conventional papers on perception and Ebbinghaus figures and alike.

Gentilucci and Negrotti, 1996; Toni et al., 1996; Gentilucci et al., 1997). Thus, perception of object size is thought to be mostly relative and rarely in physical measures (Aglioti et al., 1995). Therefore, placing an object next to surrounding objects that are smaller (or bigger) can 'fool' the size perception. At the other hand, the information required for movements towards objects is likely to be processed within an egocentric frame of reference, that is, a frame of reference centered on the body of the agent in order to encode target position in space (Soechting and Flanders, 1989; Gentilucci et al., 1997). This body scaled information about object size remains unaffected by the contextual information, and thus will not be 'fooled' by visual illusions.

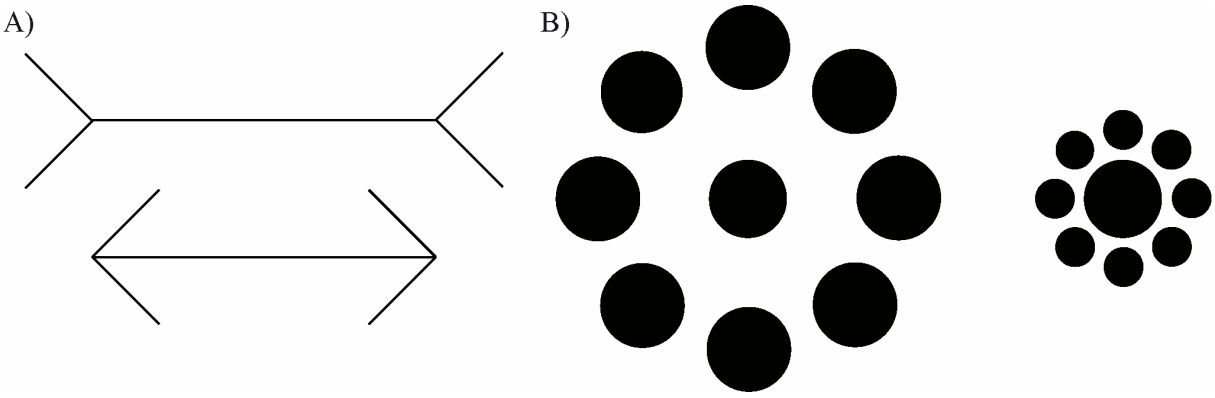

Figure 1.1 Examples of geometrical size-weight illusions, with in **(A)** the Müller-Lyer illusion and **(B)** Ebbinghaus illusion (also called Titchener circles).

Many psychophysical tasks have been performed to falsify the TVSH in pointing and grasping tasks. Aglioti, DeSouza, and Goodale (1995) surrounded poker-chips with smaller and bigger circles (the Ebbinghaus illusion, Fig. 1.1 B) and asked participants to perceptually judge the size in the pre-test phase, and pick up a poker-chip in the test-phase. The Ebbinghaus illusion had a powerful effect on the perceptual judgment of object size, but grasping the same object remained largely scaled according to the actual object's size. The authors concluded that the "calibration of grip aperture is quite refractory to the compelling size-contrast illusion" (p. 684). These results were confirmed by multiple studies implementing various contextual illusions in perception or/and action (mainly grasping and aiming) tasks (Ganel et al., 2008; Haffenden and Goodale, 1998; Stöttinger et al., 2010;

van Doorn et al., 2009; Haffenden et al., 2001; Stöttinger et al., 2012; Fischer, 2001; Alphonsa et al., 2014). Though these numerous studies have shown a functional distinction between the ventral and dorsal stream, the body of studies contradicting these findings and interpretations is accumulating (e.g., Franz et al., 2000, 2001; Pavani et al., 1999; Vishton et al., 1999; Franz, 2001; van Donkelaar, 1999; Brenner and Smeets, 1996; Smeets and Brenner, 1995).

These conflicting results from psychophysical studies have been partly explained by methodological differences in grasping and pointing tasks (Bruno et al., 2008; Bruno and Franz, 2009). Some methodological concerns have been raised with regard to the validity of the way perception and action were compared (Franz and Gegenfurtner, 2008; Pavani et al., 1999; Franz et al., 2000), and how (if at all, see van Donkelaar, 1999; Jackson and Shaw, 2000; Westwood et al., 2000; Ellenbürger et al., 2012) perception was quantified (e.g., Smeets and Brenner, 2006). These methodological weaknesses, and the variety of the applied measures, leave scientists, to date, with an insuperable gap with regard to the debate whether the visual system is functionally distinct.

1.2.3 The perception of Ebbinghaus figures

The Ebbinghaus figure is applied to experimental paradigms for over 100 years. The application of Ebbinghaus figures for studying the possible dissociation of the ventral and dorsal stream gained popularity since the landmark paper of Aglioti, DeSouza and Goodale (1995). However, to date, a rule describing the illusion effects as a function of the parameters that create this illusionary effect is absent. A few studies have systematically tested several parameter combinations to find the principal factors evoking the illusion effect (Massaro and Anderson, 1971; Roberts et al., 2005; Nemati, 2009). These studies found different factors contributing to the illusion effect: the size of the center circle, the context circle size, the number of context circles (Massaro and Anderson, 1971; Roberts et al., 2005), the distance between the context circle and the center circle (Roberts et al., 2005; Im and Chong, 2009), and the size of the area of empty space between the context circles (Nemati, 2009). However, the rules proposed by the latter authors did not specify the interplay

of the parameters. Therefore, the source(s) of the illusion effects remains unknown, which hinders predictions of illusion effects in the application of Ebbinghaus figures in experiments.

1.3 Illusion effects on movement

Like the various methods to capture the illusion effects on visual perception, numerous methods have been applied to capture the illusion effects on movements. Next to grasping movements, pointing movements have been a popular method mainly since the work of psychologist Paul M. Fitts who proposed a quantification of difficulty in pointing tasks. The law proposed by Fitts finds it origin in information theory. It describes the relation between target size, target distance, and the result on the performance (i.e., movement time) (Fitts, 1954). Fitts' law poses that the required time to successfully execute an aiming movement increases linearly with task difficulty. The prediction of movement time with regard to the target size and the distance allows for verification of the influence of perceived target size on the movement time. This idea resulted in Fitts' tasks with the Ebbinghaus (like) figure as target (Fischer, 2001; Alphonsa et al., 2014; van Donkelaar, 1999; Handlovsky et al., 2004; Ellenbürger et al., 2012; Lee et al., 2002). This way of studying the TVSH did not, however, resolve the conflicting results that were pointed out in the section 1.2.2.

1.3.1 Dynamical systems underlying movement

An important question is how all the components (i.e., cells, tissue, organs, muscles) of a human body can lead to controlled motor behavior in order to achieve a goal. Motor behavior such as motor coordination is viewed as self-organized pattern formation processes. In 1980 Kugler, Kelso and Turvey presented a concept of movement and control in terms of dynamical structures. Coordination dynamics aims to identify generic principles of pattern formation by searching for phenomenological laws of perceptual-motor behavior. Coordinated movements are spontaneously performed following characteristic stable patterns of behavior. The focus lies on the stability properties of the system under study, changes in stability and number and type of solutions as a function of parameters (bifurcations), and associated phenomena like critical fluctuations, hysteresis, etcetera (Kelso, 1995). One

famous example is a bimanual finger wiggling experiment at some relative phase and at a certain frequency. The fingers are wiggled in the same direction (to the mid-line), and are moving in-phase when the fingers move in the same direction and with the same frequency and phase. Two stable relative phases were found, 0° and 180°. All other relative phases are highly unstable. Furthermore, 0° is more stable that 180°. If the frequency of finger wiggling is increased while moving at 180°, the participants will spontaneously make a transition to 0°. The opposite, transitioning from 0° to 180°, is not true.

Since the late 1990s the behavior resulting from the Fitts' pointing tasks has been studied with respect to the principles of the dynamical systems theory. Fitts' tasks have been studied with respect to the question whether discrete and continuous movements can be considered to be distinct, driven by different control processes. The dynamical systems theory (DST) offers a classification principle based on phase flow topologies, which identify all behavioral possibilities within a class. This classification is model-independent; every behavior within a class can be mapped upon others, whereas maps between classes do not exist. Systems belong to the same class if, and only if, they are topologically equivalent. Motor control and timing mechanisms governed by different topologies can thus not be reduced to each other: they belong to different equivalent classes.

The relation between task difficulty and movement time has been shown to be continuous. However, discontinuities have been observed in both reciprocal as well as discrete Fitts' tasks (Huys et al., 2010a; Sleimen-Malkoun et al., 2012). The discontinuity has been mainly ascribed to an abrupt transition between two distinct dynamic regimes that occurs with increasing the task difficulty. These two dynamic regimes that have been identified are *limit cycle* and *fixed* point behavior (Huys et al., 2010a; Buchanan et al., 2004). A limit cycle is a trajectory that returns to its starting point, thus describes a closed orbit in the state space, which is spanned by the position of the movement $x(t)$ at time t and its change in time $\mathrm{d}x(t)/\mathrm{d}t$. Limit cycle behaviour is typically used to describe rhythmic activity. A fixed point instead is a location in the state space at which there is no movement, that is, no changes in time

$dx(t)/dt = 0$. The behaviour around a fixed point is discrete (attracting or repelling). Thus the start position and the target can be ascribed as repelling and attracting for movements in discrete Fitts' tasks. By observing this abrupt transition from limit cycle behaviour to fixed-point behaviour suggests that the human nervous system abruptly engages a different control mechanism when task difficulty increases.
Again, task difficulty comprises the target width and the distance to the target, and thus task difficulty can be changed by changing target width or distance. However, it remains unclear whether the transition between limit cycle behavior and fixed-point behavior are evoked similarly under the distance and width induced scaling of task difficulty.

Another factor that might influence a transition from one behavior to the other is the perceived target width or distance. For example, if a target is perceived as being smaller than it is, the question arises whether the behavior then follows the perceived or the physical target size. To date, however, it remains unknown whether the subjectively perceived target width can influence this transition and the corresponding movement dynamics underlying the Fitts' task. Possibly, the contradicting results identified in motor tasks with incorporated size-weight illusions share one common denominator: the sensitivity of motor regimes to size-weight illusions is different.

1.4 Outline of the thesis

The conflicting results of various studies incorporating size-weight illusions lead to the main aim of this thesis, that is, to unravel whether the relative size perception of a target influences the movement towards it. More precisely, the objective is to quantify the perception of the Ebbinghaus figure, the movement dynamics of Fitts' tasks, and finally how the quantified Ebbinghaus figures influence movement dynamics of the quantified Fitts' tasks. In order to shed light on the influence of relative size perception on movements, a structured and thorough study of visual perception, and the perception-action interaction is called for.

Therefore, *chapter 2* is dedicated to the quantification of the Ebbinghaus figure size percept for a set of 30 conditions that are Fitts' task compatible. In this chapter, the range of parameter combinations are studied in a systematic fashion with a method that is well known in psychophysics and vision research, but has not yet found its way in the study of size-weight illusions. In order to identify how the parameters of Fitts' task (i.e., the target size and the distance to the target) are influencing the transition between motor control regimes, an experiment that quantified discrete and reciprocal aiming movements is presented in *chapter 3*. In this chapter a systematic scaling of a large range of parameter combinations of a classical Fitts' task leads to a further detailed description of Fitts' law.

Chapter 2 and *Chapter 3* subsequently lay the foundation for *Chapter 4* in which the effect of the perception of Ebbinghaus figures on the motor control in a set of Fitts' tasks is reported. In *Chapter 5* we elaborate on the possible mechanisms that underlie perception and action. The thorough examination of perception (*Chapter 2*) and movement (*Chapter 3* and *4*) with a carefully designed analysis lead to novel insights concerning the influence of the Ebbinghaus figure on motor control, and leaves space for a debate on the general coupling of perception and action (*Chapter 5*). Finally, *Chapter 6* comprises a discussion about alternative dichotomies of visual information processing, and a reflection on the results from a constructivist and ecological approach. The thesis concludes with indications for future research that could foster our knowledge of the visual system and the link between perception and action.

Chapter 2 | *Perception* : Quantifying the Ebbinghaus figure effect[2]

"No two people see the external world in exactly the same way. To every separate person a thing is what he thinks it is -- in other words, not a thing, but a think."

- Penelope Fitzgerald

2.1 Abstract

Over the last 20 years, visual illusions, like the Ebbinghaus figure, have become widespread to investigate functional segregation of the visual system. This segregation reveals itself, so it is claimed, in the insensitivity of movement to optical illusions. This claim, however, faces contradictory results (and interpretations) in the literature. These contradictions may be due to methodological weaknesses in, and differences across studies, some of which may hide a lack of perceptual illusion effects. Indeed, despite the long history of research with the Ebbinghaus figure, standardized configurations to predict the illusion effect are missing. Here, we present a complete geometrical description of the Ebbinghaus figure with three target sizes compatible with Fitts' task. Each trial consisted of a stimulus and an

[2] Published as Knol H, Huys R, Sarrazin J-C, Jirsa VK (2015) Quantifying the Ebbinghaus figure effect: target size, context size, and target-context distance determine the presence and direction of the illusion. Front. Psychol. 6:1679. doi: 10.3389/fpsyg.2015.01679

isolated probe. The probe was controlled by the participant's response through a staircase procedure. The participant was asked whether the probe or target appeared bigger. The factors target size, context size, target-context distance, and a control condition resulted in a 3×3×3+3 factorial design. The results indicate that the illusion magnitude, the perceptual distinctiveness, and the response time depend on the context size, distance, and especially, target size. In 33% of the factor combinations there was no illusion effect. The illusion magnitude ranged from zero to (exceptionally) ten percent of the target size. The small (or absent) illusion effects on perception and its possible influence on motor tasks might have been overlooked or misinterpreted in previous studies. Our results provide a basis for the application of the Ebbinghaus figure in psychophysical and motor control studies.

2.2 Introduction

Optical illusions evoke a perceived image, color, contrast, lightness, brightness, or size that differs from the physical 'reality' of the figure. These illusions have mainly been used to test theories predicting the successes and failures of the perceptual system, particularly by the Gestalt school (Robinson, 1998). Optical illusions have been classified based on the behavioral manifestation of forty-five illusions (e.g. Coren et al., 1976). One commonly mentioned class is the one of size-contrast illusions, in which the size of an element is affected by its surrounding elements. A famous size-contrast illusion is the Ebbinghaus figure (see Figure 2.1), also called Titchener circles.

For over a century the Ebbinghaus figure has been used in experimental psychology to evoke an optical illusion of the perceived circle size. The Ebbinghaus figure consists of a target circle (*a* in Figure 2.1A) that is surrounded by multiple context circles (*b* in Figure 2.1A). It is thought that by surrounding the target with small or big circles, the target will appear bigger or smaller, respectively (Obonai, 1954; Massaro and Anderson, 1971). More than ten theories have been trying to explain the physiological mechanism(s) responsible for the over- and underestimation of the target (for a review see: Robinson, 1998). However, attempts

to quantify the illusion magnitude of this widely used geometrical visual illusion have not resulted in a (complete set of) geometrical rule(s), which is in all likelihood at least partly due to the broad spectrum of parameters involved. Several rules have been developed to identify the principal factors influencing the perceptual judgment evoked by the Ebbinghaus figure (e.g. Massaro and Anderson, 1971; Roberts et al., 2005; Nemati, 2009). Principle factors that have been identified are the size of the target (*a* in Figure 2.1A), the context circle size (*c* in Figure 2.1A), the number of context circles (Massaro and Anderson, 1971; Roberts et al., 2005), the target-context distance (b in Figure 2.1A; Im and Chong, 2009; Roberts et al., 2005) and the size of the area of empty space between the context circles (Nemati, 2009). However, these proposed rules do not specify the exact interplay between the three parameters specified in Figure 2.1A, which makes utilization of these rules for parameter selection and the prediction of the corresponding illusion effect tricky if not impossible. Furthermore, these rules have barely been validated. Indeed, Franz and Gegenfurtner (2008) concluded their review stating that: "…currently not much is known on the exact sources of the Ebbinghaus illusion."

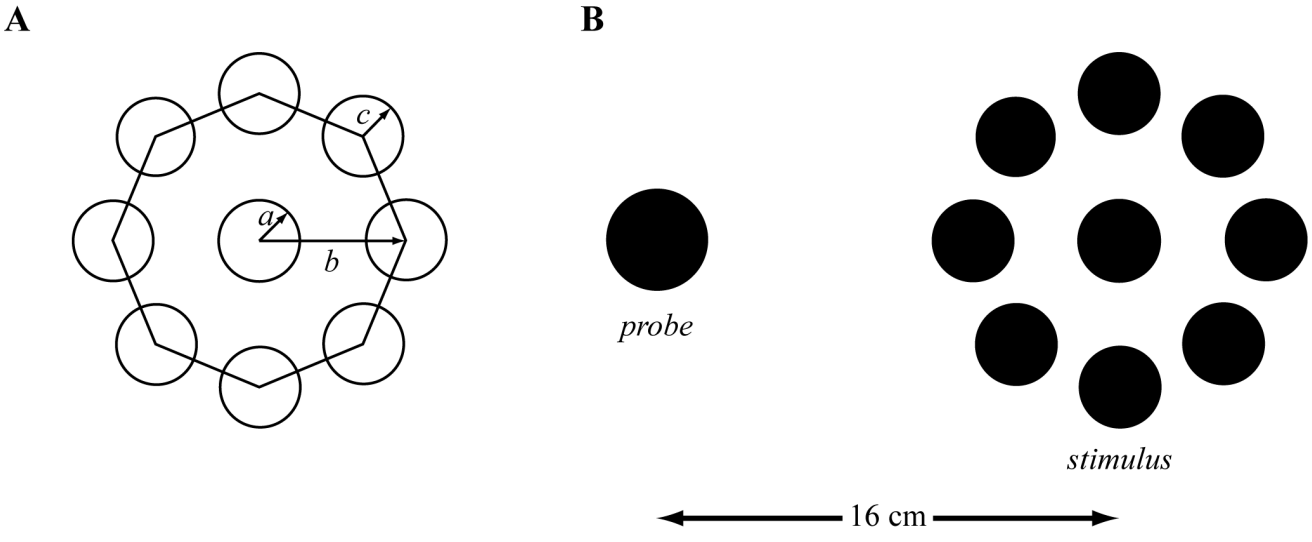

Figure 2.1 (A) The parameters of the Ebbinghaus figure with the radius of the target (*a*) and the context (*c*), and the distance from the target center to the context center (*b*). **(B)** Example of the Ebbinghaus stimulus with the scaling probe (not scaled to real size). The distance between the center of the probe and the center of the target was 16 cm. The context circles covered approximately 75 % of the circumference.

This lacuna did not withhold experimentalists to employ this figure to shed light on the so-claimed distinction between the ventral and dorsal visual pathway (see the review of Franz and Gegenfurtner, 2008). Accordingly, the visual system contains two distinct streams: the ventral pathway is specialized in processing information leading to conscious perception whereas the dorsal pathway is specialized in processing information for sensory-motor action (Goodale & Milner, 1992; Milner & Goodale, 1995). The dorsal stream encodes visual information into the required coordinates for skilled motor behavior, and does this in absolute metrics determined relative to the observer (egocentric frame of reference), whereas the ventral stream encodes the information into object properties relative to the properties of other objects (scene based frame of reference), and therefore provides a rich and detailed representation (Goodale, 2014). Based on this hypothesis, online control and the programming of movements would recruit the dorsal stream and, since absolute metrics are determined relative to the observer and not relative to the context of the object, would therefore be insensitive to visual illusions (Goodale, 2014; Milner & Goodale, 2008).

Several studies have reported evidence for the illusion insensitivity during grasping movements (Aglioti et al., 1995; Franz and Gegenfurtner, 2008; Stöttinger et al., 2010, 2012; Haffenden et al., 2001). However, these findings seem to mismatch with studies that show a clear effects of visual illusions on grasping (Franz et al., 2000; Pavani et al., 1999) and pointing (Gentilucci et al., 1996; van Donkelaar, 1999). These seemingly contradicting results led to the hypotheses (for a review see Franz & Gegenfurtner, 2008) that a clear functional dissociation between perception and action cannot be made (Franz et al., 2000; Gentilucci et al., 1996), that the ventral pathway would have to be partially involved (Carey, 2001; Aglioti et al., 1995), and that two dorsal pathways (e.g., the use and grasp system) exist in stead of one (Binkofski and Buxbaum, 2013).

Seemingly conflicting results of studies that quantified the illusion effect in perception and movements tasks may be explained in various methodological ways (Bruno et al., 2008; Bruno and Franz, 2009). Franz (2001) classified two measurement

types, to which he referred as the standard and the non-standard perceptual measures. In the standard method, participants either compare the size of two illusion stimuli or of one probe and one illusion stimulus. In the non-standard method, participants scale the aperture (with or without vision of the hand) to indicate the perceived size. Potential problems arising in the standard method are: First, by changing the size of the inner circle of an Ebbinghaus figure, as in Aglioti et al. (1995), it is not just the target size that is changed but also the distance from the target to the context circle, and therefore also the illusion magnitude (Roberts et al., 2005). Second, sometimes a stimulus-stimulus configuration is used in the perceptual task whereas a stimulus-probe configuration is used in the motor task (as in Aglioti et al., 1995). Third, if a task consists of comparing stimulus A with stimulus B, the question comes up which stimulus evokes an illusion effect (if any). For the non-standard method, a potential problem is that it is questionable that studying the perceptual illusion effect by asking participants to scale their aperture indeed provides a 'pure' perceptual measure. Note that this method has generated conflicting results (Haffenden and Goodale, 1998; Daprati and Gentilucci, 1997). Across methods, if graspable targets are used (in the perceptual task), the minimum stepsize of the target or probe might be relatively big compared to the illusion magnitude. Furthermore, Franz & Gegenfurtner (2008) identified methodological biases and statistical corrections in the comparison of perception and movement task data. There are, however, also studies that have not quantified or reported the illusion effect on perception (e.g. van Donkelaar, 1999; Ellenbürger et al., 2012; Jackson and Shaw, 2000; Westwood et al., 2000), or have not used a control condition (Ellenbürger et al., 2012). To recapitulate, the conflicts in the reported results may well be due to the various methods used, and potential weakness therein as discussed here above. Consequently, it is hard, if possible at all, to draw strong conclusions about the proposed dissociation of the ventral and dorsal stream in perceptuomotor tasks based on research using optical illusions.

With the aim to (partly) fill this gap, we here provide a fully parameterized Ebbinghaus figure, and systematically quantified the illusion effect for parameter ranges that are relevant for behavioral experiments. Thereto, we used a methodology

that is well established in the psychophysics literature, namely, the staircase procedure. We predicted that target size, context size, and target-context distance would affect the perceived target size of the Ebbinghaus figure, but that some parameter combinations, in particular those involving small target sizes (Massaro and Anderson, 1971), would fail to elicit a significant illusion effect. Intuitively, we further expected that some stimulus configurations, in particular those evoking a strong illusion effect, would be perceptually more distinct than others, and that this would affect the decision making as expressed in the response times. That is, we expected response time to scale inversely with perceptual distinctiveness. Our results will be able to guide future experimentalists, which, we hope, will contribute in clarifying the role of the ventral stream in the guidance of motor behavior.

2.3 Materials and methods

2.3.1 Participants

Twelve participants (6 females and 6 males, age mean ± SD = 28.9 ± 3.5) with normal or corrected to normal vision volunteered in the experiment. The experiment was performed in accordance with the Helsinki Declaration and all participants gave a written informed consent prior to their participation.

2.3.2 Apparatus

The visual stimuli were drawn and generated using the Psychophysics Toolbox in Matlab R2009b (The MathWorks Inc., Natick, MA) (Brainard, 1997; Kleiner et al., 2007). Black stimuli were presented against a white background (see Figure 2.1) and multisampled to control for aliasing effects. To prevent interference from previous trials and to control hemispace bias the stimuli were randomly presented on the left or the right side of the screen while an isolated probe (i.e., target without context circles) was presented simultaneously on the opposite side of the screen at a distance of 16 cm from the stimulus (and at the same height). The stimuli were displayed with a Dell Precision T3610 and Nvidia Quadro K2000 video card on a Dell P2714H monitor with a resolution of 1920 × 1080 pixels (597.9 × 336.3 mm, 52.96° × 29.27°)

and a frame rate of 60 Hz. The participants sat at a 60 cm distance from the monitor and their heads were supported with a chin-rest so as to ensure that the distance between the head and the monitor remained fixed.

2.3.3 Procedure

Based on a fully geometrical description (Figure 2.1A), three target sizes ($2 \times a$ in Figure 2.1A), three target – context distances (b in Figure 2.1A), three context sizes (bigger, equal, and smaller than the target; c in Figure 2.1A), and three control conditions (isolated targets) were selected, resulting in a $3 \times 3 \times 3 + 3$ factorial design. The equidistantly spaced context circles covered approximately 75 percent of the circumference in all conditions to control for the completeness of the surround (Roberts et al., 2005). Consequently, the number of context circles varied as a function of context size and target-context distance. The stimuli diameters were 0.5, 1.0 and 2.0 cm. (These sizes were chosen with an eye on planned future studies involving Fitts' task; the corresponding indices of difficulty (i.e., $ID=\log_2(2D/W)$, where D and W represent the distance between the targets and the target width (Fitts, 1954), were 6, 5 and 4, respectively.) Context sizes were 20, 100 and 180 percent of the target size; i.e., 0.1, 0.5 and 0.9 cm for the small target, 0.2, 1.0, and 1.8 cm for the medium target, and 0.4, 2.0, and 3.6 cm for the big target. Three distances from the center of the target to the center of the context circles (i.e., b in Figure 2.1A) were calculated based on the smallest distance being 10 percent bigger than the radius of the target plus the radius of the biggest context; i.e., 0.8 cm for the small target, 1.6 cm for the medium target, and 3.0 cm for the big target. The other two distances were incremented with 0.6 cm for each distance. All dimensions were corrected for pixel size and rounded to the nearest integer.

A two-down, one-up staircase procedure was used to find the perceptual threshold between the probe and the target in which the probe size was adjusted (García-Pérez, 1998). Two staircases per condition were used, one in which the initial condition of the probe was 0.4 cm bigger than the target size, and one in which it was 0.4 cm smaller. Each staircase started with a probe diameter step size of four pixels (i.e., 0.12 cm). The participants were tasked with pressing a key (A or L) for the

bigger appearing target or probe on the left (*A*) or right side (*L*) of the keyboard corresponding to the target and probe location on the screen. Depending on the response of the participant, the probe size was adjusted according to the two-down, one-up staircase procedure. In a sequence of responses, a reversal is the event where the response to probe n deviates from that at n-1. After each reversal the step size was halved, until the minimum of one pixel (i.e., 0.03 cm) was reached, which was then retained. The participants were instructed to respond as soon as they had decided which key to press, but it was made clear that it was not a reaction time task. After each key press, the stimulus disappeared and a random noise window was displayed for one second followed by a fixation cross (duration: 0.5 s). Then the next stimulus with the adjusted probe appeared. A staircase was terminated and removed from the cue after a participant had reversed the direction of the staircase 11 times. After five conditions, the participants could take a small pause. Upon completing the first half of the experiment, the participants took a ten to fifteen minutes break. The entire experiment lasted for about 2 hours.

2.3.4 Data analysis

From the last 10 reversals, the perceptual threshold (*PT*) was calculated according to equation 2.1,

$$PT = \frac{1}{m}\Sigma_{j=1}^{m}\left(\frac{1}{n}\Sigma_{i=1}^{n}SC_{up_i} + \frac{1}{n}\Sigma_{i=1}^{n}SC_{low_i}\right) \qquad (2.1)$$

in which *m* corresponds to the number of staircases (here 2), *n* represents the number of reversals taken into account (here 10), Explicitly, the mean of SC_{up} and SC_{low} are calculated based on the last 10 reversals and are referred to as the upper and lower staircase threshold respectively. The range between the mean SC_{up} and mean SC_{low} reflected the area of uncertainty (*AU*; Equation 2.2).

$$AU = \frac{1}{n}\Sigma_{i=1}^{n}SC_{up_i} - \frac{1}{n}\Sigma_{i=1}^{n}SC_{low_i} \qquad (2.2)$$

To control for inter-individual differences in the judgment of the target sizes in the control condition, and to allow for inter-individual and inter-trial comparisons, the judgments were corrected by subtracting the perceptual threshold of the control

trial ($PT_{control}$) from the corresponding perceptual threshold of each trial (PT_{trial}), i.e., $IM = PT_{control} - PT_{trial}$, where IM stands for illusion magnitude. For the statistical analyses and the visualizations, the illusion magnitude was used.

Response time was defined as the time between stimulus presentation onset and the participant's response. We next computed the average response time before a participant crossed one of the staircase thresholds for the first time (referred to as RT_{base}). For this procedure, the first response was omitted. The average response time following this threshold crossing was referred to as RT_{AU}.

Three-way repeated measures ANOVAs with target size (*a* in Figure 2.1A), distance (*b* in Figure 2.1A), and context size (*c* in Figure 2.1A) as within participants factors were performed to investigate the effects on the illusion magnitude and the area of uncertainty**.** If significance levels were met ($a = .05$), the tests were followed up by Bonferroni post-hoc tests ($a = .05$). A four-way repeated measures ANOVA with target size (*a*), distance (*b*), context size (*c*), and response moment (RT_{base}, RT_{AU}) as within participants factors was used to investigate significant effects on response time. The degrees of freedom were corrected according to the Greenhouse-Geisser method to control for non-sphericity of the data if necessary. If this was the case, the adjusted degrees of freedom were reported below. In order to examine if the perceived size of the targets of the illusion trials were significantly different form those of the control trials, a paired samples t-test was performed for each condition. Pearson correlation coefficients were calculated to investigate potential (linear) correlations between response time, area of uncertainty and illusion magnitude, and between the response time before the area of uncertainty for the upper and lower staircase.

2.4 Results

2.4.1 Illusion magnitude

Recall, for the statistical analysis the control perceptual threshold ($PT_{control}$) per target size was subtracted from the PT_{trial} to control for the participants' ability to judge targets of different sizes. Figure 2.2A displays the results of the paired samples t-tests to investigate if the illusion magnitudes were significantly different from the control

trials. There, it can be seen that a target appeared only bigger than it was when the context and distance were small (i.e., 20 percent of the target size and 110 percent of target plus biggest context size, respectively) and the target size small or medium (i.e., 05 or 1.0 cm). In 33 percent of the cases, there was no significant illusion effect. For all other conditions the target was perceived as smaller than it actually was.

Significant main effects for illusion magnitude were found for context size ($F(2,22)=40.698$, $p=.000$, $\eta_p^2=.787$), distance ($F(2,22)=24.181$, $p=.000$, $\eta_p^2=.687$) and target size ($F(1.244, 13.686)=28.973$, $p=.000$, $\eta_p^2=.725$). The illusion magnitudes of all target sizes were significantly different (all $p < .005$; mean ± SD for the small (-.01 ± .01), medium (-.04 ± .01), and big (-.11 ± .02) target size), as well as for all context sizes (all $p < .001$; mean ± SD for the small (-.01 ± .01), medium (-.05 ± .01), and big (-.10 ± .02) context). For target – context distance, small distances differed significantly from the medium ($p < .000$) and big distances ($p < .005$), however, medium and big distances did not differ significantly from each other ($p > .05$; mean ± SD for distance small (-.03 ± .01), medium (-.07 ± .01) and big (-.06 ± .01)).

The analysis further revealed a significant interaction between target size and target-context distance ($F(4,44)=3.933$, $p=.008$, $\eta_p^2=.263$; see Figure 2.2B), as well as between target size and context size ($F(2.244,24.687)=12.822$, $p=.000$, $\eta_p^2=.538$; see Figure 2.2C), indicating that context size and distance influenced the illusion effect differently for the different target sizes. If significantly different from the baseline, the big and medium target-context distances always had a diminutive effect on the perceived target size (Figure 2.2A). The illusion magnitude under the small distance was always smaller than that of the medium and big distance, except when the illusion had a magnifying effect on the perceived target size. Except for the small distance, the big context size always had a stronger diminutive effect on the perceived target size than the medium context size, and the medium context size always had stronger diminutive effect than the small context size (see Figure 2.2C). The interaction of the three factors distance, context and target size approached significance ($F(3.857, 42.431)=2.427$, $p=.065$, $\eta_p^2=.181$). The target-context distance by context size interaction was not significant.

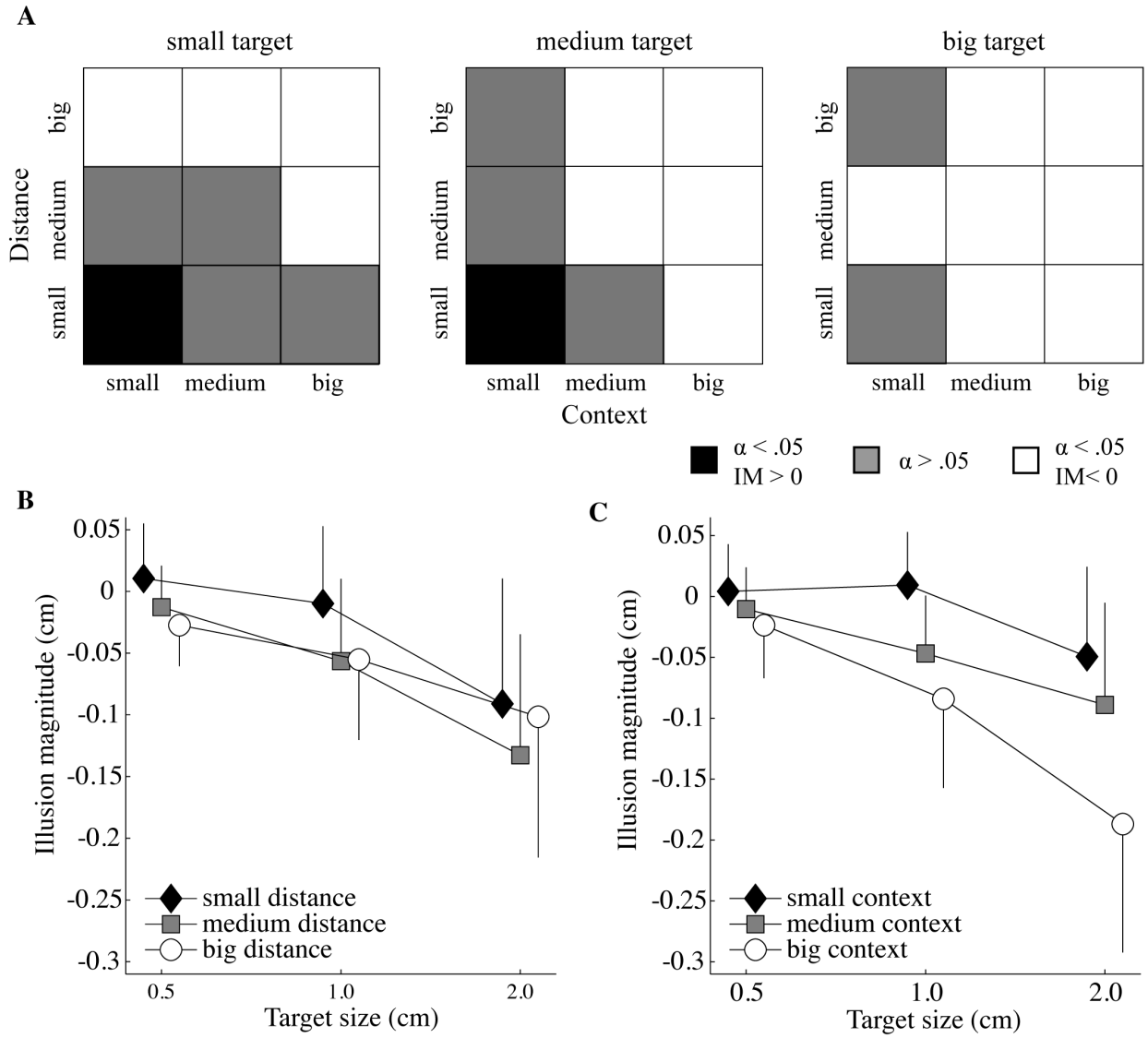

Figure 2.2 Illusion effects as a function of target size, context size, and target-context distance. **(A)** Significance levels resulting from paired sample t-tests and the direction of the illusion magnitude (IM) for each target size as a function of the context-target distance and context size. The black and white squares indicate a significant effect for bigger perceived targets and smaller perceived targets, respectively. The gray squares show conditions that were not significantly different from the control trials (a = .05). **(B)** Mean IM (and standard deviation) as a function of target size and distance. **(C)** Mean IM (and standard deviation) as a function of target size and context size.

2.4.2 Area of uncertainty

The area of uncertainty was only significantly influenced by target size (F(1.260,13.855)=22.731, p=.000, η_p^2=.674). Post-hoc tests indicated that it increased in

the control conditions as well as in the illusion trials as target size increased (for illusion trials: big versus medium or small target size ($p < 0.005$), medium versus small target size ($p < 0.05$)).

2.4.3 Response time

The response times for the three target sizes for the baseline (RT_{base}) and area of uncertainty (RT_{AU}) control conditions were not significantly different ($p > .05$; mean ± SD RT_{AU} for target small (.89 ± .38), medium (.89 ± .47) and big (.96 ± .57)). Presentation of the Ebbinghaus figures, however, provoked longer response times compared to the control conditions ($F(1,11)=35.795$, $p=0.000$, $\eta_p^2=.765$). In addition, for the illusion trials, RT_{AU} was significantly higher than RT_{base} ($F(1,11)=7.8$, $p=0.017$, $\eta_p^2=.415$; Figure 2.3A). Further, a significant main effect of target-context distance ($F(2,22)=6.1$, $p=0.008$, $\eta_p^2=.356$; Figure 2.3B) and of target size ($F(2,22)=4.9$, $p=0.17$, $\eta_p^2=.310$; Figure 2.3C) on the response time was found. Post-hoc tests revealed that response times were significantly longer at small distances compared to big distances ($p < 0.01$) and in the big target size conditions than in the small target size conditions ($p < 0.05$). Furthermore, an interaction effect between target size and distance was found ($F(4,44)=2.9$, $p=0.034$, $\eta_p^2=.207$) which was mainly caused by the medium distance. For the small and big distance, the response times increased with increasing target size, whereas for the medium distance the response time was shortest at the medium target size.

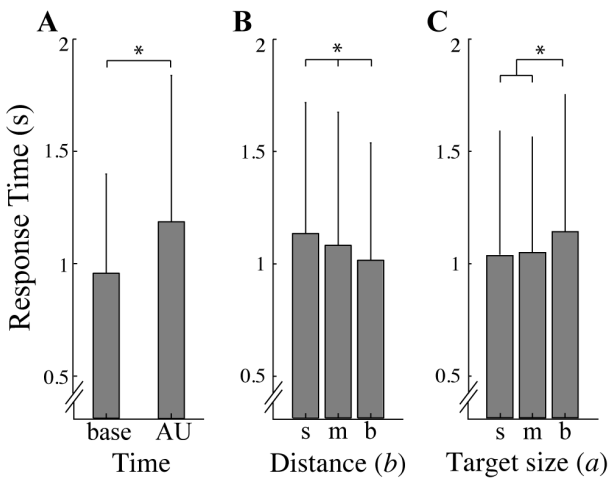

Figure 2.3 Response times. **(A)** Average response time (and standard deviation) as a function of time; *base* refers to the baseline responses and *AU* refers to responses in the area of uncertainty. Panel B and C represent the average response time (and standard deviation) over a small (*s*), medium (*m*) and big (*b*) distance **(B)** and target size **(C)**. Asterisks indicate significant effects ($a = .05$).

2.4.4 Correlations between illusion magnitude, area of uncertainty, and response time

A significant but weak correlation was found between the absolute illusion magnitude and the area of uncertainty ($r(322)=.12$, $p<.05$). Further, as the absolute illusion magnitude increased, the response time (moderately) increased ($r(322)=.25$, $p<.001$). In contrast, if the area of uncertainty increased, the response time decreased ($r(322)=-.41$, $p<.001$). Further examination of the relation between the area of uncertainty and response time across participants revealed that it was exponential, and that the exponent decreased with target size (Figure 2.4).

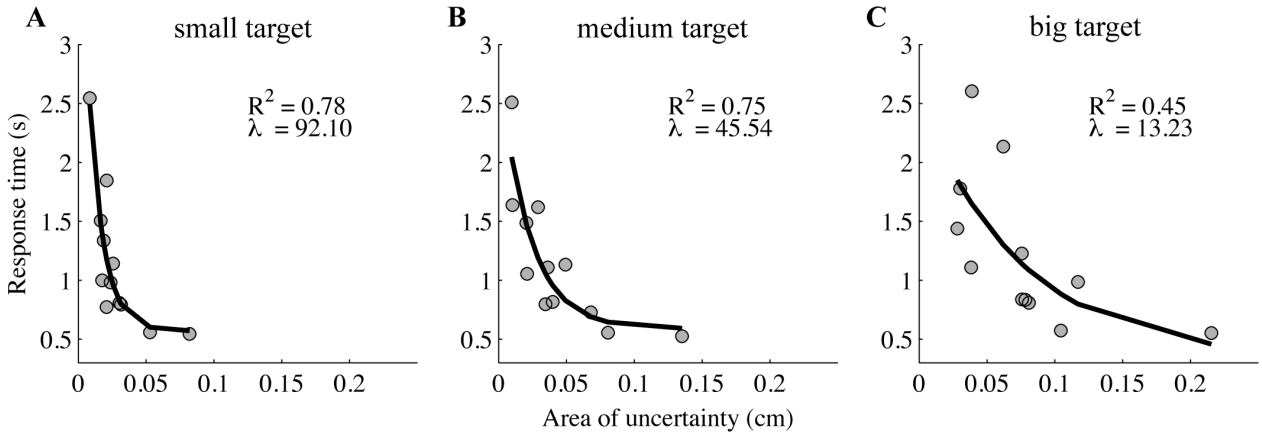

Figure 2.4 Response time in the area of uncertainty as a function of the area of uncertainty. The response time decays exponentially as a function of the area of uncertainty, and the decay increases with the increasing target size (the small **(A)**, medium **(B)**, and big target **(C)** are represented in the left, middle, and right panel, respectively).

2.5 Discussion

2.5.1 Summarize findings

We investigated the role of context size, target-context distance, and (actual) target size on perceived target size using a staircase procedure. In accordance with our hypotheses, we found no significant illusion effect in 33 percent of the 27 applied parameter combinations. Whenever there was an illusion effect, all three factors affected the perceptual threshold. A target circle appeared bigger in only two out of 27 conditions (i.e., 7 percent), namely, when presenting a small or medium target with small context circles at a small distance. In all other cases (i.e., 60 percent) the target appeared smaller. The area of uncertainty grew with a growing target size and with a decreasing target-context distance. Furthermore, the response time increased whenever context circles surrounded the target, and with increasing target size. The response time correlated positively with the illusion magnitude, but opposing our prediction, correlated negatively (but weakly) with the area of uncertainty.

Illusion magnitude

Massaro and Anderson (1971) formulated an equation according to which the illusion effect scales positively with target size. In accordance therewith, the authors reported two experiments that both showed increased illusion effects as a function of increasing target size (more specifically, 1.3, 1.5 and 1.7 cm). Our findings are in agreement with theirs, and we showed that this effect holds for a wider range of target sizes (namely, 0.5, 1.0, and 2.0 cm).

Nemati (2009) argued that illusionary effects of the Ebbinghaus figure are the result of a combination of a size contrast effect and the area of empty space (i.e., the area of the stimulus that is not filled by the context). The size contrast effect holds that smaller or bigger context circles, relative to the target, cause an overestimation or underestimation, respectively, of the perceived target size due to contrast mechanisms (Massaro and Anderson, 1971). If so, our findings should reflect only size contrast effects since we controlled for the empty space area by covering 75 percent of the circumference in all stimulus configurations. In accordance with Roberts et al. (2005), we reported, however, that small context circles did not always make the target appear bigger (i.e., only in 22 percent of the cases a target with a

small context was perceived as being bigger). That is, the Ebbinghaus figure cannot be reduced to 'just' a size-contrast effect in which a target is always perceived as being bigger when the context is smaller than the target size. In other words, we oppose earlier work describing magnifying and reducing effects of the smaller and bigger surround on a target, respectively (Obonai, 1954; Massaro and Anderson, 1971).

As compared to Roberts et al. (2005), fewer parameter combinations resulted in positive illusion magnitudes (i.e., overestimation of target size) and, furthermore, the absolute maximum illusion magnitude was bigger. Differences in the direction and size of the illusion effect could possibly be explained by the different target sizes (Roberts et al., 2005 employed target sizes of 1.05 and 1.4 cm whereas we used 0.5, 1.0 and 2.0 cm), since target size played a big role in the size of the illusion magnitude, and interacted with target-context distance and context size.

Target-context distance has been suggested to be more important than the size-contrast effect for the illusion magnitude (Im and Chong, 2009). This suggestion, however, is not supported by our results: although a significant effect of target-context distance on illusion magnitude was found, this effect was weaker than the effect of context size and target size.

Whereas a target-context distance larger than 1.9 cm (3.5 degrees) was found to decrease the perceived target size (Roberts et al., 2005), a small target-context distance (0.3-1.2 cm in Girgus et al., 1972) has been shown to increase the perceived target size (Girgus et al., 1972; Oyama, 1960). That is, perceived target size seems to reveal an inverted u-shape as a function of context distance. In line therewith we found increased perceived target sizes for small distances (0.8 and 1.6 cm for the small and medium sized target, respectively) when combined with a small context whereas a distance of 1.4 cm in combination with a small context size did not result in an increased perceived target size. For all other target-context distances (i.e., 2.0 to 4.2 cm), if there was an effect, the perceived target size was smaller than the actual target size. However, this was also the case for the smallest target-context distance for the biggest target (2.4 cm). In fact, the largest target was never perceived as being bigger, which could be due to the target-context distances that for this target size always exceeded the 0.3-1.6 cm range, or other protocol variations (*a, b* in figure 2.1).

An increase in distance up to 3.6 cm (all conditions except the large distance – large target condition) resulted in a larger illusion magnitude. A distance greater than 3.6 cm (i.e., 4.2 cm; large distance – large target) reduced the illusion magnitude (see Figure 2.2B), which could explain the interaction effect between target size and target-context distance. That is, these findings agree with an inverted u-shape of the illusion magnitude over target-context distance. This might stroke with what Sarris (2010) called Ebbinghaus' law of relative size-contrast, in which he describes a general inverted u-shape trend for size-contrast effects. (Note, though, that Ebbinghaus pointed at the relative size comparison of dwarfs, men and dolls; Ebbinghaus and Dürr, 1902; Sarris, 2010). However, to confirm this hypothesis, a broader range with smaller and larger target-context distances should be tested.

We did not find a significant interaction effect between target-context distance and context size. In Roberts et al. (2005), this interaction was tested for in two experiments. In their experiment 3, which was similar to our experiment – they reported an illusion magnitude from 0.084 to 0.12 cm for a target size of 1.4 cm, a context size of 0.35 and 1.4 cm, and a target-context distance of 1.05 to 4.67 cm – the interaction turned out to be significant whereas in the other (experiment 1) it did not. Our results indicate that the illusion magnitude was affected by target-context distance and context size in a similar fashion (illusion magnitude of 0.1 - 0.13 cm for target size 1 and 2 cm, context size 0.2 – 3.6 cm, and a target-context distance of 1.6 - 4.2 cm).

Area of uncertainty

We quantified the distance between the points as asymptotically reached by the upward and downward staircases, and refer to it as the area of uncertainty. The area of uncertainty represents a measure of the perceptual distinctiveness of the illusion. We showed that it increased as the target size increased. This might be a simple demonstration of Weber's law (or the Weber-Fechner law) according to which sensitivity to changes in perception decreases when stimulus intensity increases (i.e. the ratio between the 'just-noticeable difference' in a physical property and its magnitude is invariant). Schmidt et al. (1979) proposed that variability (in force production) would increase proportionally with the absolute magnitude (of the

forces) (Schmidt et al., 1979). Along the same line, it might be that the variability represented by the area of uncertainty scales linearly with target size. Interestingly, it has been shown that internal noise increases with letter size (Pelli and Farell, 1999). It may well be that our scaling of target size similarly increased internal noise. In that regard, investigating variations in internal noise as a function of the various Ebbinghaus figure parameters (Figure 2.1A), as well as relative to control conditions, may well shed novel insights into the (strength of the) illusion effect and its perceptual distinctiveness.

The increase of the area of uncertainty confirms the use of a minimum of two staircases and shows the directionality imposed by the procedure. By taking the mean of the two staircases, information about the distance between these two staircases is lost, even though this contains valuable information about the perceptual and decision-making processes, and thus the illusion effect.

Response time

Our response time data showed a complex effect of the illusion. First of all, the response time in the control conditions was unaffected by target size, which stands in contrast to reports of an inverse relation between target size and reaction time (Marzi et al., 2006; Osaka, 1976; Payne, 1967). The illusion conditions, however, showed two contrasting effects: the influence of target size on the response time (response time increased with target size; Figure 2.3C), and the influence of target-context distance on the response time (response time decreased with increasing target-context distance; Figure 2.3B). Furthermore, the response time correlated positively (but weakly) with the absolute illusion magnitude and negatively with the area of uncertainty. Since, to our knowledge, most of the Ebbinghaus studies neglected the response time, we can only refer to a study with schizotypal traits in which the authors measured the illusion magnitude and the response time of two Ebbinghaus figures (small and big context circles with a fixed target size and target-context distance; Bressan and Kramer, 2013), and reports of simple reaction time studies (Sperandio et al., 2010). Whereas Bressan and Kramer found that individuals with a longer response time tended to show less illusion effects (Bressan and Kramer, 2013), others reported that the reaction time was shorter when the target appeared

bigger/longer (Sperandio et al., 2010; Ponzo illusion: Plewan et al., 2012). We found that strong illusion effects went hand in hand with long response times. Thus rather than being scaled according to the perceived target size, we found that the response time scaled with the (absolute) illusion magnitude. It may be that, at least to some extent, these discrepancies are due to methodological differences: in the reaction time studies quickness of response was stressed and the illusions were presented briefly only (ranging from 10 to 250 ms), unlike our study. Regardless, the question remains what the origin of the increase in response time is, and how response time and illusion magnitude causally relate (if so). Given the widely accepted view that response time somehow reflects the cognitive processes involved in a given performance, and the more easily comprehendible effects relative to the control condition and the moment of assessing it (i.e., baseline versus the area of uncertainty), we believe that response time, which is typically discarded in studies using visual illusion as a means to investigate the ventral-dorsal visual pathway distinction, may provide an interesting novel entry point to its effects. We will return to this issue in the section below.

2.5.2 Models describing the Ebbinghaus illusion

Until now it has not been possible to predict the illusion magnitude given a certain set of parameters. Massaro and Anderson (1971) and Roberts et al. (2005) described a simple model of the Ebbinghaus illusion. The model developed by Massaro and Anderson (1971), to which they refer as judgmental model, is based on the idea that the Ebbinghaus figure works as a simple size-contrast illusion with a fixed number of context circles. They did not take into account that the completeness of the surroundings would influence the illusion magnitude as Roberts et al. (2005) have shown (Massaro and Anderson, 1971; Roberts et al., 2005). Nemati (2009) extended the hypothesis of Massaro and Anderson (1971) with the idea that the area of empty space influences the magnitude and direction of the illusion effect. By controlling for the completeness of the surroundings, as in Roberts et al. (2005), we controlled for differences in the empty space. The sole remaining explaining factor, thus, would accordingly be the size-contrast effect. As said above, this was not the case. Roberts et al. (2005) proposed a model according to which the illusion magnitude scales

exponentially with inducer distance. Their model could not explain our data in 78 percent of all factor combinations. We incorporated three times the number of participants, and should therefore have shown an exponential decaying trend if the model would have been correct.

In that regard, a potential shortcoming of existing models is that they do not allow for non-linear effects like hysteresis, multi-stability, etc. Dynamical systems are described in the space spanned by its state variables. If one stable solution exists in that space (an attractor), the system will invariantly evolve towards it. If multiple stable solutions exist (multi-stability), it will evolve towards one of the attractors, dependent on the initial conditions. In a bifurcation, the number and/or nature of the system's solution changes when the so-called bifurcation parameter is (gradually) scaled. Hysteresis only occurs in multi-stable systems, and refers to the phenomenon that when changing a bifurcation parameter the system's history determines to which stable attractor the system will evolve. Such effects are the hallmark of nonlinear systems, and evidence that behavioral, perceptual, and cognitive systems belong to that class of nonlinear systems abounds (Haken et al., 1985; Tuller et al., 1994; van Gelder, 1998; Kelso, 1995). Our present results only hint at the existence of nonlinear effects (note that the experiment was not designed so as to reveal them). The response time data and, in particular their exponential decay as a function of the size of the area of uncertainty (Figure 2.4), may provide indications that are consistent with nonlinear effects. Within the borders of the area of uncertainty, the responses are at chance level. Outside this area of uncertainty the participants perceive a clear difference between the target and the probe. This observation is open to interpretation in terms of the existence of two distinct 'states' or regimes (multi-stability). In this sense, the borders of the area of uncertainty are linked to the bistability regime of the coexistent two distinct states (see Figure 2.5). They are, however, not synonymous therewith. Intuitively, it makes sense to assume that response time scales with the degree of (perceptual) uncertainty. Consequently, the shorter an observer's distance to the area of uncertainty, the slower her/his response. In the present staircase procedure, the participants' initial conditions were the same, but the size of their area of uncertainty varied. In other words, their distance to the

area of uncertainty, which scales inversely with its size, was different (see Figure 2.5). Consistent with our present argument, the results in Figure 2.4 indicate an exponential relation between the size of the area of uncertainty and response time. For the argument to hold, however, a similar trend should exist for the participants individually. We tested this in two ways: first, for each participant we calculated the distance to the area of uncertainty for the upper and lower staircase and the corresponding response times for the second response. For most of the participants (11 out of 12), the distance was larger for the upper staircase and the response times were shorter. Both effects were significant (paired *t*-test; both $p<.001$). Second, we linearly regressed each participant's response times against the distance to the area of uncertainty. Unfortunately, due to the high variability, only three out of twelve regressions were significant at $a = .05$. Their average slope was -1.23. Regardless, all regressions had a negative slope; the mean slope of the non-significant regressions was -0.49. That is, across participants the response time tended to decrease as the area of uncertainty increased. In combination, these results argue in favor of a relation between the distance to the area of uncertainty and response time, and are suggestive of the existence of distinct regimes of operation. Clearly, however, future efforts will be needed to either falsify or reject this idea.

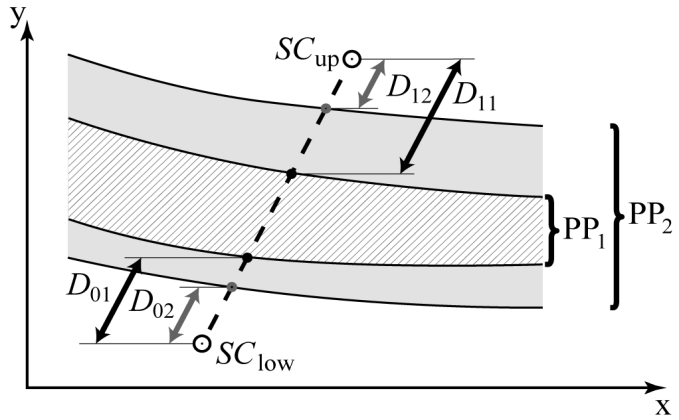

Figure 2.5 Cartoon illustration of the Ebbinghaus figure parameter space. PP_1 and PP_2 contain the area of uncertainty for two different participants; the black (D_{01}, D_{11}) and grey arrows (D_{02}, D_{12}) represent the corresponding distances to the area of uncertainty from the start of the two staircases (SC_{up}, SC_{low}), respectively. The non-shaded versus shaded areas (PP_1, PP_2) may represent distinct regimes in parameter space in which perceptual decision-making is deterministic versus random, respectively.

2.5.3 Illusion effects in motor tasks

The combination of an increased illusion magnitude, standard deviation (as suggested by visual inspection of Figure 2.2B and 2.2C), and the increase in response time as target size and, concomitantly, the area of uncertainty decreased, might indicate that strong illusion effect evoking parameters induce instability in the participants' decision-making. But which processes underlie this change in stability is uncertain. As discussed in section 4.2, possibly the area of uncertainty and the longer response time hint at hysteresis. If hysteresis indeed exists, then the mechanism underlying the change of strength of the illusion effect is linked to multistability and transitions from one state to another. The parameter space in figure 2.2 offers a starting point to develop experimental paradigms, in which the Ebbinghaus illusion is used to drive parametrically coordination behavior through a "perceived" parameter such as size in contrast to the "physical" parameter, the actual size. It should be noted, however, that it should not be naively assumed that the parameter space of the illusion effects in figure 2.2 is the same, when the Ebbinghaus illusion is used in sensorimotor coordination experiments. This assumption holds, from the dynamical system perspective, only for weak coupling of the perception-action system. Weak coupling means that two dynamic systems, when coupled, display the same qualitative dynamics as in absence of coupling, and undergo changes that can be regarded as small perturbations. For instance, two systems that display oscillations in absence of coupling can realize arbitrary relative phase relations; when weakly coupled, they still display oscillations, but now only certain relative phase relations are stable, others unstable. For strong coupling, the intrinsic oscillation may disintegrate and different behaviors may occur that cannot be understood anymore through the notion of relative phase. This limitation should be kept in mind when developing applications of the Ebbinghaus illusion parameter space, in which the perception-action coupling, if strong, may alter the system dynamics significantly.

How visual illusion figures affect perception and action has previously been shown to be a complex puzzle, and highly depending on the research method and selected parameters (Bruno and Franz, 2009). In the present perceptual study, the

effect sizes and direction of the effects resulting from the perception of the Ebbinghaus figure appeared to be highly dependent on the selected parameters. Observed illusion effects, if present, up to (exceptionally) ten percent of the target size might explain why illusion effects in motor tasks have sometimes failed to materialize.

Fitts' law predicts the time required to rapidly move between two targets as a ratio of the width of the target and the distance to the target (Fitts, 1954). The Ebbinghaus (like) figure has been implemented in a Fitts' task to test whether a perceptual illusion would affect the motor behavior (Ellenbürger et al., 2012; van Donkelaar, 1999; Fischer, 2001). Van Donkelaar (1999) and Ellenbürger et al. (2012) found that movement was affected by the illusion (in terms of movement time (Van Donkelaar, 1999), dwell time, and harmonicity (Ellenbürger et al, 2012)). However, Van Donkelaar and Ellenbürger and colleagues did not quantify the illusion magnitude of their Ebbinghaus figures. In contrast, Fischer (2001) found an effect of context size and context-target distance on perception but no effect on movement (at least, in the absence of stimulus-movement delays). The perceptual effects, while significant, were rather small; they ranged from -0.3 to 0.2 mm, that is, about an order of magnitude smaller than the range reported here. It remains to be seen, however, to which degree the method used by Fischer to quantify the illusion effect on perception, namely scaling a probe until it matches the perceived target size, provides robust results (see also Introduction). In fact, we found no illusion effect in 33 percent of the parameter combinations for a similar target size as in Fischer's study (1 cm versus 1.2 cm, respectively). Thus, if the reported perceptual results fail to be robust, the results of Fischer's movement study might simply be due to the lack of illusion effects. Furthermore, since the illusion magnitude was often found to be relatively small, it might be that the measures used for motor studies were too coarse to capture small effects of the illusion. In conclusion, studies like these hamper drawing firm conclusions on how perceptual and motor effects relate, and to what degree the ventral and dorsal stream operate in a functionally distinct manner.

2.5.4 Methodological concerns

Both the Ebbinghaus figure and the staircase procedure can be adapted by changing numerous parameters such as parameters *a, b, c* in the Ebbinghaus figure (Figure 2.1A), and the (adaptive) stepsize, procedure, starting point, and number of reversals for the staircase procedure. Due to the contradictory results of various methods to quantify the illusion effect, and due to the large number of Ebbinghaus figure configurations tested in this study, the widely studied and applied two-up, one-down staircase procedure was chosen, which is a two alternative forced choice method (2AFC). Several previous studies also applied the staircase procedure to study different features of the Ebbinghaus figure (Roberts et al., 2005; Im and Chong, 2009; McCarthy et al., 2013). Another version of the 2AFC method to study perception is the method of constant stimuli, in which a fixed number of combinations of (Ebbinghaus) figures are shown a certain number of times in a random order. In this case, the sampling is random and every possible stimulus-pair combination is presented equally often. This method allows for the full sampling of a so-called psychometric function. The slope and the horizontal shift of this psychometric function (i.e. a cumulative probability distribution) and the X_{50} value (also called the Point of Subjective Equality) then specify the illusion effect. A big area of uncertainty might be linked to a shallow slope of the psychometric function, and the perceptual threshold should be equal to the point of subjective equality. McCarthy et al. (2013) have performed 4 experiments with using both the staircase procedure (experiment 2) and the method of constant stimuli (experiment 1, 3 and 4) showing that both methods result in similar points of subjective equality. Considering the long history of staircase procedures in the field of psychophysics (García-Pérez, 1998), and the magnitude of the illusion effect being in a similar range as in the similar study of Roberts et al. (2005) the staircase procedure opens new doors in order to quantify the Ebbinghaus illusion effect in a systematic way.

Clearly, this method has its own limitations and assumptions. For example, to which percent-larger responses (referred to as percent-correct responses in visual contrast and luminance studies) the staircases converge using different protocols, is still under debate (for a review see: García-Pérez, 1998). At chance level, a two-up, one-down procedure will bias responses in the 'up' direction rather than the 'down'

direction. However, a two-up, one-down procedure also assures a better precision than a one-up, one-down procedure (García-Pérez, 1998). Two staircases that start from positions bigger and smaller than the actual target size, assure a fully symmetrical procedure, and a bias in both the 'up' and 'down' direction, for the upper and lower staircase respectively. Anyhow, regardless these limitations, visual illusion research, be it in the context of the visual stream dissociation or otherwise, may benefit from these (and potentially other) more or less standardized and in-depth investigated methods.

2.5.5 Conclusion

Concluding, since the Ebbinghaus figure is widely used but no clear rule is set, inter-comparison of the broad range of parameters remains difficult. We haven shown that the illusion magnitude highly depends on an interplay of target size, context size and target-context distance, and that a third of the parameter combinations here used did not evoke an illusion effect. Importantly, however, even if the group-averaged illusion magnitude can be predicted by a set of stimulus configuration parameters (or established rules), the predictive value for individual performances would likely be limited given the marked inter-individual variability. Thus, the implementation of the Ebbinghaus figure in various fields of research needs to be handled with care and quantified per study.

Chapter 3 – *Action* : Does changing Fitts' index of difficulty evoke transitions in movement dynamics?[3]

"Take action! An inch of movement will bring you closer to your goals than a mile of intention."

- Steve Maraboli

3.1 Abstract

The inverse relationship between movement speed and accuracy in goal-directed aiming is mostly investigated using the classic Fitts' paradigm. According to Fitts' law, movement time scales linearly with a single quantity, the index of difficulty (*ID*), which quantifies task difficulty through the quotient of target width and distance. Fitts' law remains silent, however, on how *ID* affects the dynamic and kinematic patterns (i.e., perceptual-motor system's organization) in goal-directed aiming, a question that is still partially answered only. Therefore, we here investigated the Fitts' task performed in a discrete as well as a cyclic task under seven *IDs* obtained either by scaling target width under constant amplitude or by scaling target distance under constant target width. Under all experimental conditions Fitts' law approximately held. However, qualitative and quantitative dynamic as well as kinematic differences for a given *ID* were found in how the different task variants were performed. That is, while *ID* predicted movement time,

[3] Published as Huys R, Knol H, Sleimen-Malkoun R, Temprado J-J, Jirsa VK (2015) Does changing Fitts' index of difficulty evoke transitions in movement dynamics? EPJ Nonlinear Biomed. Phys. 3:8. doi: 10.1140/epjnbp/s40366-015-0022-4

its value in predicting movement organization appeared to be limited. We conclude that a complete description of Fitts' law has yet to be achieved and speculate that the pertinence of the index of difficulty in studying the dynamics underlying goal-directed aiming may have to be reconsidered.

3.2 Introduction

More than 60 years ago, Paul Fitts initiated a novel paradigm when he asked participants to cyclically move a stylus between two targets characterized by a width W and separated by a distance D (Fitts, 1954). By systematically varying D and W, he found that movement time MT related linearly to the ratio of D and W, $MT = a + b \times \log_2(2D/W)$. This linear relation, now known as Fitts' law, was next found to hold also for discrete aiming (Fitts and Peterson, 1964). In Fitts' law, the index of difficulty $ID = \log_2(2D/W)$ quantifies task difficulty as an informational quantity in bits (Fitts and Peterson, 1964; Shannon and Weaver, 1949). Over the years, several authors have voiced criticism as to the functional form of the scaling of MT with ID as well as on whether the ID as formulated by Fitts is the most appropriate one (MacKenzie, 1992; Meyer et al., 1988; Schmidt et al., 1979; Guiard, 2009; Welford et al., 1969). Regardless, few will debate that as a first approximation, MT scales linearly with the ID, which has been repeatedly shown in discrete and cyclical performances alike (Buchanan et al., 2006; Guiard, 1997; Mottet and Bootsma, 1999; Sleimen-Malkoun et al., 2012; Smits-Engelsman et al., 2006).

Fitts' law, however, is silent on how the movements' organization changes as the ID is scaled. In addressing this issue, one prominent class of models (sub-movement models) focuses on the presence and features of primary and corrective secondary (and sometimes more) sub-movements as a function of W and D (Crossman and Goodeve, 1963; Meyer et al., 1988; Schmidt et al., 1979). The features associated with these movements, and those that deemed most relevant, are typically scalar variables (duration, [average] velocity, proportion of corrective movements, etc.).

Another prominent class of models (dynamical models) seeks to understand how the movements' kinematic and underlying dynamics change when *D* and/or *W* are systematically changed. In this case, the focus is geared towards trajectories in the Hooke's plane and/or phase space (Bongers et al., 2009; Guiard, 1993; Mottet and Bootsma, 1999), and the identification of the dynamics as observable in the latter (Huys et al., 2010a; van Mourik et al., 2008). In that regard, deterministic, autonomous, and time-continuous systems are unambiguously described by their flow in phase (or state) space (or vector field), i.e., the space spanned by the system's state variables (Strogatz, 1994). For movements along a single physical direction, as in a (sliding) Fitts' task, it is commonplace to use the movement's position and its time-derivative velocity as the state variables (Haken et al., 1985; Kay et al., 1987; Mottet and Bootsma, 1999) (but see (Daffertshofer et al., 2014; Kay, 1988) for a critical discussion). The attractors that may live in such two-dimensional spaces are limited to (different kinds of) fixed points (i.e., points where velocity and acceleration are zero) and limit cycles (nonlinear closed orbits), which are associated with discrete and rhythmic movements, respectively (Jirsa and Kelso, 2005; Schöner, 1990). Changing the system's parameter(s) modifies the phase flow, and may evoke a bifurcation (i.e., a change in the system's solution(s)). If so, the parameter is referred to as a control or bifurcation parameter. Grounded in this latter perspective, the present study aimed to identify the dynamics, and further characterize the movements' kinematics, when changing the *ID* by varying *W* and *D* independently, in both discrete and cyclic versions of Fitts' task.

In that regard, for the cyclic Fitts' task version it has been shown that gradually changing *ID* induces a gradual adjustment of the movement kinematics (Bongers et al., 2009; Mottet and Bootsma, 1999), albeit less so when changing *D* than when changing *W*. In the latter case, the gradual adjustment may evoke an abrupt transition in the dynamics underlying the performance (Huys et al., 2010a; Buchanan et al., 2004) via a homoclinic bifurcation (i.e., from a limit cyclic dynamics to (two) fixed points, each having one stable and one unstable direction [i.e., saddles]); (Huys et al., 2010a)). As hinted at, changing *ID* via target width *W* and distance *D* affects the aiming movement's velocity profiles differently (Guiard, 2009; Mottet and Bootsma,

1999; Thompson et al., 2007): increasing *D* mainly stretches the (bell-shaped) velocity profile, while increasing *W* renders it skewed (the deceleration phase lengthens relative to the acceleration phase). Thus, it is not clear if the scaling of *ID* per se induced the bifurcation in (Huys et al., 2010a) or if effectively the manipulation of *W* did so. For discrete task performance, the pattern of kinematic changes as a function of *ID* (including the *D* and *W* differentiation) yields some similarities with those observed in the cyclic task version (Sleimen-Malkoun et al., 2013, 2012). The discrete and cyclic task, however, are fundamentally different in that, in the former, but not the latter, movement velocity and acceleration must be zero before initiating the movement and upon ending it (Guiard, 1997). In this case, it seems self-evident to assume the existence of a fixed-point dynamics in the discrete task version. Various fixed-point dynamics scenarios, next to the above-mentioned connected saddles, are realizable, however. For instance, Schöner (Schöner, 1990) has proposed that a fixed point (at location A) vanishes so as to temporally give way to a limit cycle—causing the movement, after which the limit cycle vanishes and the fixed point (at location B) re-occurs. Alternatively, a fixed point may be driven through phase space, more or less continuously changing the phase flow so that the system is 'dragged behind it" (Perdikis et al., 2011). This scenario constitutes an interpretation of equilibrium point models (Feldman, 1986) in the framework of dynamical systems (Kugler et al., 1980). In this case, the trajectories in the phase space can be expected to be 'wiggly' and reveal little local convergence (i.e., overlaid trajectories can be expected to have a similar thickness throughout). Yet another possible realization involves a competition in which an active fixed point at location A vanishes while simultaneously another at location B comes into existence (Perdikis et al., 2011). Indeed, while the discrete Fitts' task must involve fixed points, what remains unknown is: i) whether they are similar under *D* and *W* induced *ID* scaling, ii) if *ID* changes evoke a transition between mechanisms, and iii) if the fixed points assumed in the discrete task are the same as those found for the cyclic (*W* induced *ID* scaling) cyclic task. In fact, for the cyclic task, it is not known either if a transition occurs if *ID* is altered via target distance *D*. Teasing apart the contributions of *D* and *W* to the scaling of the *ID* will allow us to investigate whether *ID*, which plays a primordial

role in the Fitts' paradigm, acts as bifurcation parameter or if effectively either *D* or *W* or both do so.

Based on the above reasoning, in the discrete task, we predicted to observe fixed-point dynamics under all conditions. Under the distance manipulation, for low *ID,* the (average) velocity can be expected to be very low. We therefore expected to find indications for the existence of a driven fixed-point scenario. For the cyclic task, in line with previous findings we predicted to observe a bifurcation from a limit cycle dynamics to a fixed-point dynamics with decreasing target width (Huys et al., 2010a). Finally, we expected to find evidence either for a limit cycle dynamics or the driven fixed-point at small target distances and time-invariant fixed points at large target distances.

We examined our predictions primarily by investigating the underlying Fitts' task performance under discrete and rhythmic task versions and identifying bifurcations (if existent). In addition, to further characterize task performance, we also extracted various kinematic features of the movements. Thereto, we designed a Fitts' task that was performed in the discrete and cyclic mode, and in which task difficulty was scaled via *D* and *W* separately in different sessions. We found that while *ID* predicted movement time, it did not uniquely predict the dynamics and kinematics associated with the task performances.

3.3 Methods

Thirteen (self-declared) right-handed participants (7 females; age: 29.3 ± 3.8 years) performed aiming movements from a starting point to a target (discrete mode) or between two targets (cyclic mode) with a hand-held stylus (18 g, 156.5 × 14.9 mm, ~1 mm tip) across a digitizer tablet (Wacom Intuos XL, 1024 × 768 pixel resolution) under instructions stressing both speed and accuracy. Position time series were acquired from the tablet via custom-made software (sampled at 250 Hz). The targets were printed in red on white A3 paper that was positioned under the transparent sheet of the tablet. In the *cyclic* mode, for each condition two trial repetitions

consisting of 50 horizontal reciprocal aiming movements each (i.e., 25 cycles) were performed in the transversal plane, once starting from the left target and once from the right target. In the *discrete* mode, four blocks consisting of 25 single aiming movements were performed twice; in two blocks movements were made toward a target positioned on the right side; in the two other blocks the direction was inversed. *Cyclic* trials with more than 6 errors and *discrete* blocks with more than 3 errors were redone (i.e., a 12% error rate was tolerated). In both task modes target *distance* and target *width* were manipulated independently, and chosen so as to allow for a large sampling of distance and width, respectively. In the *width* manipulation, target distance was set at 20 cm, and target width varied as follows: 4.20, 2.50, 1.49, 0.88, 0.53, 0.31, and 0.19 cm. In the *distance* manipulation, target width was set at 0.31 cm, and target distance was varied from 1.47, 2.48, 4.17, 7.01, 11.80, 19.84, and 33.37 cm. In both cases, this resulted in seven *ID*s (from 3.25 to 7.75, step size 0.75), which were administered randomly. Participants were familiarized with all task mode (discrete, cyclic) by manipulation (distance, width) conditions by performing 5 to 10 movements (until fast and successful performance) with *ID*=3.25 and *ID*=7.00. The familiarization ended when the participant reached a stable behaviour (i.e., moving fast and not missing the target). The *width* and *distance* manipulations were assessed in two experimental sessions lasting about 1½ hour each. Both the *width* and *distance* manipulations, as well as the *cyclic* and *discrete* tasks were counterbalanced across participants.

For the rhythmic movements, the peaks in the (horizontal) position time series were taken as movement initiations and terminations. The discrete movements' initiation and termination were defined as the moment its (absolute) velocity exceeded versus fell below 0.1 cm/s, respectively. For the termination, the additional criterion was used that the movement velocity had to remain below this velocity criterion for minimally 60 ms (Meyer et al., 1988). A secondary movement was deemed present if it lasted for minimally 100 ms, the velocity criterion was exceeded for at least half of the burst's time, and if the covered distance was minimally either 2 mm or ¼ of the target width. If present, the secondary movement's endpoint was taken as the movement's termination. (For movement time, we verified whether the inclusion of the secondary movement changed the patterns of results, which was not

the case.) Movement time (*MT*) was defined as the average of the temporal differences between movement termination and onset. For each movement, the acceleration duration (*AT*) was defined as the moment of peak velocity minus movement initiation. The ratio *AT/MT* ($R_{AT/MT}$) measures of the degree of symmetry of the movement velocity's profile. Effective amplitude (A_e) was computed as the average distance traversed across repetitions, and effective target width (W_e) as 2×1.96 times the mean standard deviation at the movement terminations (Kostrubiec et al., 2012). Next, effective *ID* was calculated as $ID_e = \log_2(2A_e/W_e)$.

In order to reconstruct the vector field underlying the movements (Plamondon and Alimi, 1997; Welford, 1968), we computed the conditional probability distributions $P(x,y,t \mid x_0,y_0,t_0)$ that indicated the probability to find the system at a state (x,y) at a time t given its state (x_0, y_0) at an earlier time t_0. These distributions were computed using all aiming movements in each condition using a grid size of 28 bins. Drift coefficients (i.e., the deterministic dynamics) were computed according to:

$$D_x(x,y) = \lim_{\tau \to 0} \frac{1}{\tau} \iint (x' - x) P(x', y', t+\tau \mid x, y, t)\, dx'\, dy$$

$$D_y(x,y) = \lim_{\tau \to 0} \frac{1}{\tau} \iint (y' - y) P(x', y', t+\tau \mid x, y, t)\, dx'\, dy$$

These coefficients are the numerical representations of the *x*-, and *y*-component of the vector at each phase space position. From these coefficients, we computed the angle θ_{max} for each bin between its corresponding vector and that of each of its neighbours (if existent), and extracted the corresponding maximal value in order to visualize the phase flows in terms of so-called angle diagrams (Huys et al., 2010a, 2008).

We performed a principal component analysis (PCA) to investigate trajectory variability (x,y). For each participant and condition all trajectories were resampled to 100 samples, and subjected to principal component analysis (Huys et al., 2010a). A PCA was done separately for the 50 left-to-right and 50 right-to-left aiming movements. The 1st eigenvalue l_1 was next averaged.

The ANOVA on ID_e showed multiple effects, we therefore created ID_e block averages of MT, $R_{AT/MT}$, θ_{max}, and l_1 that were subjected to a repeated measures ANOVA with *Task* (2), *Manipulation* (2), and ID_e (7) (i.e., a total of 28 conditions) as within participant factors. The Greenhouse-Geisser correction was applied whenever necessary. Significant main effects (α=.05) were followed up by Bonferroni-corrected post hoc tests. (For completeness, the same analyses were performed for acceleration and deceleration time, and peak velocity; they are reported in section 3.7 *Supplementary information*).

The protocol was in agreement with the Declaration of Helsinki. Informed consent was obtained from all participants prior to the experiment.

3.4 Results

What participants do in a Fitts' task typically (slightly) deviates from the imposed task constraints. That is, the produced end-point variability and movement amplitude do not map one-to-one on the task defined target width W and distance D. As commonly done, we therefore computed the effective amplitude and the effective target width (see *Methods*) and calculated the effective ID as $ID_e = \log_2(2A_e/W_e)$. We report our results based on the ID_e.

As a first step in our analysis, we examined how MT changed under the different experimental factors. MT was lower in the discrete task (mean±SD = 0.75±0.04) than in the cyclic task (mean±SD = 0.80±0.04; $F(1,12)=10.270$, $p<.01$, $h^2=.461$) and higher in the distance manipulation (mean±SD = 0.82±0.05) than in width manipulation (mean±SD = 0.73±0.03; $F(1,12)=23.975$, $p<.0001$, $h^2=.666$). The Task × Manipulation interaction ($F(1,12)=22.203$, $p<.005$, $h^2=.649$) showed, however, that the effect of Task only held for the distance manipulation (Figure 3.1A). As expected, MT increased with ID_e ($F(1.449,17.383)=148.827$, $p<.0001$, $h^2=.925$), but did so in a manner that interacted with Task ($F(2.903,34.842)=18.228$, $p<.0001$, $h^2=.603$; Figure 3.1B), and Task and Manipulation ($F(2.770,33.236)=3.376$, $p<.05$, $h^2=.220$; Figure 3.1C,D). For each task and manipulation combination we linearly regressed

MT against effective ID (for each participant), and investigated the regressions' slopes with a 2 (Task) × 2 (Manipulation) ANOVA. The average R^2 equalled .91 (±0.08). The slopes in the discrete task (mean±SD = 0.19±0.01) were smaller than in the cyclic task (mean±SD = 0.24±0.02; $F(1,12)=56.856$, $p<.0001$, $h^2=.826$), and those in distance conditions (mean±SD = 0.18±0.01) were smaller than those in the width conditions (mean±SD = 0.24±0.02; $F(1,12)=75.028$, $p<.0001$, $h^2=.862$). The significant Task × Manipulation interaction ($F(1,12)=6.929$, $p<.05$, $h^2=.366$) indicated that the effect of Manipulation was stronger in the cyclic task (mean±SD = 0.20±0.02 versus 0.28±0.02 for distance and width scaling, respectively) than in the discrete task (mean±SD = 0.16±0.01 versus 0.19±0.01 for distance and width scaling, respectively). Thus, both the task version (discrete, cyclic) and how *ID* was varied (via *D* or *W*) altered the rate of *MT* increase with ID. At the same time, as a first approximation, the linear relation predicted by Fitts' law held in all Task × Manipulation conditions.

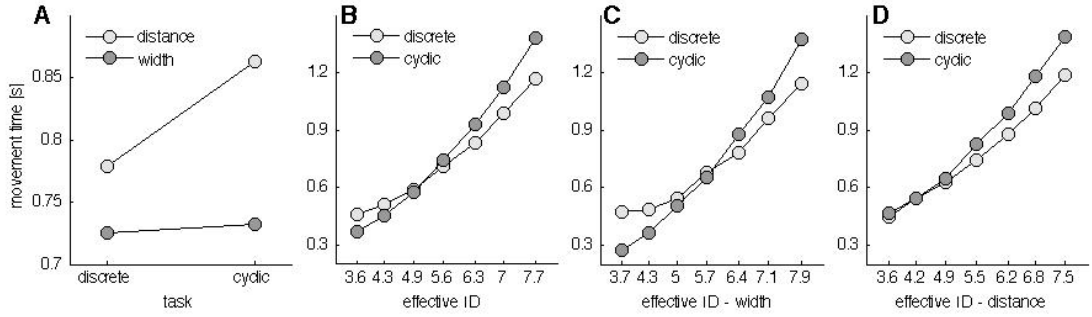

Figure 3.1 Average movement time. **(A)** MT it is lower in the discrete than in the cyclic task in the distance but not in the width conditions. **(B)** At low ID_e MT is higher in the discrete task than in the cyclic task, while at higher ID_e this is inversed. **(C)** This effect owes largely to the width conditions. **(D)** For distance, the cyclic MT equals the discrete MT at low ID_e but is (again) higher at high ID_e.

To investigate the dynamics associated with the movements in the various conditions, we computed the vector fields, and statistically analysed the maximal angle θ_{max} (Huys et al., 2010a). In that regard, each vector *k* in a vector field has (up to) eight neighbouring vectors whose direction relative to vector *k* can be represented

by an angle. θ_{max} represents the maximum of the angles of vector k with its neighbouring vectors. For θ_{max} > 90°, we consider that the movements in the corresponding trial pertained to a fixed-point dynamics. In almost all conditions, except for the cyclic-width condition at a low ID and for a few trials in the cyclic-distance condition, indications for the existence of fixed points in the target regions were found (see Figure 3.2 and Table 3.1). This observation was statistically corroborated by the ANOVA on θ_{max} (*Supplementary information,* Figure *S3.1*), which indicated that θ_{max} was higher in the discrete task (mean±SD = 171°±0.6) than in the cyclic one (mean±SD = 130°±3.5; $F(1,12)=123.893$, $p<.0001$, $h^2=.912$), and higher in the distance conditions (mean±SD = 160°±2.3) relative to those of width (mean±SD = 142°±1.4; $F(1,12)=99.556$, $p<.0001$, $h^2=.892$). As expected, θ_{max} became larger as ID_e increased ($F(3.765,45.180)=28.289$, $p<.0001$, $h^2=.702$). The distance versus width effect, however, was only observed for the cyclic task (Task × Manipulation, $F(1,12)=54.782$, $p<.0001$, $h^2=.820$). In addition, the increase of θ_{max} with ID_e occurred primarily in the width (Manipulation × ID, $F(3.010,36.126)=18.737$, $p<.0001$, $h^2=.610$) and in the cyclic conditions (Task × ID, $F(3.552,42.267)=43.048$, $p<.0001$, $h^2=.782$). Finally, the Task × Manipulation × ID interaction ($F(3.022,36.261)=9.456$, $p<.0001$, $h^2=.441$) showed that θ_{max} was high (>130°) and varied little only with ID_e in all task–manipulation combinations except for that of cyclic–width. Finally, as can be seen in Table 1 (see also *Supplementary information,* Figure *S3.2*), the number of participants in which fixed point were identified (in correspondence with the criterion outlined above) always equalled the total number of participant (i.e., n=13) in all discrete task conditions. In the cyclic-discrete task conditions, fixed points were always found for the higher ID_e. However, all but one (2 ID_e) or 3 participants (1 ID_e) did not show a fixed-point dynamics at low ID_e. Two of the participants that did not adhere to a fixed-point dynamics at ID_e = 4.9 were 'stand-alone' incidences. In one participant no fixed points were found for the first three ID_e's, that is, this participant's behaviour in all likelihood showed a true transition. In the cyclic-width task conditions, all participants showed a transition from a limit cycle dynamics to a fixed points dynamics with increasing ID_e, albeit at different ID_e. Thus, across the board (with a single exception), a limit cycle dynamics was operative in the cyclic–width condition at ID_e up to about 5.6, and that a fixed-point dynamics governed all other conditions.

Topologically, the vector fields of all conditions in which a fixed-point dynamics was identified were indistinguishable. For cyclic Fitts' task performance the gradual up-scaling of task difficulty, in particular through manipulation of target width, gradually increases the degree of system nonlinearity (Mottet and Bootsma, 1999). Figure 2 suggests that this was also the case for the discrete task performances (see also (Sleimen-Malkoun et al., 2012)). The degree of nonlinearity does not uniquely map onto a system's topological organization. Its evolution as a function of *ID*, however, does provide inside into the quantitative changes in the movement dynamics. We summarize these changes via $R_{AT/MT}$, which quantifies the degree of symmetry of the movement velocity profile. $R_{AT/MT}$ was lower in the discrete task (mean±SE = 0.35±0.02) than in the cyclic task (mean±SD = 0.39±0.04; $F(1,12)=28.982$, $p<.0001$, $h^2=.707$), but primarily so in the width conditions (Task × Manipulation ($F(1,12)=53.321$, $p<.0001$, $h^2=.816$; Figure 3.3A). In line therewith, $R_{AT/MT}$ was lower in the distance manipulation (mean±SD = 0.34±0.02) than in that of width (mean±SD = 0.39±0.01; $F(1,12)=36.564$, $p<.0001$, $h^2=.753$). At first glance, this latter finding appears to contradict established knowledge (Guiard, 2009; Mottet and Bootsma, 1999; Sleimen-Malkoun et al., 2012; Thompson et al., 2007); it is important to recall therefore, that in the present distance manipulation, the fixed target width was always very small (0.31 cm). As expected, $R_{AT/MT}$ decreased as ID_e increased ($F(2.205,26.458)=136.922$, $p<.0001$, $h^2=.919$). This decrease was stronger for discrete than for the cyclic conditions, and at high ID_e the task mode differences vanished (Task × ID; $F(2.908,34.899)=14.305$, $p<.0001$, $h^2=.544$; Figure 3.3B). Similarly, the interaction between Manipulation and ID ($F(2.068,24.822)=42.956$, $p<.0001$, $h^2=.782$) indicated that the manipulation differences vanished with increasing ID_e. Finally, the Task × Manipulation × ID interaction ($F(3.625,43.504)=7.302$, $p<.0001$, $h^2=.378$) indicated that $R_{AT/MT}$ decreased faster in the cyclic than in the discrete task mode with increasing ID_e for the width conditions but not so for the distance conditions (Figure 3.3 CD). Thus, the velocity profiles became more skewed with increasing ID_e (i.e., the nonlinearity increased). Whereas this effect was similar for both tasks in the

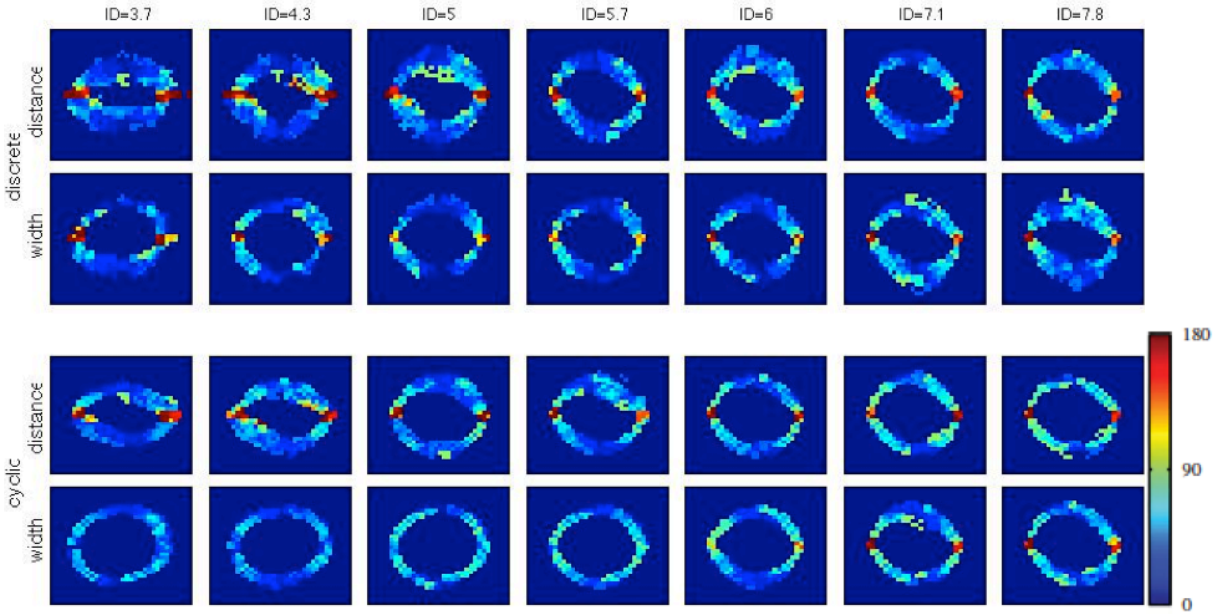

Figure 3.2 Angle diagrams. The upper versus lower two rows represent angle diagrams from a single participant of the discrete and cyclic mode, respectively. For both row pairs, the upper panels show the distance conditions while the lower ones display the width conditions. ID_e increases form left to right. The colour coding (at the right) represents the maximal angle between neighbouring vectors. Red areas indicate locally opposing angles, implying the existence of a fixed point. Their absence suggests the existence of a limit cycle.

distance manipulation, for the width manipulation the profiles were more symmetric at low ID_e in the cyclic task than in the discrete task. This latter difference vanished as in both task modes the profiles became more asymmetric (i.e., the movements became more nonlinear).

Table 3.1 Number of participants for whom fixed points were identified per condition.

		IDe						
		3.6	*4.3*	*4.9*	*5.6*	*6.3*	*7.0*	*7.7*
Task	***Manipulation***							
Discrete	Distance	13	13	13	13	13	13	13
	Width	13	13	13	13	13	13	13
Cyclic	Distance	12	12	10	13	13	13	13
	Width	0	0	2	7	12	13	13

As indicated in the *Introduction*, we expected that under the distance manipulation at low *ID* a driven fixed point would govern the movements. In such a dynamic system, the phase space trajectories can be expected to be wiggly (and show little local convergence), and thus to be variable from one trial to the next. We therefore examined the trajectory variability using PCA (see also *Supplementary information* Figure *S3.3*), and subjected the first eigenvalue to an ANOVA. Please note that the more variable the trajectories are, the smaller the first eigenvalue is. In fact, the variance that is not accounted for by the first principal component is orthogonal to it so that the first eigenvalue can be interpreted as reflecting the degree of convergence towards the trajectory associated with the first principal component. Neither the effect of Task nor that of ID_e was significant (p>.1 and p>.05, respectively). In contrast, the trajectories were more variable (i.e., the 1st eigenvalue smaller) in the distance conditions (mean±SE =.76±0.01) than in those of width (mean±SE =.84±0.01; $F(1,12)=140.683$, $p<.0001$, $h^2=.921$). The Task × Manipulation interaction ($F(1,12)=17.132$, $p<.0005$, $h^2=.588$) indicated that the difference between task manipulations was larger in the cyclic task mode than in the discrete one. The significant interaction between Task and ID ($F(3.374,40.486)=26.453$, $p<.0001$, $h^2=.688$), Manipulation and ID ($F(2.713,32.559)=43.106$, $p<.0001$, $h^2=.782$), and Task, Manipulation and ID ($F(3.061,36.734)=7.385$, $p<.005$, $h^2=.381$) are displayed in Figure 3.4. In combination, these interactions showed that at low ID_e, the trajectory variability in the discrete task was larger than that of the cyclic task, which inversed at high ID_e (Figure 3.4A). Further, the trajectories were most variable at low ID_e in the

distance manipulation, and the variability decreased as ID_e increased (Figure 3.4B), The inverse was observed for the width conditions. The effect of increasing ID via target distance was comparable for both tasks (Figure 3.4CD). Decreasing target width, however, hardly affected the trajectory variability in the discrete task, but it led to an increased variability in the cyclic task. For the latter, at low ID_e, that is, when a limit cycle dynamics was invariantly present, the trajectories were the least variable in the entire dataset.

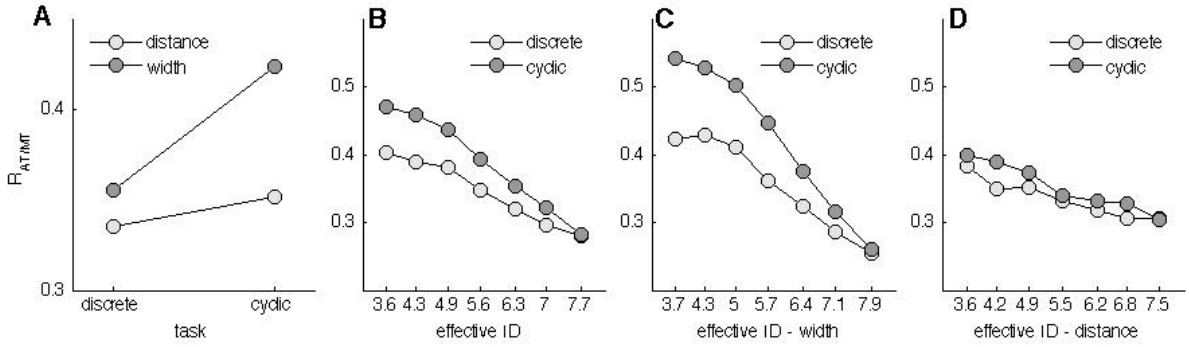

Figure 3.3 Ratio AT/MT. **(A)** The larger $R_{AT/MT}$ in the width condition relative to the distance conditions is most pronounced in the cyclic task mode. **(B)** At low ID_e $R_{AT/MT}$ is lower in the discrete task than in the cyclic task, while at higher ID_e $R_{AT/MT}$ is similar. **(C)** This interaction is due to the width conditions. **(D)** In the distance conditions $R_{AT/MT}$ is similar and decreasing with ID_e for both task modes.

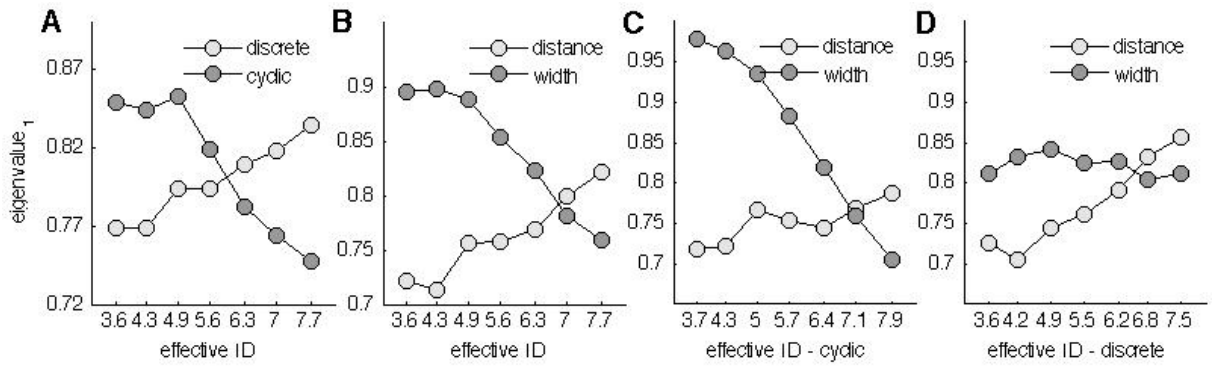

Figure 3.4 PCA: 1st eigenvalue. **(A)** Trajectory variability decreased with increasing ID_e for the discrete task mode whereas it increased in the cyclic mode (from the 3rd ID_e onwards). **(B)** Similarly, trajectory variability in the distance conditions decreased with increasing ID_e whereas that in the width conditions increased. **(C)** This effect, however, was most pronounced for the cyclic task. **(D)** In the discrete task trajectory variability in the width condition stayed about the same for all ID_e.

As for the movement organization under the different conditions, our results have revealed identical topological organizations (fixed-point dynamics) under all but the cyclic-width task version at low ID_e (and for one participant in the cyclic-distance task at low ID_e). At the same time, however, the discrete and cyclic task modes are set apart in terms of the degree of symmetry of movement velocities, and particularly, trajectory variability. By hypothesis, this distinction may imply that in the cyclic task mode, the dynamical organization (i.e., the phase flow) remains invariant throughout the entire trial, independent of whether a fixed-point or limit cycle dynamics is adhered to. For the discrete task mode, this will actually be the same. In this case, however, prior to and following each single aiming the movement-task organization will be (has to be) 'dismantled' (to return to the home position) and assembled for the execution of the next trial. Consequently, additional performance variability can be expected for the discrete task mode relative to the cyclic one as the trial-to-trial re-establishment of the movement organization adds a source of variability for the former task mode relative to the latter. In terms of Saltzman and Munhall's (Saltzman and Munhall, 1992) wording, additional variability in repeated discrete aiming relative to continuous cyclic aiming is introduced in terms of parameter

dynamics. We tested this hypothesis by focussing on the variability (through the coefficient of variation) of the variable central to Fitts' law, that is movement time. Consistent with the hypothesis, the movement time's coefficient of variation (CV_{MT}) was larger in the discrete task (mean±SD = 1.18±0.01) than in the cyclic one (mean±SD = 1.12±0.01; $F(1,12)=63.735$, $p<.0001$, $h^2=.842$), and also larger in the distance conditions (mean±SD = 1.16±0.01) than in the width conditions (mean±SD = 1.13±0.01; $F(1,12)=43.829$, $p<.0001$, $h^2=.785$). This latter effect was stronger in the cyclic than in the discrete task (Task × Manipulation; $F(1,12)=5.271$, $p<.05$, $h^2=.305$; Figure 3.5A). Further, CV_{MT} decreased with increasing ID_e ($F(4.306,51.667)=6.812$, $p<.0001$, $h^2=.362$); this effect, however, was confined to the discrete task (Task × ID; $F(3.201,38.417)=7.810$, $p<.0001$, $h^2=.394$; Figure 3.5B). Finally, the interaction between Manipulation and *ID* ($F(3.526,42.317)=55.529$, $p<.0001$, $h^2=.822$) indicated that at low ID_e, the CV_{MT} under the distance manipulation, which decreased strongly as ID_e increased, was almost twice as high as that under the width manipulation, which increased moderately as ID_e increased (Figure 3.5 C).

The pattern of intra-participant $R_{AT/MT}$ variability (coefficient of variation) strongly resembled that of CV_{MT}, and is reported in *Supplementary information S3.4*.

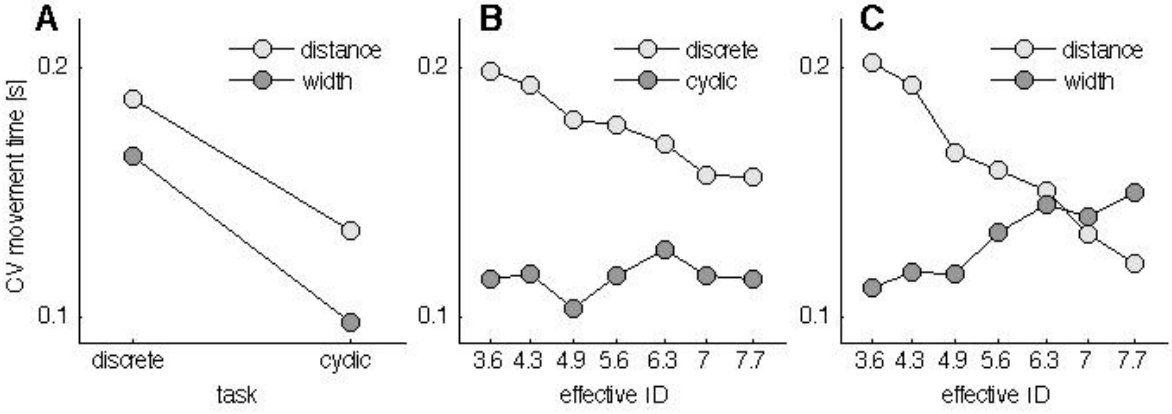

Figure 3.5 CV movement time. **(A)** The distance-width CV_{MT} difference is moderately stronger in the cyclic than in the discrete task mode. **(B)** In the *discrete* task CV_{MT} increases with ID_e whereas in the *cyclic* task it decreases. **(C)** In the *distance* conditions CV_{MT} decreases with increasing ID_e whereas in the *width* conditions it increases.

3.5 Discussion

In the present study, we investigated both the dynamics and kinematics underlying Fitts' task performance during discrete and cyclic task modes when ID was varied through distance and width independently. Most importantly regarding the dynamics, consistent with previous observations (Huys et al., 2010a), in the cyclic task setting, a transition from a limit cycle to a fixed-point dynamics occurred when scaling the ID via target width. In contrast to the expectation voiced in that study, a similar transition was not observed here when varying ID via the distance separating the targets. Indeed, varying target distance did not affect the observed movement's topology, at least not in the presently studied range. In this case, fixed points were found throughout the entire ID range (except for a few cases, mainly one participant). This result suggests that, in general, the index of difficulty *per se* does not uniquely dictate the dynamical organization of rapid aiming movements, thereby disqualifying as a bifurcation parameter. That function, however, appeared to be fulfilled by target width, even though only so for the cyclic task mode. Indeed, varying target distance did not affect the movement's topology observed, at least not in the presently studied range. It cannot be ruled out, however, that the smallness of the target (0.31 cm) under the present distance manipulations hindered the occurrence of a limit cycle dynamics (or any other; see below) at specific target distances.

Furthermore, trajectory variability changed in opposing direction with decreasing target width for the discrete and cyclic task. This observation seems hard to reconcile with the idea that the kinematic re-organization as a function of (varying) target width for both task modes is the same. That is, even if varying target width drives the sensorimotor system through a bifurcation when operating in the discrete task mode, it is unlikely that the bifurcation type matches the one observed in the cyclic task. Confirmation (or not) of this hypothesis, however, will require further investigation.

Concerning the effects on the movement kinematics, we found that how ID was varied (i.e., via D or W) as well as the nature of the task (i.e., discrete or cyclic)

had pronounced effects on the movement kinematics investigated. In that regard, it is often stated that scaling target distance versus its width 'simply' stretches the velocity profile or skews it, respectively (Guiard, 2009; Mottet and Bootsma, 1999; Sleimen-Malkoun et al., 2012). Here, we found that although increasing the ID by scaling target width reduced the degree of the movement's velocity profile more than under the distance scaling, the latter also reduced it (Figure 3.3B). Again, this may to some extent be due to the smallness of the target under the present distance scaling. By comparison, we here used a target width smaller than used by (Sleimen-Malkoun et al., 2012) and (Mottet and Bootsma, 1999) under a (modestly; relative to Guiard, 1997) larger distance scaling. A closer look at these studies, however, shows that while, indeed, the degree of asymmetry increases markedly more under the width than distance scaling. Categorically setting apart the effects of these variations in terms of skewing versus stretching the velocity profiles appears a simplification that does not do justice to the observations.

Further, the degree of asymmetry increased with decreasing target width. In that case, at low ID, the discrete movements were more asymmetric than the cyclic ones, while at high ID this difference vanished as for both task modes the asymmetry increased. The initial difference as well as the evolution can be understood when considering that discrete movements always contain a zero velocity and acceleration start and end point, which emerge at higher ID only for cyclic movements. Indeed, under the distance scaling, the symmetry reduction was similar for the discrete and cyclic task mode (Figure 3.3D), which was always governed by a fixed-point dynamics.

The effects of varying target distance versus width were not limited to the movement's velocity symmetry. Specifically, increasing target distance (under constant target width) reduced the movement's trajectory variability irrespective of task mode. As peak velocity also increases with increasing distance (*Supplementary information Figure S3.5*), this effect contrasts the signal-dependent noise perspective (Harris and Wolpert, 1998). Reasoning from a dynamical perspective, and assuming noise to be approximately constant, a reduction in trajectory variability may come

about by an increased (more or less local) convergence of the phase flows underlying the movements (i.e., an increased tendency of the vectors pointing towards a manifold in the state space) and/or by an increased contribution of the deterministic dynamics relative to the stochastic dynamics (i.e., an increased length of the vectors). Under this perspective, increasing the ID via target distance is likely to result in an increased flow convergence for both task modes, which indeed occurs (reduced trajectory variability; see Figure 3.2 and *Supplementary information* Figure *S3.4*). The marked reduction in inter-aiming movement time variability (CV_{MT}; Figure 3.5C) is consistent therewith. In contrast, varying ID via target width did not (globally) affect the trajectory variability in the discrete task mode, but resulted in a marked variability increase in the cyclic task mode: In these conditions, at low ID and governed by a limit cycle dynamics, trajectory variability was the lowest observed but it noticeably (but rather gradually) increased as the non-linearity increased ($R_{AT/MT}$; Figure 3.3D) and a fixed point dynamics was created (Figure 3.2).

We found support for the hypothesis that the variability across aiming movements is bigger in the discrete task mode than in the cyclic one. This might result from the dynamical organization (i.e., the phase flow) being more or less invariant throughout the entire trial, depending on the type of task: in the discrete task mode, the perceptual-motor system prepares the movement for each upcoming action (leading to more variability) while across repeated aiming movements (in the cyclic task mode), the dynamical organization is more invariant (less variable). To further investigate this interpretation, we calculated the Pearson correlation for the movement time variability (CV_{MT}) between all Task, Manipulation, and low and high ID condition pairs (NB: in order to obtain more data points, the lowest two ID conditions and the highest two ID conditions were taken together to form a 'low ID' and 'high ID' category). Our reasoning was that, if tasks share specific processes relevant for their (timed) behaviour, their variability ought to be correlated and, conversely, if not, no correlation is to be expected (Robertson et al., 1999). Accordingly, we expected that all correlations between pairs involving a discrete and cyclic condition would be non-significant, and that for the cyclic task the low ID –

width condition would show no significant correlation with any of the others as the dynamics in the former condition (limit cycle) differed from the latter (fixed points). As it can be appreciated in Figure 3.6, these expectations turned out to be correct. Further, for the rhythmic task, all pairs except for those involving the low ID – width condition turned out significant, which fits the observation of similar dynamics (fixed points) and the proposition of being governed by an invariant dynamics across repetitive aiming movements. For the discrete task, however, the correlations were less straightforward: the CV_{MT} of multiple pairs correlated, but not all did, and the 2 × 2 matrix was not symmetric. We therefore abstain from any further interpretations.

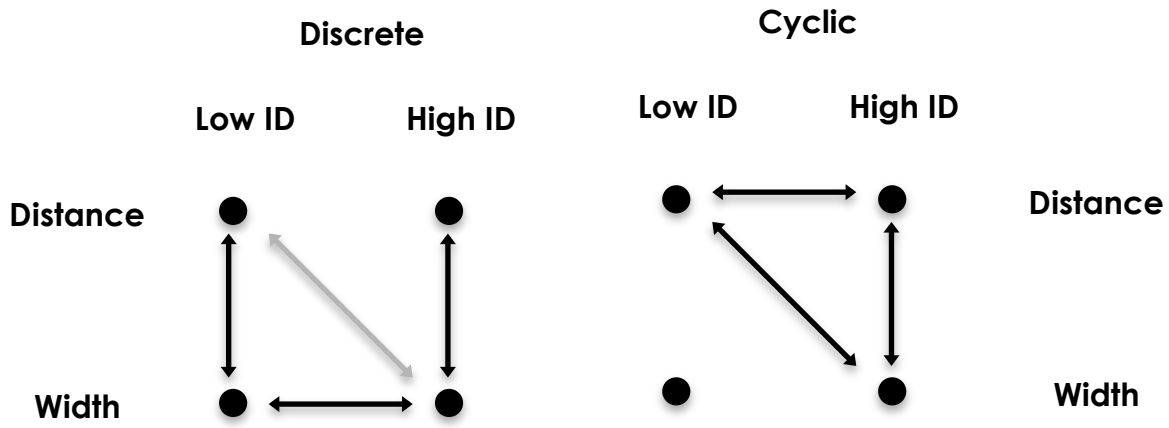

Figure 3.6 Pearson's correlation r for CV_{MT} between conditions. Black arrows indicate significant correlations ($p < .05$; across correlations $.41 < r < .70$), the grey arrow indicates a marginal significant correlation ($.1 < p < .05$; $r = .36$). The absence of arrows indicates that the correlation was not significant. No correlations between any of the discrete and cyclic conditions were found; within the cyclic task mode, no correlation was found between the low ID – width condition and the others. For the discrete task mode, several significant correlations were identified.

As discussed above, we found evidence that in a subset of these combinations limit cycle dynamics were observed, while in another subset, fixed points regimes were found. Some indications (not conclusive) were found that the nature of the fixed points might have been dissimilar in the later subset dependent on the experimental factors. Regardless, in all task and manipulation combinations,

movement time increased as the ID increased. That is, this trade-off appeared independent of the dynamical organization underlying Fitts' task performance. The question then arises of what could be the origin of the increase of *MT* with ID? The different models available in the literature do not provide satisfying answers in this respect. For instance, the dynamical model proposed by Mottet and Bootsma (Mottet and Bootsma, 1999) fails for discrete movements—for these an *N*-shape in the Hooke plane appears independent of ID. Similarly, models from the 'corrective (sub)movements class' ((Meyer et al., 1988; Crossman and Goodeve, 1963); see *Introduction*) fail to deal with performances in (at least a large part of) the limit cycle regime since no corrective sub-movements are made (acceleration is about highest around the targets, (Mottet and Bootsma, 1999)) but *MT* still gets larger with increasing ID. That is, while both models have their merits in their respective domains, neither of them is able to explain the MT increase with increasing ID across the range of task conditions that is reported here, and in the literature more at large.

3.6 Conclusions

Consistent with the Fitts' law, movement time scaled (approximately) linearly with the index of difficulty ID under all task and manipulation conditions. However, the system's functional organization underlying task performance differed both qualitatively and quantitatively as a function of task mode (cyclic vs. discrete) and manipulation (*D* vs. *W*). Within the cyclic task mode, low IDs were associated with limit cycles or fixed points dependent on whether target width or distance was manipulated, respectively. In this respect, target width was the parameter causing a bifurcation at a critical value. Conversely, for the discrete task mode, we did not observe such a bifurcation. Both behavioural modes adhere to distinct functional organizations; for instance velocity and acceleration always have to vanish at the target in discrete task mode. Consistent herewith, analysis of movement time variability (CV_{MT}) set apart the discrete and cyclic task mode, even for IDs in which both task modes appeared governed by a fixed-point dynamics. We argue that their difference is due to the inherent need for the perceptual-motor system to instantiate every single aiming in the discrete but not cyclic task mode, thereby introducing variability at another level of the perceptual-motor organization (i.e., that of the

parameter dynamics; (Saltzman and Munhall, 1992)). In addition, it cannot be ruled out that the nature of the fixed-points, or the space within which they exist, is dissimilar across both task modes and ID-manipulations. While our present data do not allow us to either conclusively refute or confirm this hypothesis, the differential trajectory variability evolution as a function of the task modes and distance versus width manipulation provides a hint thereto.

Regardless, the functional organization underlying task performance at various IDs varied markedly as a function of task mode and manipulation. In fact, our results counter the idea that change in a single parameter (as a function of ID) of the dynamics and/or bifurcation structure can account for Fitts' law. Explanations in terms of correction strategies, however, as discussed above, also have their limitations. That is, explaining Fitts' law in terms of a single dynamical organization or movement strategy remains problematic. In fact, this may indicate that a full description of Fitts' law may require more than one control (or bifurcation) parameter. The remaining question, then, is which one? We found evidence that target width, rather than task difficulty, acts as a control parameter. No clear indication was found that target distance did so too (except for a single participant) even though changing target distance had the opposite effect (of width) on trajectory variability. This may be due to a differential effect of the degree of convergence of the phase flow for both parameters. This, however, is of yet an open question. Regardless, this discussion resonates with previously expressed doubts as to whether the notion of task difficulty as quantified through target distance divided by width is appropriate. For instance, Welford and colleagues proposed a definition incorporating two additive logarithmic D and W terms (Welford et al., 1969). Further, task difficulty is insensitive to energetic cost (Guiard et al., 2011), which is higher at the easy task difficulty spectrum. Also, anecdotal reports from our participants suggest that subjective difficulty does not map uniquely onto the index of difficulty (the low ID small width-small distance conditions were experienced as particularly difficult). That is, the explicit identification of the nature of the fixed points in the various task conditions as well as the control parameter(s) implicated seems of a particular interest for the Fitts' paradigm. If a second control parameter indeed

exists, its identification may well alter the notion of task difficulty as currently understood.

3.7 Supplementary information

Maximal vector field angles θ_{max}.

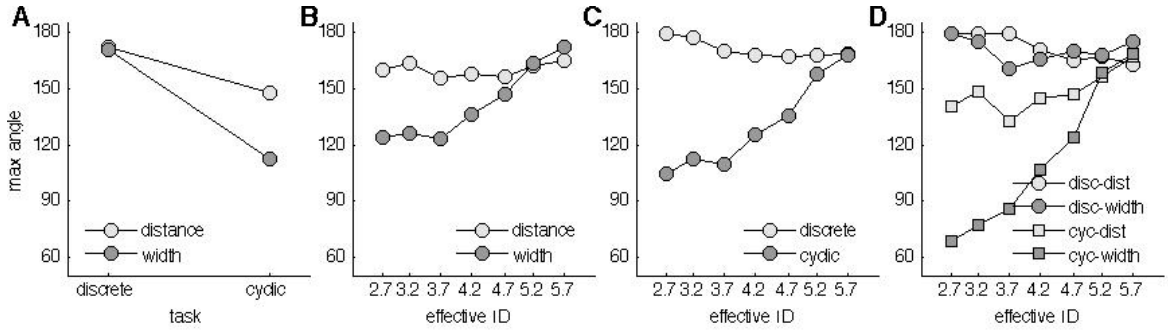

Figure S3.1 Maximal vector field angles. (**A**) θ_{max} is smaller in the width condition than in the distance for the *cyclic* task only. (**B**) In the *distance* conditions, θ_{max} is always large (>156°) while in the *width* conditions it was about 125° for the first three ID_e and then steadily increased to levels comparable to the *distance* condition. (**C**) In the *discrete* conditions, θ_{max} is always large (>168°) while in the *cyclic* conditions it was below 113° for the first three ID_e and then steadily increased to levels comparable to the *discrete* condition. (**D**) In both *discrete* tasks (*distance*, *width*) θ_{max} is high (>160°), while in the *cyclic* task θ_{max} is smaller at low ID_e, in particular for the first three ID_e in the *cyclic* conditions (< 90°).

Classification of dynamics for the cyclic task.

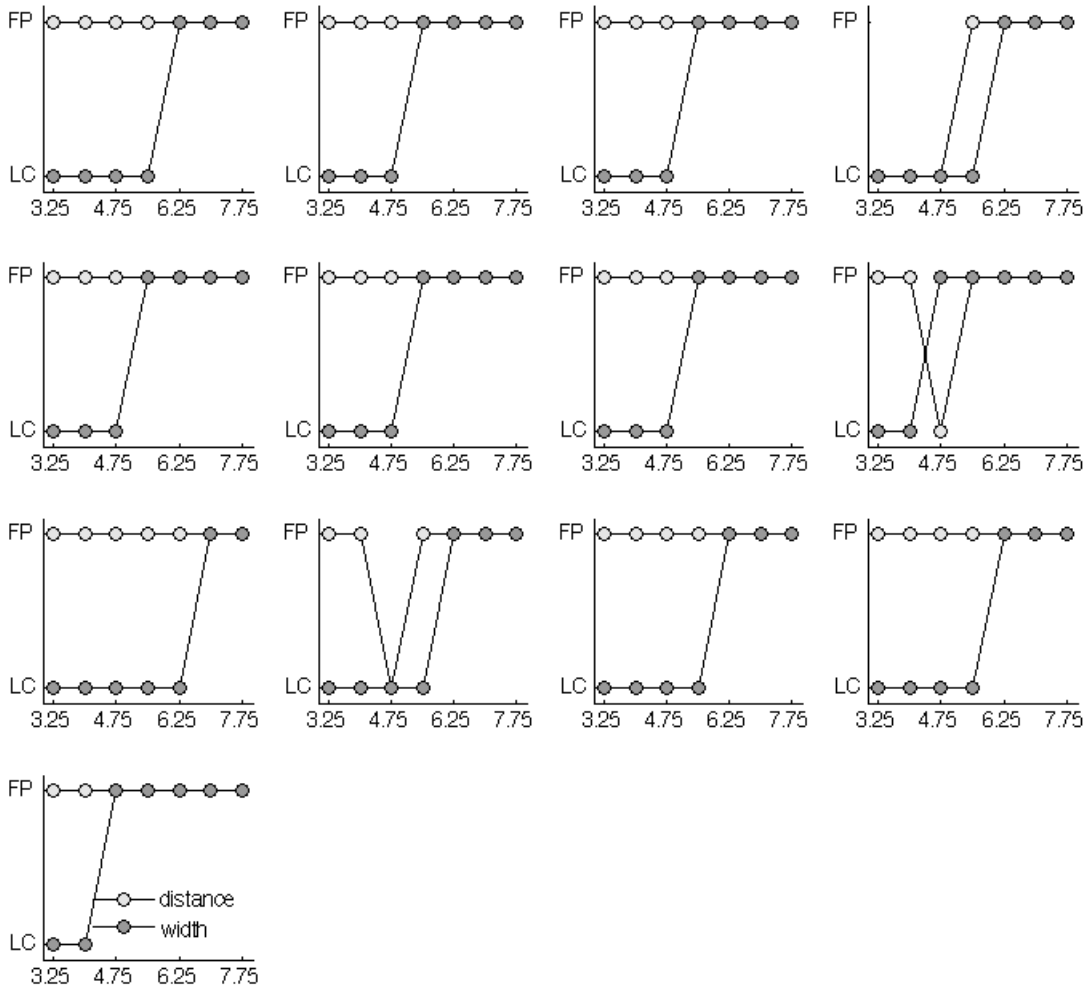

Figure S3.2 Identified attractor structures in the cyclic task for the width and distance conditions. White dots represent conditions in which fixed points were identified (θ_{max} > 90°; see main text); gray dots represent conditions in which a limit cycle was identified (legend in the lower panel only). The horizontal axis displays ID, the vertical axis sets fixed point trials ("FP") and limit cycle trials ("LC") apart. Each panel contains the data of one participant.

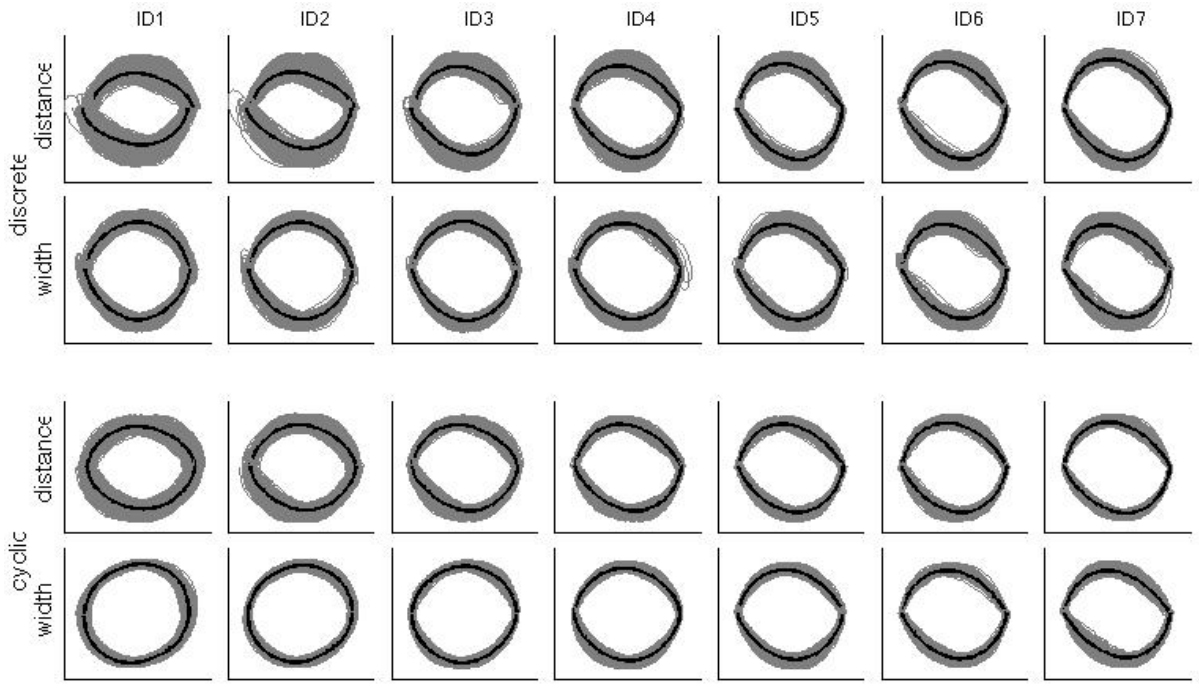

Figure S3.3 Phase plane trajectories. The upper versus lower two rows represent phase space trajectories from a single participant of the discrete and cyclic mode, respectively. For both row pairs, the upper panels show the distance conditions while the lower ones display the width conditions. *ID* increases form left to right. Following PCA for each participant and condition separately, grey lines were obtained by summing the product of the first two eigenvectors and their time coefficients for all participants. Black lines represent the mean trajectories. Clearly, at low (but not high) *ID*, the trajectory variability in the distance conditions is greater than that in the width conditions. Also, the trajectory variability is quite evenly spread at low *ID*s but contracts around the target positions at high *ID*s. Finally, at low *ID*s trajectory variability is higher in the discrete task than in the cyclic one; at high ID this effect inversed.

Intra-participant $R_{AT/MT}$ variability CV $R_{AT/MT}$.

The intra-participant coefficient of variation for the ratio acceleration time – movement time revealed a significant main effect of *Task* (*F*(1,12)=58.306, *p*<.0001, h^2=.829), which showed that the *CV* $R_{AT/MT}$ was higher in the discrete task (mean±SD = 0.20±.01) than in the rhythmic one (mean±SD =0.15±.01). Further, it was significantly larger in the distance conditions (mean±SD =0.20±0.01) than in the width conditions (mean±SD =0.20±0.01; *F*(1,12)=147.628, *p*<.0001, h^2=.925). The main effect of ID_e did not reach significance (*p*>.1). The significant interactions between *Task* and *Manipulation* *F*(1,12)=8.503, *p*<.05, h^2=.415), *Task* and *ID* *F*(3.974,47.690)=6.721, *p*<.0001, h^2=.359), and *Manipulation* and *ID* *F*(3,792)=96.253, *p*<.0001, h^2=.889) are shown in Figure S3.4 below (panel A, B, and C, respectively).

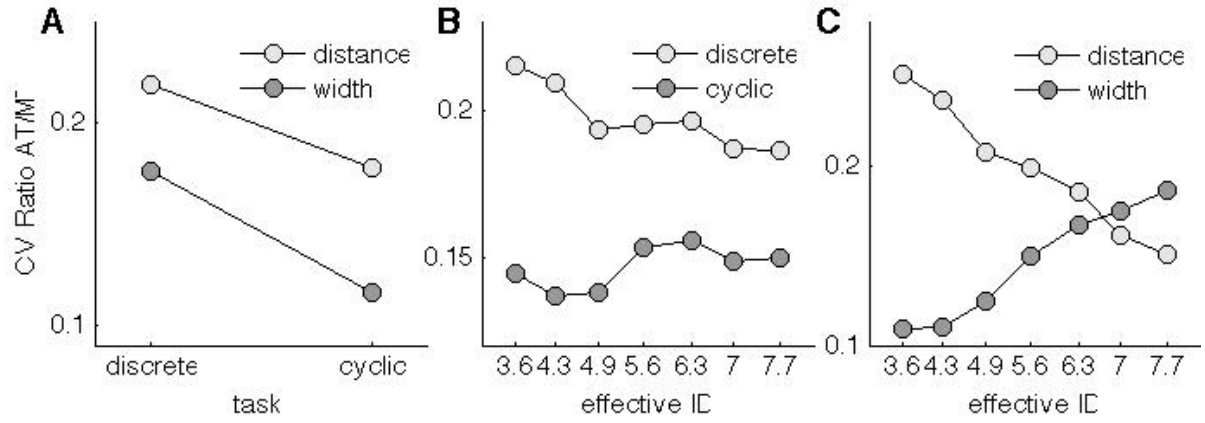

Figure S3.4 CV $R_{AT/MT}$. (**A**) The decrease in *CV* $R_{AT/MT}$.the discrete versus cyclic condition is greater in the width than in the distance conditions. (**B**) In the discrete condition *CV* $R_{AT/MT}$ decreases with inxcreaidng ID while in the cyclic conditions it changes hardly. (**C**) In the width condition *CV* $R_{AT/MT}$ almost doubled with increasing ID while in the distance conditions it reduces to about half its value at low ID.

Peak velocity (PV)

A significant main effect of *Task* ($F(1,12)=8.524$, $p<.05$, $h^2=.415$) occurred because PV was higher in the discrete task (mean±SD =57.50±3.21) than in the cyclic task (mean±SD =51.47±1.88). Moreover, PV was significantly lower in the distance conditions (mean±SD =31.12±1.94) than in those of width (mean±SD =77.85±3.07) (Manipulation ($F(1,12)=749.193$, $p<.0001$, $h^2=.984$). No significant interaction was found between *Task* and *Manipulation*. The significant main effect of ID ($F(1.729,20.637)=16.741$, $p<.0001$, $h^2=.582$) revealed that PV was U shaped as a function of ID. The interactions between *Task* and *ID* ($F(1.802,21.630)=10.860$, $p<.005$, $h^2=.475$), *Manipulation* and *ID* ($F(1.954,23.445)=286.696$, $p<.0001$, $h^2=.960$), and *Task*, *Manipulation*, and *ID* ($F(2.525,30.300)=9.642$, $p<.0001$, $h^2=.446$) are shown in Figure S3.5 below (panel A, B, and C, respectively).

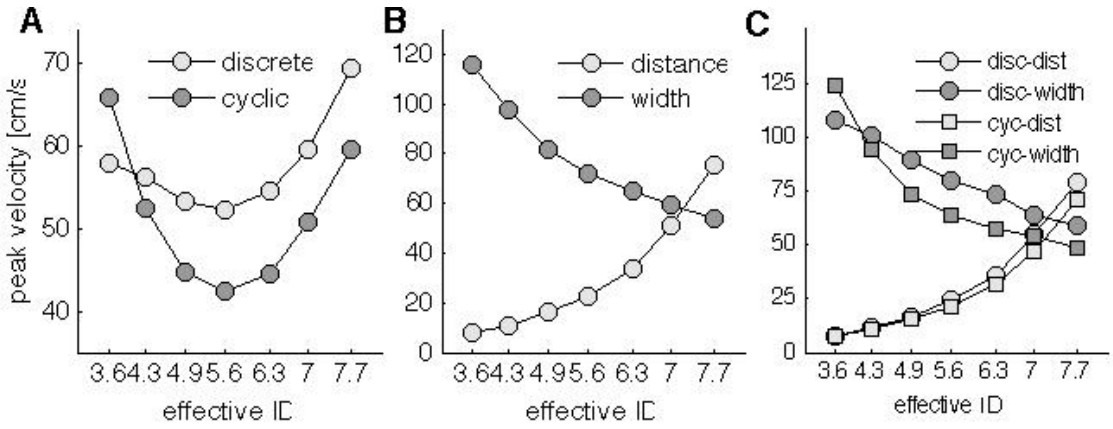

Figure S3.5 PV. (**A**) The U shaped PV as function of ID is slightly asymmetric for both task modes; for the discrete task it is highest at high ID while this is the inverse for the cyclic task. (**B**) PV increases with ID in the distance conditions but decreased in the conditions. (**C**) The rate of PV increase and decrease for the distance and width task varies moderately as a function of manipulation.

Acceleration time (AT)

The significant main effect of *Task* (*F*(1,12)=24.281, *p*<.0001, h^2=.669) showed that the AT was smaller in the discrete condition (mean±SD =0.25±.02) than in the cyclic one (mean±SD =0.28±.01). Further, a main effect of *Manipulation* (*F*(1,12)=4.919, *p*<.05, h^2=.291) occurred because significantly more time was spent in the distance condition (mean±SD =0.27±.02) than in the width condition (mean±SD =0.26±.02), even though the effect was small. AT significantly increased with increasing ID (*F*(1.113,13.353)=40.472, *p*<.0001, h^2=.771). The interactions between *Task* and *ID* (*F*(2.107,25.290)=22.764, *p*<.0001, h^2=.655), *Manipulation* and *ID* (*F*(1.915,22.985)=12.740, *p*<.0001, h^2=.515) as well as between *Task*, *Manipulation* and *ID* (*F*(2.406,28.873)=6.225, *p*<.005, h^2=.342) are shown in Figure S3.6 below (panel A, B, and C-D, respectively).

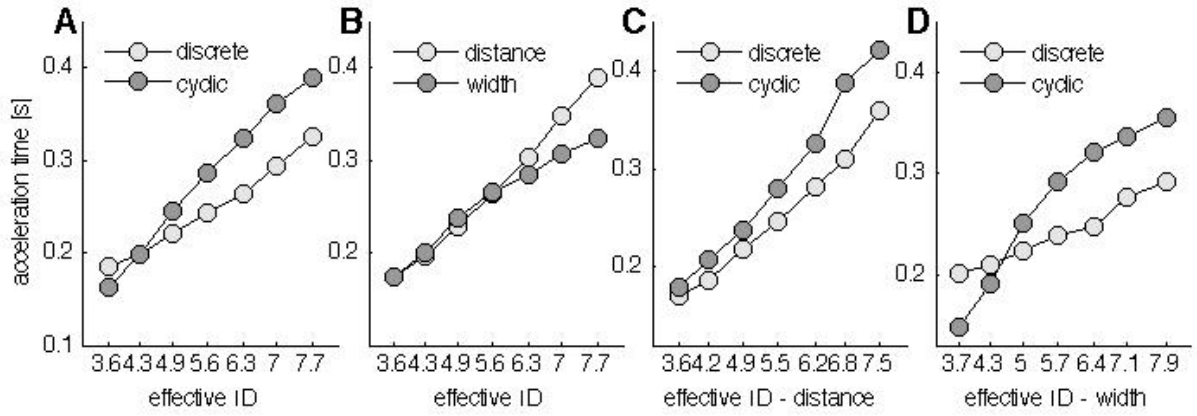

Figure S3.6 AT. (**A**) AT increased stronger with ID in the cyclic condition than in the discrete one. (**B**) At low IDs, AT is about the same for the distance and width conditions; at higher IDs the increase of AT in the width conditions decreased while that in the distance conditions remains steady. (**C,D**) In the distance condition (**C**) AT increases for both task modes, albeit slightly less in the discrete than in the cyclic task. In the width condition (**D**) At increases about linearly with ID in the discrete task; in the width condition, AT initially increases more than the discrete task but its increase diminishes with increasing ID.

Deceleration time (DT)

No significant effect of *Task* was found. A significant main effect of *Manipulation* ($F(1,12)=22.307$, $p<.0001$, $h^2=.650$) revealed that *DT* was higher in the distance conditions (mean±SD =0.55±.04) than in the width conditions (mean±SD =0.47±.03). A significant effect of *ID* ($F(1.605,19.254)=164.863$ $p<.0001$, $h^2=.932$) showed that DT increased with ID at faster rates as ID increased (see Figure S3.7 B and C). The significant interactions between *Task* and *Manipulation* ($F(1,12)=26.901$, $p<.0001$, $h^2=.692$), *Task* and *ID* ($F(3.073,36.872)=14.127$, $p<.0001$, $h^2=.541$), and *Manipulation* and *ID* ($F(3.495,41.935)=9.231$ $p<.0001$, $h^2=.435$) are shown in Figure S3.7 below (panel A, B, and C, respectively). The 3-way interaction between *Task*, *Manipulation*, and *ID* just failed to reach significance ($.05 < p < .1$).

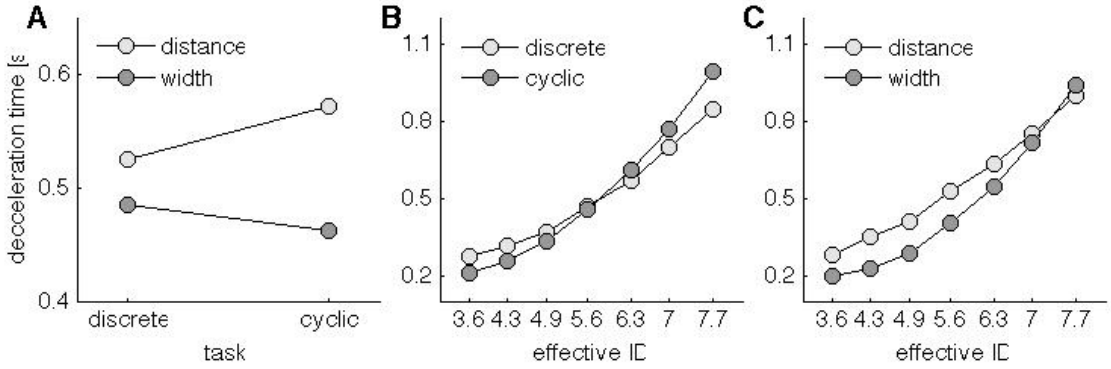

Figure S3.7 DT. (**A**) The difference in DT for the distance and width conditions is greater in the cyclic task than in the discrete one. (**B**) DT increases faster with ID in the cyclic than tin the discrete condition. (**C**) At low ID DT is larger in the distance than in the width condition, but this difference vanishes with increasing ID.

Chapter 4 | *Perception-Action* : Ebbinghaus figures that deceive the eye do not necessarily deceive the hand[4]

"Nothing is permanent about our behaviour patterns except our belief that they are so."

- *Moshé Feldenkrais*

4.1 Abstract

In support of the visual stream dissociation hypothesis, which states that distinct visual streams serve vision-for-perception and vision-for-action, visual size illusions were reported over 20 years ago to 'deceive the eye but not the hand'. Ever since, inconclusive results and contradictory interpretations have accumulated. Therefore, we investigated the effects of the Ebbinghaus figure on repetitive aiming movements with distinct dynamics. Participants performed a Fitts' task in which Ebbinghaus figures served as targets. We systematically varied the three parameters that influence the perceived size of the Ebbinghaus figure's target circle, namely the size of the target, its distance to the context circles and the size of the context circles. In contrast, solely context size significantly affected the movements, in particular the approach phase towards the target, regardless of the movement dynamics. Thus, consistent with the dissociated visual stream hypothesis, the Ebbinghaus figure affected perception and action differently. The hand, however, was also deceived when manipulating context size, which speaks against a strict segregation. To

[4] Under review as Knol H, Sarrazin J-C, Spiegler A, Huys R, Jirsa VK Ebbinghaus figures that deceive the eye do not necessarily deceive the hand.

reconcile these findings we argue that different informational variables are used for vision-for-perception and vision-for-action irrespective of whether certain variables induce (perceptual) illusions.

4.2 Introduction

The importance of vision for humans can hardly be overstated: we use vision to guide movements, to identify objects, and to manipulate them. While it is well known that the visual system comprises two anatomically distinct streams, a ventral and a dorsal stream, if and how they function differently has been debated for over three decades. In the early 1980's, Ungerleider and Mishkin (1982) proposed that the ventral and dorsal stream were associated with processing of 'what' and 'where' attributes of objects in the visual field (Ungerleider and Mishkin, 1982). Later, Goodale and Milner (1995) proposed that the ventral and dorsal visual stream are dedicated to vision for perception and vision for action, respectively (Milner and Goodale, 1995). Accordingly, allocentric information about an object and its contexts proceeds through the ventral stream and evokes a conscious percept. Egocentric information, in particular information about the location of objects for guiding our movements, passes through the dorsal stream in absolute measures.

The functional dissociation attributed to the two visual streams was originally based on clinical studies. These studies demonstrated that lesions to the ventral stream are uniquely associated with functional deficits, often severe, in reporting physical attributes of various objects while retaining the possibility to manually interact with them. Inversely, lesions in the dorsal stream severely disrupt motion-related information affecting actions. However, ever since Aglioti et al. (1995) published their landmark study (Aglioti et al., 1995), visual illusions have become popular to study the proposed dissociation between conscious perception (ventral stream) and (unconscious) perception for the control of movements (dorsal stream) in grasping and pointing tasks. Context-induced visual illusions make targets look smaller or bigger than they are, through for example small context circles around one big 'target' circle (i.e., the Ebbinghaus figure; see Figure 4.1a). If a strict functional dissociation between the ventral and dorsal stream exists, then conscious perception

should be related to the relative size of an object, whereas actions should be affected by the absolute size of an object. In other words, conscious perception is thought to be sensitive to visual illusions. In return, movements guided by egocentric information should be unaffected by visual illusions.

Several studies, both in the context of grasping and pointing, have provided evidence in favour of a functional dissociation between the ventral and dorsal stream (Aglioti et al., 1995; Haffenden et al., 2001; Stöttinger et al., 2012; Haffenden and Goodale, 1998; Stöttinger et al., 2010). In these studies perception was affected by the illusion, but the grip aperture (Aglioti et al., 1995; Haffenden et al., 2001; Stöttinger et al., 2010, 2012) and movement time remained unchanged (Fischer, 2001; Alphonsa et al., 2014). Others, though, found that perception and action were equally affected by visual illusions and thus concluded that the same representation of object size guides perception and action (Franz et al., 2000, 2001; Pavani et al., 1999; Vishton et al., 1999; Franz, 2001; van Donkelaar, 1999). These contradictory findings and interpretations are opposed by authors claiming that the illusion effects do not depend on whether the task is perceptual or motor, but rather on the spatial attributes that are used to execute a task (Smeets et al., 2002; Smeets and Brenner, 2006). For example, in the same movements the lift and grip force are sensitive to a size illusion, but grip aperture is not (Brenner and Smeets, 1996; Jackson and Shaw, 2000). Yet another view was forwarded by Glover (2002), who proposed that visual illusions affect the planning of actions, but not their on-line control (Glover, 2002). Since experimental support exists for each of the aforementioned approaches, numerous methodological differences suggest that a clear interpretation of the repeatedly contradictory results will be impossible unless systematic and well-parameterised experimental studies disentangle the role of the visual system in perception and action.

One task that has been implemented to test whether the visual system is functionally dissociated, is Fitts' task (Handlovsky et al., 2004; van Donkelaar, 1999; Alphonsa et al., 2014; Skewes et al., 2011). In a Fitts' task, a participant is asked either to move a stylus on a tablet from a start position to a given target of width (*W*) in distance (*D*) (i.e., single or discrete movement) or to cyclically move between two

targets of width (*W*), which are separated by a distance (*D*). By systematically varying *D* and *W*, Fitts (Fitts, 1954) linearly related the movement time (*MT*) to the ratio of movement distance (*D*) to target width (*W*) through the index of difficulty *ID* = $\log_2(2D/W)$ by $MT = a + b\,ID$. The index (*ID*) expresses the difficulty of the task in bits(Fitts, 1964, 1954). The robustness and insensitivity to experimental contexts of this so-called Fitts' law, as well as it quantitative nature, render Fitts' paradigm a powerful tool to investigate the dissociation of visual streams.

The question arises whether the linear relationship between the *MT* and the *ID* is affected by a visual context. It is unknown what the effect on the *MT* is when the subjective target size (i.e., perceived *W*) is smaller, or bigger, than it physically is. Therefore, Ebbinghaus-like figures have been implemented in Fitts' tasks to investigate the effect of perceptual illusion on motor behaviour (Ellenbürger et al., 2012; van Donkelaar, 1999; Fischer, 2001; Alphonsa et al., 2014; Lee et al., 2002; Handlovsky et al., 2004). The results of these studies, however, show many contradictions.

Van Donkelaar (1999) was the first to find an effect of the Ebbinghaus illusion on discrete movements in a Fitts' task, by showing an increase in *MT* when the targets looked smaller (or at least, were thought to have looked smaller; see below). Later, Fischer however failed to reproduce these findings in a similar task and reported an insensitivity of the movements to the Ebbinghaus-like figure (Fischer, 2001). Up to now, to our best knowledge, Fischer's study remains the only discrete Fitts' task that failed to show an effect of visual illusions on movement time. Indeed, several studies found that pointing movements were affected by the visual illusion (see Table 1 for a summary of the results of these studies). In one study movements were found to be faster towards bigger looking targets (Handlovsky et al., 2004). This contrasts yet another study that showed *MT* to remain unaffected by a combined Ebbinghaus-Müller-Lyer figure. However, precision and amplitude for a certain effective *ID* resembled the perceived *ID* in a discrete Fitts' task (Alphonsa et al., 2014). Thus, the discrete pointing tasks have rendered ambiguous results.

Table 4.1 Effects of Ebbinghaus-like figures on perception and pointing movements.

	Feedback	Target (mm)	Delay (ms)	Perception (%)	Relative *MT* (%)	Protocol
Discrete movements						
Van Donkelaar (1999)	OL	30	-	-	**S: 94%, B: 100%**** (control: 318 ms*)	a
Fischer (2001, exp 1)	CL	12	-	**S: 100, M: 96, B: 98** (control: 12.2 mm)	S: 105.6%, M: 104.2% B: 106.4% (control: 359 ms)	b
Fischer (2001, exp 2)	LV	12	650	S: 100, B: 95	S: 100%, B: 102.5% (control: 437 ms)	b,f
Handlovsky (2004)	OL	50	-	**S: 107**, B: 98 (control: 51.0 mm)	**S: 94-96%**, B:95-99% (control: 464 ms)	c
Alphonsa (2014, exp 1)*	CL	19	5000	**S: 110**, B: 96 (control: 17.9 mm)	p >.05, no values reported	d,e
Reciprocal movements						
Ellenbürger (2012)	CL	14; 40	-	-	**S: 575/655 ms, B: 625/690 ms**	a
Alphonsa (2014, exp 2)*	CL	19	-	**S: 110,** B: 96 (control: 17.9 mm)	not significant; no values reported.	d

All illusion effects are relative to the control condition in percentage if the control condition was present, and marked bold if significance at the p <.05 level. Else, the values in mm or ms were reported. The illusion conditions consist of Ebbinghaus figures with a small (S), medium (M), or big (B) context size. The visual feedback is classified as open-loop (OL), closed-loop (CL), and limited vision tasks.
*The exact *MT*s are not reported. **The *MT*s are not related to a control condition in the study.
Experimental conditions: (a) simultaneous presentation of target with small context on one side, and big context on the other side, (b) only the target is surrounded by contexts, (c) the home position as the target could be surrounded symmetrically and asymmetrically by a small, big, or no context size, (d) symmetric display of left and right target with, or without context circles, (e) display offset and movement onset after time delay, (f) movement onset after delay.

Next to discrete Fitts' tasks, reciprocal Fitts' tasks have also been combined with visual illusions (see Table 1). In a reciprocal aiming task with Ebbinghaus illusions, a longer *MT* and dwell time was reported for big context circles relative to small context circles (note that the authors did not report a control condition)(Ellenbürger et al., 2012). This result is supported by a different size illusion (i.e., the Müller-Lyer trapezoids) that was implemented in a reciprocal

tapping task for which *MT* increased and the endpoints of the movements were more tightly distributed when the target looked smaller (Skewes et al., 2011). However, in yet another study, *MT* and accuracy measures appeared insensitive to the combined Ebbinghaus-Müller-Lyer figure (Alphonsa et al., 2014). Thus, ambiguity in the reported results in the reciprocal Fitts' task lines up with that in the discrete task version.

The ambiguity in the reported results may well be traced back to methodological differences. Fischer (2001) reported perceptual illusion effects ranging from -0.3 to 0.2 mm relative to physical target size. This leaves the discussion open as to whether illusion effects are big enough to identify changes in movement since the perceived *ID* (between 4.09 and 4.15) hardly changes. Van Donkelaar (1999) did not quantify the perceptual illusion effect, so that a lack of illusion and its effects in some of the parameter combinations cannot be excluded, which may explain why he only found significant results for the 'looking smaller' condition (Knol et al., 2015). Also, different stimulus presentation protocols were applied in the studies in which the Ebbinghaus figure was used to make targets look bigger or smaller. In some experiments, participants were asked to move from the centre between two targets to one of the two simultaneously displayed targets: small context circles surrounded one of the two targets, and big context circles surrounded the other target (van Donkelaar, 1999; Ellenbürger et al., 2012). In contrast, Alphonsa et al. (2014) used the same target as starting and ending point. Others displayed only one target with or without surrounding circles (Fischer, 2001; Handlovsky et al., 2004). Another factor of concern is related to the visual feedback before and during movement execution. The timing and duration of the visibility of the targets, as well as the visibility of the hand during movement execution differs across the protocols (see Table 1). In some cases, the targets had to be memorized due to a delay between stimulus presentation and movement onset (Alphonsa et al., 2014; Fischer, 2001). In other cases, targets were permanently visible (van Donkelaar, 1999; Fischer, 2001; Ellenbürger et al., 2012), or appeared with movement initiation (Handlovsky et al., 2004) (see Table 1). Delayed movements and judgments are more likely to be based on conscious perception (i.e., associated with the ventral stream) than on visuomotor information

(i.e., reflected in dorsal stream activity)(Gentilucci et al., 1996; Hu and Goodale, 2000). Memory based, delayed actions lead to stronger illusion effects (Bruno et al., 2008). The visibility of the hand during the execution of the task was restricted in some studies (commonly referred to as an open-loop task), whereas others did not constrain the visibility of the hand (closed-loop; see Table 4.1). The availability of visual feedback during aiming tasks allows for online control of movements, which is ascribed to the dorsal stream. The illusion effects for reciprocal, closed-loop aiming movements (see Table 4.1) speak against a strict functional dissociation of the visual system. Hence, the contradicting results relative to ventral-dorsal stream dissociations might be explained in terms of differences in methodology, the lack of perceptual quantification of the illusion effect, and relatively small perceptual illusion effects.

Another source of variation that has, to our best knowledge, not been considered so far is in the type of movements elicited in different experiments. In particular, it might be that the presence (or absence) of illusion and its effects on movements is restricted to the certain control mechanism governing the movements. Dynamical models have sought to disentangle the changes in the movement organization underlying the *MT* in a reciprocal Fitts' task (Huys et al., 2010a; van Mourik et al., 2008; Huys et al., 2015; Mottet and Bootsma, 1999; Bongers et al., 2009). By analysing movement kinematics, two types of dynamics have been identified, namely of limit cycle and fixed point (Huys et al., 2010a; Buchanan et al., 2004). A limit cycle is a closed orbit in the state space, which is spanned by the position of the movement x and its change in time $\mathrm{d}x/\mathrm{d}t$. A trajectory on the limit cycle thus periodically returns to its starting point. Therefore, limit cycles are typically used to describe rhythmic activity. A fixed point instead is a location in the state space at which there is no movement, that is, no changes in time $\mathrm{d}x/\mathrm{d}t = 0$. The behaviour around a fixed point is discrete (depending on the nature of the fixed point, attracting, repelling or both but in different directions, as in Fitts task performance; see 31 for details). Thus, the start position and the target can be ascribed as repelling and attracting for movements in discrete Fitts' tasks. In a reciprocal Fitts' tasks, a sudden transition from limit cycle to fixed point behaviour can be evoked by

increasing the *ID* (Huys et al., 2010a). In the latter regime, the reciprocal movements are effectively concatenated discrete movements. When the perceived target width differs from the physical width, the question is whether it is the perceived or the actual width (*W*) that governs the *ID* and the corresponding movement kinematics. As the kinetics are distinct, it may well be that the answer to this question lies in the type of movement underlying the task performance. Movements of the limit cycle type can be expected to be less susceptible to visual perturbation such as introduced by the Ebbinghaus figure. Two arguments that support this hypothesis are that the evolutionary older rhythmic movements owe their functional integrity to a large part to body-related information (in particular kinaesthesia and proprioception), whereas the evolutionary younger discrete movements rely in particular on the visual system (Bernstein, 1996). A second argument is found in the aiming literature in describing larger effects of reducing the availability of visual information on tasks of high level difficulty (typically associated with fixed-point behaviour) compared to low levels of task difficulty (typically associated with limit cycle behaviour)(Bootsma et al., 2002). To date, however, the control mechanisms governing the movements have not been related to the effects of visual illusions on pointing movements.

This leads us to test three hypotheses:

i) A functional visual-stream dissociation exists. In this case, Ebbinghaus figures that evoke perceptual illusions will not affect movements.

ii) Vision for perception and vision for action cannot be dissociated, i.e., a one-to-one mapping of effects on perception and action exists. In this case, perceived target size will determine the movement (i.e., its duration and other features).

iii) Whether the movement is influenced by visual illusions depends on the dynamics that govern the movement.

It should be noted that the first hypothesis (i) does not rule out the existence of interactions between the two streams, as already pointed at by Milner and Goodale (1992). Functionally, however, these interactions are not such that figures causing perceptual illusions lead to 'motor illusions'. We will test these three hypotheses in

the present study in order to clarify if and how the ventral and dorsal streams are functionally dissociated. By structurally testing a broad range of parameters that have been previously identified in a visual perception study, we will evaluate movements with both classical methods (i.e., that have been traditionally used to analyse Fitts' tasks), and the underlying dynamics. As visual feedback is thought to favour the dorsal stream processing of information, we implemented the Ebbinghaus figures in a reciprocal, closed-loop Fitts' task.

4.3 Methods

4.3.1 Participants

Nine (self-declared) right-handed participants (5 females; age 29.5 ± 3.7 years) who reported having normal or corrected to normal vision volunteered in the experiment. The participants were naïve to the purpose of the experiment. This study was approved by the local ethics committee (CPP Sud-Méditerranée I) and was in accordance with the Helsinki Declaration. All participants gave a written informed consent prior to their participation.

4.3.2 Apparatus

The participants performed aiming movements between two targets with a hand-held stylus (18 g, 156.5 mm long, ø 14.9 mm, ~1 mm tip) across a digitizer tablet (Wacom Intuos XL; with a resolution of 200 lines per mm (5080 lpi)) under instructions to move as fast as possible. Position time series were acquired from the tablet via custom-made software (250 samples per second). The targets were displayed and designed using the Psychophysics Toolbox (Kleiner et al., 2007; Brainard, 1997) in Matlab R2014b (The MathWorks Inc., Natick, MA). Filled black circles were presented against a white background and multisampled (open GL) to control for aliasing effects. The tip of the hand-held stylus was represented by a red dot on the monitor (Dell P2714H with a size of 597.9 by 336.3 mm (1920 x 1080 pixels) that displayed 60 frames per second. The participants sat at a 60 cm distance from the monitor (establishing a viewing angle of 52.96° x 29.27°) and their head was supported with a chin-rest so as to ensure that the distance between the head and the monitor remained fixed.

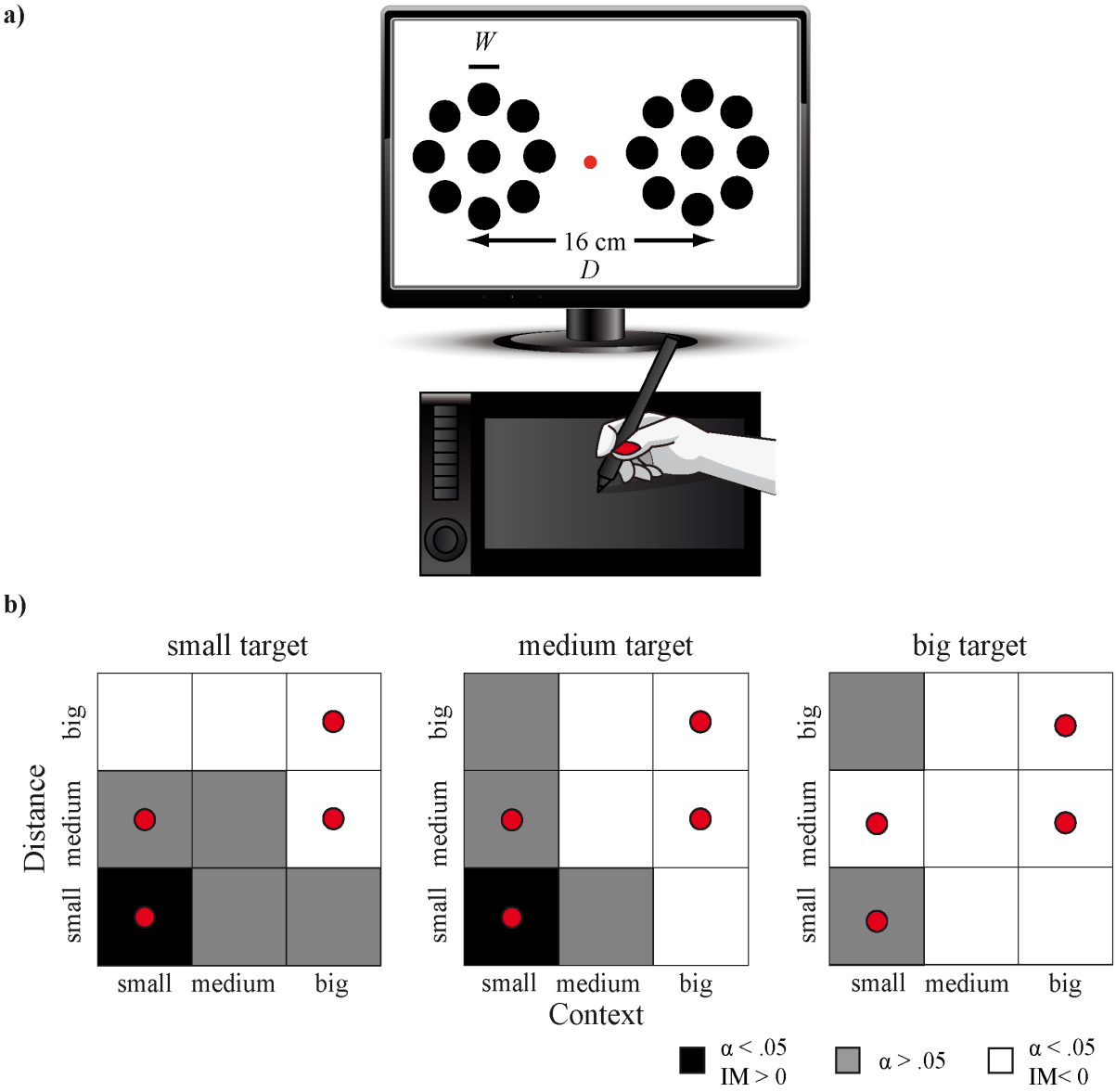

Figure 4.1 (A) Experimental set-up of the horizontal sliding task, with *W* representing the target size and *D* the distance between the targets on the left and right side. **(B)** Selected parameter combinations adopted from Knol et al. (2015) are marked with a red dot for each quantified target size, context size, and target—context distance. The black and white squares indicate a significant illusion magnitude (IM) for bigger perceived targets and smaller perceived targets, respectively. The grey squares show conditions that were not significantly different from the control trials (α = 0.05; see Knol et al. (2015) for details).

4.3.3 Procedure

Participants read instructions on the screen, which explained that they were required to slide with the stylus as fast as possible between two targets (i.e., the centre of the left and right figure in Figure 4.1). After a familiarization phase in which the participants performed up to 5 sliding movements on the tablet between two plain target circles, the participants performed two trials of 25 reciprocal movements per condition. The conditions consisted of an identical Ebbinghaus figure on the left and right side of the screen with one out of three possible target sizes (i.e., 5, 10, or 20 mm). Each target size was combined with a small or big context of target-surrounding circles displayed at a small/medium and medium/large distance between target and context circles, respectively (indicated with a red dot in Figure 4.1b). This resulted in 12 conditions (i.e., 3 target sizes × 2 context sizes × 2 target—context distances) for the Ebbinghaus figure. Three control conditions were added, in which the three plain target sizes were presented, that is, without context circles. Participants were asked to take breaks after each block of five trials but could also take a break whenever they felt it was necessary. The order of trials was randomized. After each trial, the participants got feedback on the number of errors to emphasize the importance of the precision.

4.3.4 Movement parcellation

To calculate the moments of movement onset and offset, the velocity along the trajectory of the movement and its position data (x,y) on the plane of the tablet were analysed. The position data (x,y) were analysed with the aim to restrict the analysis to the horizontal plane (x). This movement parcellation allowed to classify and to quantify the movement errors, and to assess whether the Ebbinghaus illusion affected these measures. Figure 4.2 shows the analysis of the movement in a target (in this case, the left target), in which valid movements are defined as those in which the angle between the ingoing and outgoing intersection points of the line (φ_{in}, φ_{out}) was smaller than 120 degrees, and the angle (α) between the vectors at the intersection points with the target border (V_{in}, V_{out}) did exceed a threshold of 42°. Note that these valid movements have one target 'entry' and one target 'exit' ($\varphi_{in,}$). One-sided overshoots were identified as movements with also one target entry and

exit but with φ_{in}, φ_{out} and/or α exceeding the corresponding threshold. Two-sided (or n-sided) overshoots were characterized by at least two entries and exits. Misses did not cross the target. Misses were further subdivided into undershoots and overshoots, based on the horizontal position and the movement velocity (see Figure 4.3).

Dwelling in the target occurred if the velocity profile showed a significant minimum inside the target (i.e., along the trajectory and not touching the target border). The minimum was significant if this period was drawn from a different distribution than the movement inside and away from the target. This was tested by a two-sided Kolmogorov-Smirnov test. Irrespective of the presence of dwelling, we determined the turning point inside the target (with respect to the x-direction). Note that both dwelling and turning can coincide.

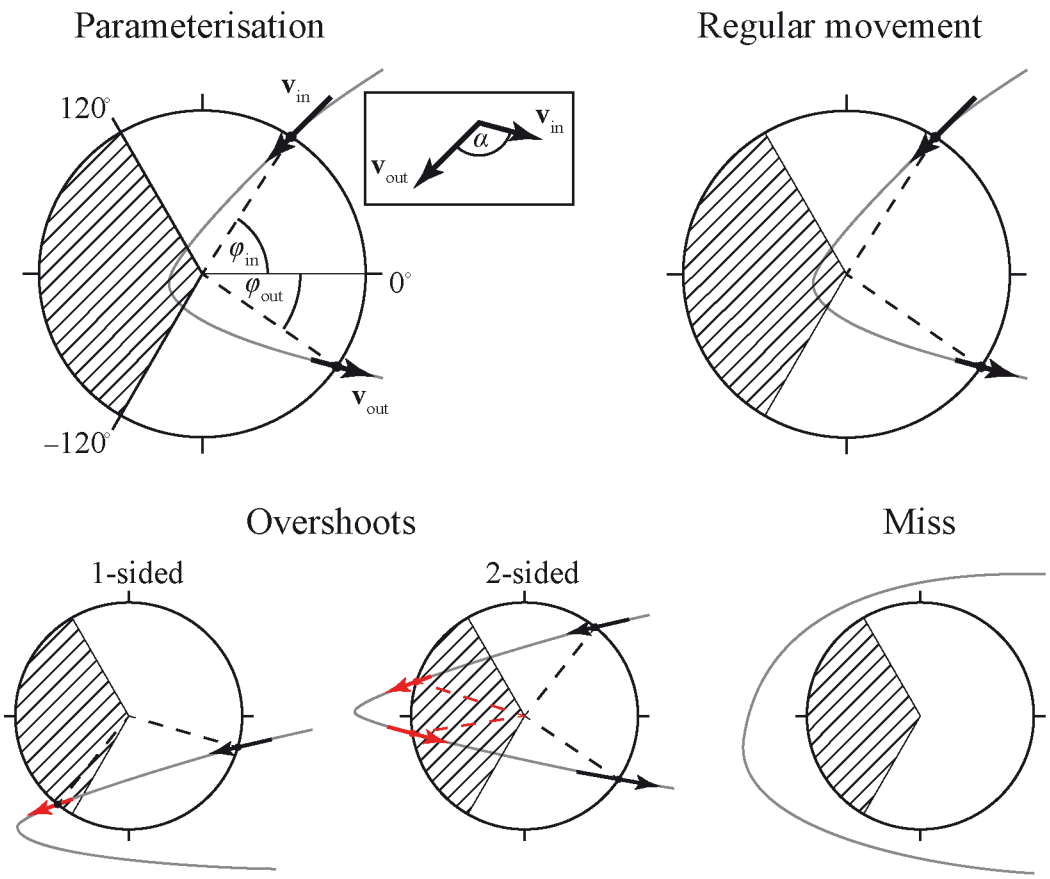

Figure 4.2 Geometrical movement parcellation and identification of the targeting phase, illustrated for a right to left movement. V_{in} and V_{out} represent the vectors and the entry and exit point, respectively, with α being the angle between the vectors. The angle between of the radius at 0° and the radius to the intersection of the movement with the target (φ_{in} and φ_{out}) should not exceed 120°. The shaded area is the area with φ_{in} and/or φ_{out} being bigger than 120 degrees. A black arrow signifies a correct entry or exit, whereas a red arrow represents an entry or exit that did not meet the requirements. Errors were identified as 1-sided overshoots if a least one entry or exit was exceeding the requirements. 2-sided overshoots had at least 2 entries and 2 exits. Misses did not have any intersections with the target.

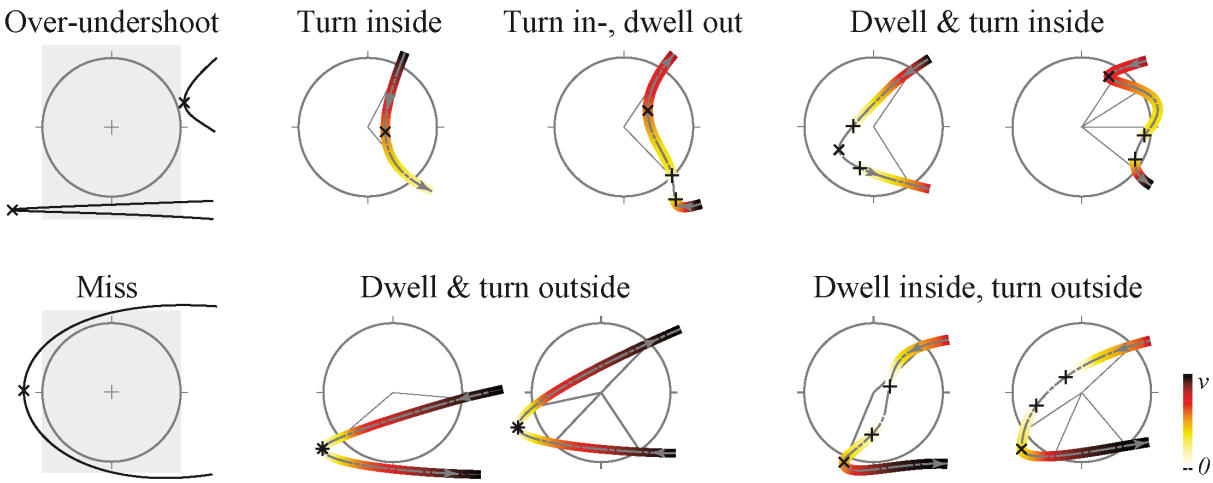

Figure 4.3 Subdivision of overshoots and undershoots and characterization of dwell time based on the velocity profiles. The color-coding signifies the speed along the trajectory. The cross (x) indicates the turning point. The plus (+) indicates the movement onset and offset. The grey block for an over-undershoot and a miss represents the area that would have been included if only the horizontal position and its first derivative would have been taken into account, illustrating the possible errors that would have been falsely taken into account.

4.3.5 Dependent measures

Movement time (*MT*) was defined as the difference between movement onset and the subsequent movement onset (see Figure 4.3). Dwell time was defined as the difference between movement offset and movement onset within (or around) one target. The ratio between the acceleration time and the movement time ($R_{AT/MT}$) was quantified as the time from movement onset to peak velocity (i.e. acceleration time, *AT*), divided by the movement time. The deceleration time (*DT*) signified the time from peak velocity till the subsequent movement onset. The perceptual illusion magnitude (*IM*) was retrieved from Knol et al. (2015) and correlated with the *MT*. The misses and overshoots (one-sided and two-sided, see Figure 4.2 and 4.3) were counted, and their sum reflected the number of invalid movements.

The probability to find a specific point at a given time in state space $(x,\dot{x})$ relative to its previous state at time t_0 is reflected by the conditional probability distribution. The conditional probability serves as a basis for the construction of

vector fields (i.e., the deterministic dynamics). To compute the probability $P(x,t)$ and the conditional probability, position time series were low-pass filtered using a fourth-order Butterworth filter, with a cut-off frequency of 10 Hz. The x and $\dot{x}$ time series were normalized from [-1, 1]. The probability distributions were computed by concatenating all aiming movements of all participants in each condition using a grid of 31 by 31 bins. Difference probability distributions were calculated as the difference between the probability distribution of the small context condition and the big context condition. The probabilities were normalized. Kramers-Moyal coefficients (i.e., to reconstruct the deterministic part of the dynamics) were computed, which allowed for the computation of angle Θ between each vector and its neighbors. Subsequently the angle with the biggest value Θ_{max} was retained. The biggest Θ_{max} around the target (7x5 bins around the target location) was taken as a measure for the existence of a fixed point (fixed points were identified as $\Theta max > 90$; Huys et al., 2015).

One principal component analysis (PCA) was performed to investigate endpoint variability as a measure of targeting precision. To test the distribution of endpoints, the principal orthogonal eigenvectors were retrieved. To test whether the distribution of endpoints got more or less dense through the experimental conditions, the endpoint distribution (*EPD*) was calculated as the range between the minimum and maximum value of the data, after outliers were excluded according to equation 4.1:

$$\left(Q_1 - 1.5 * IQR\right) \leq data \leq \left(Q_3 + 1.5 * IQR\right) \qquad (4.1)$$

in which IQR is the interquartile range (from 25-75%), Q_1 is the first quartile (25%) and Q_3 is the third quartile (75%). The *EPD* was calculated relative to the *EPD* of the control condition (100%).

Statistics

Repeated measures analyses of variance (ANOVA) were performed on the normal distributed data, with *ID*, target-context distance, and context size as within participants factor. If significance levels were met (α = .05), the tests were followed

up by Bonferroni post-hoc tests. The degrees of freedom were corrected according to the Greenhouse-Geisser method to control for non-sphericity of the data if necessary. If this was the case, the degrees of freedom were reported. Whenever the data was non-normal distributed, a non-parametric Friedman test was performed. If the Friedman test showed significant differences, the test was followed up with the Wilcoxon signed rank post-hoc tests with Bonferroni correction (α/number of comparisons). Pearson correlation coefficients were calculated to investigate potential linear correlations between the perceptual *IM* and the *MT*. Linear regression analyses were applied on the *MT* data to investigate the slope and intercept.

4.4 Results

4.4.1 Fitts' law – the effect of target size on non-normalized durations

We examined how *MT* changed as a result of changing the target size, context size, and the context—target distance of the Ebbinghaus figure (see Methods for more details). The target sizes of 5, 10, and 20 mm corresponded to an *ID* of 4, 5, and 6, respectively. We found that *MT* increased with increasing the *ID* for both the illusion and control trials (for illusion trials: $F(2,16) = 92.85$, $p < .001$, $\eta_p^2 = .921$; Figure 4.4a). Thus, Fitts' law held under both the Ebbinghaus and control conditions. Also, the acceleration time (i.e., the time from movement onset to peak velocity), *AT* (for illusion trials: $F(1,8)=50.61$, $p=.000$, $\eta_p^2=.864$; Figure 4.4b), deceleration time (i.e., the time from peak velocity to movement offset), *DT* (for illusion trials: $F(1,8)=68.36$, $p=.000$, $\eta_p^2=.895$; Figure 4.4c), and dwell time (i.e., the time from movement offset to movement onset; $F(2,16) = 3.71$, $p < .05$, $\eta_p^2 = .317$) increased with *ID*.

The ratio between the acceleration time and the movement time ($R_{AT/MT}$) quantifies the (a)symmetry of the velocity pattern. The asymmetry has previously been shown to increase ($R_{AT/MT} < .5$) as *ID* increases (Mottet and Bootsma, 1999; Huys et al., 2015). In line therewith, the $R_{AT/MT}$ significantly increased as the *ID* decreased ($F(2,16) = 54.59$, $p < .001$, $\eta_p^2 = .872$), which was mainly due to a decrease of the deceleration time as *ID* decreased.

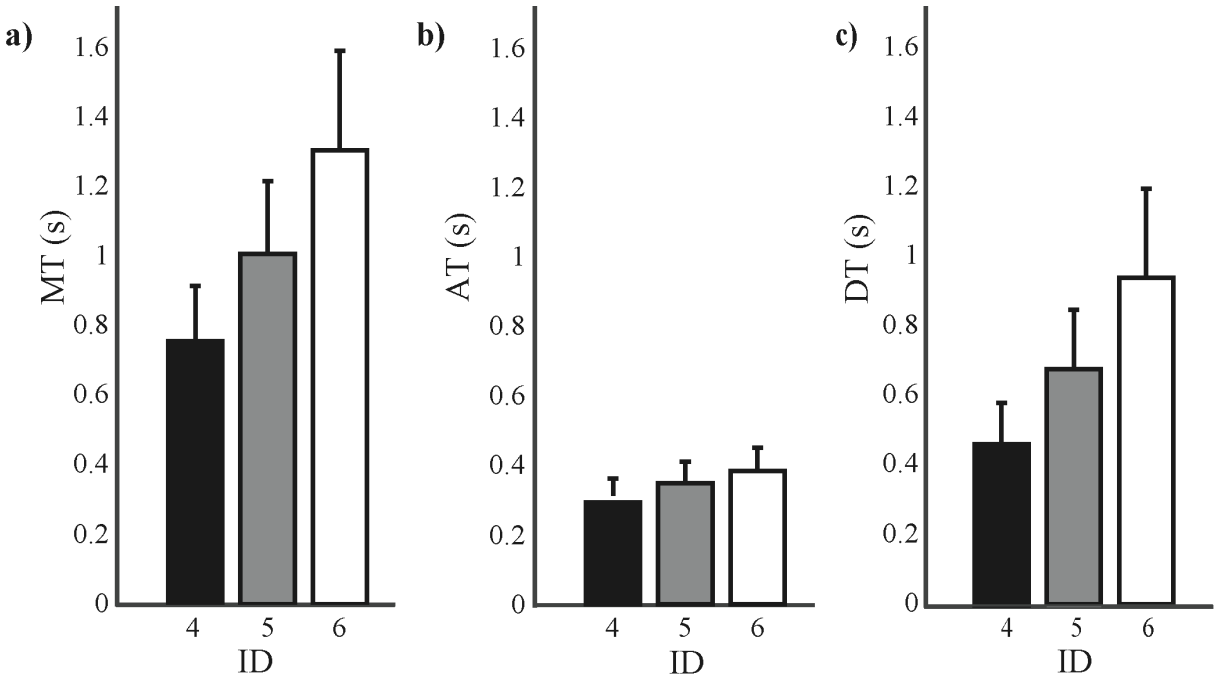

Figure 4.4 (a) Movement time (*MT*), **(b)** acceleration time (*AT*), and **(c)** deceleration time (*DT*) for ID 4 (black), ID 5 (grey), and ID 6 (white). The error bars represent the standard deviation.

4.4.2 Illusion effects

To control for the effect of target size on various dependent measures we normalized them relative to the control conditions. MT_r, AT_r, and DT_r signify the *MT*, *AT*, and *DT* relative to the corresponding observed values in the control condition in percentage. Context size significantly affected the MT_r. ($F(1,8) = 13.97$, $p < .01$, $\eta_p^2 = .640$; Figure 4.5a); MT_r was significantly bigger than 100% in the big context size condition ($t(107) = -5.41$, $p < .0001$). On a group level, linear regression on the *MT* over *ID* showed a bigger intercept (*a*) and marginally shallower slope (*b*) for the big context size condition ($a = -.28$, $b = 0.26$ in Figure 4.5d) as compared to the small context ($a = -.45$ and $b = 0.29$) and the control condition ($a = -.39$, $b = 0.28$). We additionally performed the regression analyses for each participant individually in order to assure consistency between the here-reported group level and the individual level (see supplementary information). An ANOVA on the intercept (*a*) and slope (*b*) with context size as factor indicated that the slope was not significantly affected by context size ($F(16,2) = 1.900$, $p > .1$, $\eta_p^2 = .192$,) and that the intercept just failed to reach

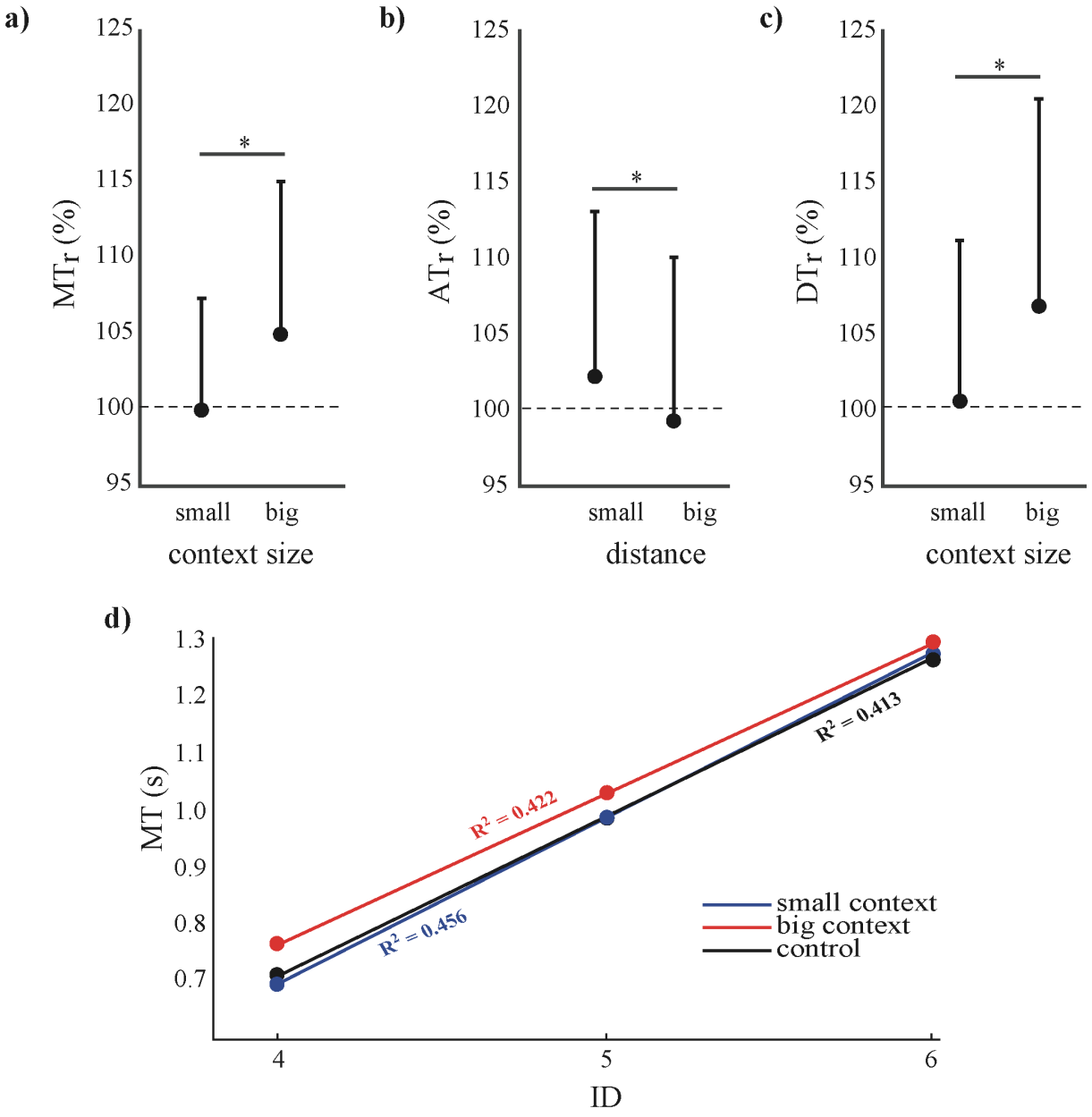

Figure 4.5 (a) The relative movement time (MT_r), **(b)** acceleration time (AT_r), and **(c)** deceleration time (DT_r) as a function of the small (black) and big (white) context circles (*a*, *c*), and target—context distance (*b*). The error bars represent the standard deviation. **(d)** The linear regressions with the corresponding R^2 value of movement time (*MT*) in seconds as a function of the index of difficulty (*ID*) for the small (blue) and big (red) context and the control condition (black).

significance ($F(16,2) = 3.227$, $p = .066$, $\eta_p^2 = .287$). This latter result contrasts that of the ANOVA on *MT*, but, as the independent variable *ID* in the regression is based on three *IDs* only, it should be interpreted with caution. The $R_{AT/MT}$ was not different from the control trials. The increase in MT_r, however, could be explained by an increase in the relative deceleration time (DT_r) ($F(1,8) = 17.22$, $p < .01$, $\eta_p^2 = .683$;

Figure 4.5c). The AT_r was affected by the distance between the target and context circle ($F(1,8) = 5.39$, $p < .05$, $\eta_p^2 = .400$; Figure 4.2b).

4.4.3 Perceptual categories

To tackle the question whether a target that looked bigger (or smaller) than it actually was resulted in faster (or slower) movements, we identified three perceptual categories based on our recent study on quantifying the Ebbinghaus figure and its effects on perception(Knol et al., 2015). The perceptual categories are conditions in which the target circle was perceived as *looking smaller, bigger,* and *no illusion effect* as compared to the control condition. The relative *MT* resulting from the 12 Ebbinghaus figure conditions (Figure 4.1) was divided into these three perpetual categories. These categories identify which illusion figures evoked a significant perceptual illusion effect and identify the direction of the effect (i.e., bigger or smaller). To compare the perceptual effect with the effects of the Ebbinghaus figure on *MT,* we calculated the illusion effects relative to the control condition (in percentage) for both the perception and *MT* data, and then correlated them. The relative MT was significantly different from 100% ($t(62) = 5.2$, $p < .001$) only when the targets were perceived as smaller than they really were (*looking smaller* category, mean = 104.6 ± 7.0). For the other two categories the MT_r was not significantly different from 100%.

4.4.4 Correlation perception and movement time

Since the complete dataset of the illusion magnitude (perception) of the same participants was at hand, we could test whether the perceptual effects correlated with the movement effects. As can be seen in Figure 3, relative perceived target size correlated negatively with the relative movement time ($r = –0.32$, $p < .001$); perceived as smaller (larger) targets were accompanied by longer (shorter) relative movement times. Since context size significantly affected MT_r, we computed the correlations for both context size conditions separately. Only the big context condition materialized in a significant (negative) correlation between the IM_r and MT_r ($r = –.29$, $p < .05$; black dots in Figure 4.6), though the slope of the small context condition was negative as well ($r = –.012$, $p > .05$; red dots in Figure 4.6).

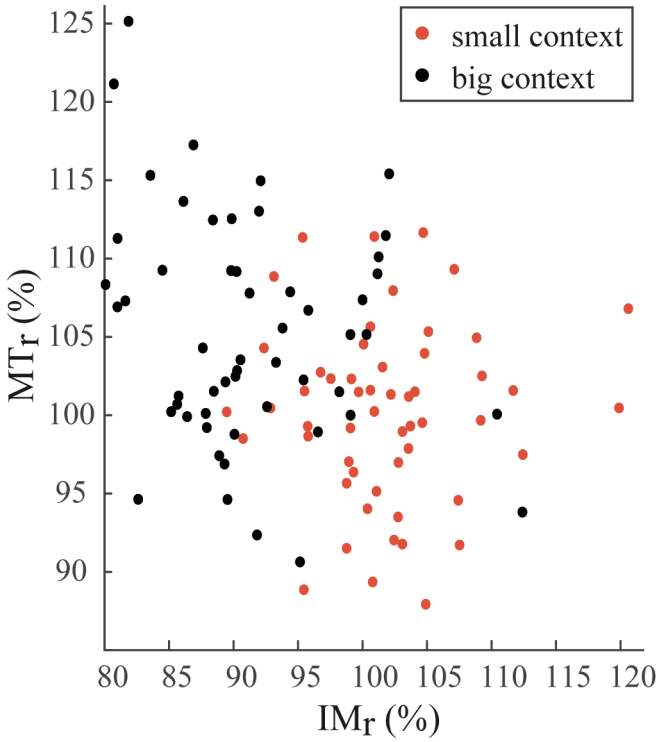

Figure 4.6 The relative movement time (*MTr*) as a function of relative illusion magnitude (*IMr*) and context size. The relative movement time is plotted against the relative illusion magnitude from Knol et al. (2015) (for the same participants). The red and black dots signify the small and big context condition, respectively.

4.4.5 Vector field angles

Since the contribution of the movements in the sagittal plane (i.e., away from the body of the participant) on the trajectory length was negligible (see Supplementary Information for further details), we only used the horizontal position data for further analyses (as is typically done: Mottet and Bootsma, 1999; Saltzman and Kelso, 1987; Huys et al., 2015). A vector field describes the change in magnitude and direction at given points in the state space of a system. With respect to the present work, the arrows indicate the magnitude and direction of the movement's rate of change at the corresponding points in the state space. Vector fields are the graphical representations of the system's dynamics (Strogatz, 1994; Huys et al., 2014) and were here reconstructed from the concatenated horizontal position data to verify whether fixed points were present at the highest *ID*s. Fixed points, that is $dx/dt = 0$, are recognisable by short arrows pointing in opposing directions. If indeed a fixed point behaviour is present, the maximum angle (θ_{max}) between the vectors close to the fixed point can be expected to be bigger than 90° (Huys et al., 2015, 2010a). For limit cycle behaviour, the vectors should point in a similar direction, and therefore the angle should not exceed 90°. θ_{max} was calculated around the end point of the movement (Huys et al., 2010a) (see Methods). There was no significant difference between the

left and right target ($t(107) = -1.7743$, $p = .08$). We therefore averaged across both targets for the remaining analyses.

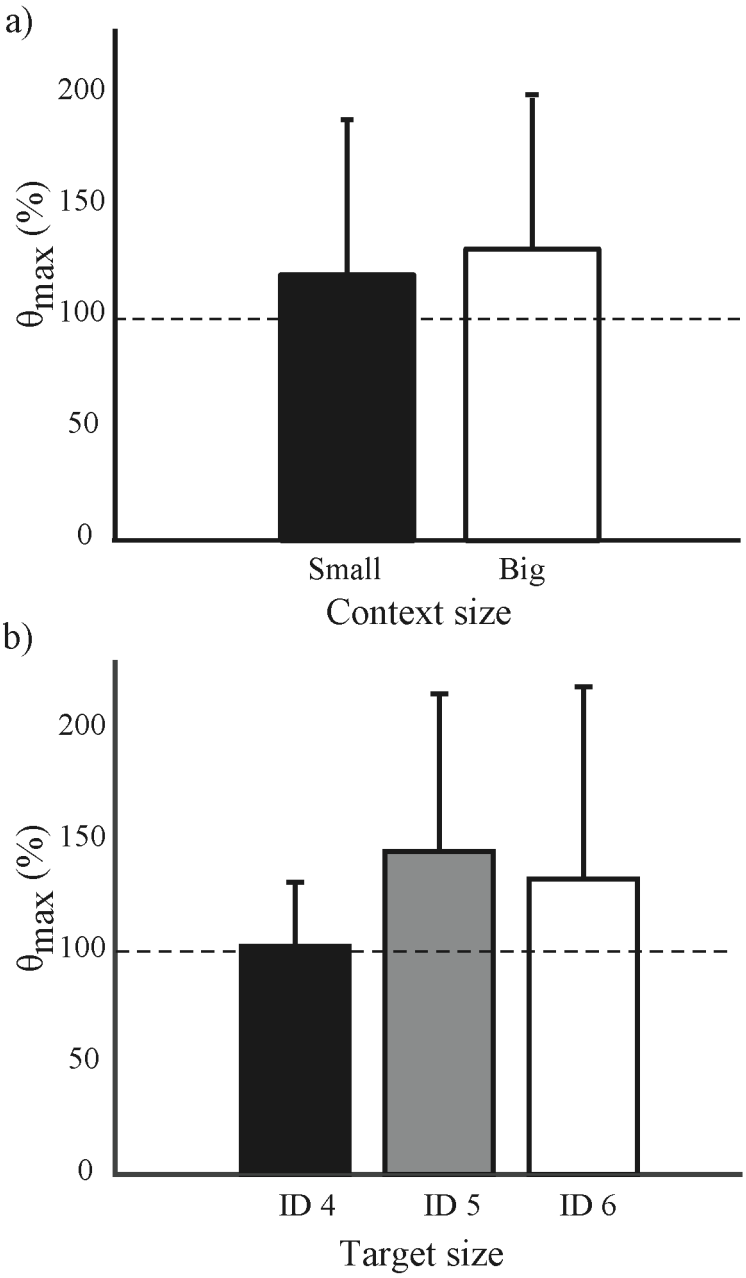

Figure 4.7 Maximum angle between vectors for **(A)** context size and **(B)** target size. In panel **(A)** the two bars represent the maximum angle in percentage (θ_{max}) between vectors in a vector field for the small (black) and big (white) context, relative to the control condition. In panel **(B)** the bars represent θ_{max} in degrees for index of difficulty 4 (black), 5 (grey), and 6 (white). The error bars represent the standard deviation.

Both *ID* and context size affected θ_{max} relative to the control condition (context size: ($F(2,34) = 4.85$, $p < .05$, $\eta_p^2 = .222$; Figure 4.7a; *ID*: ($F(2,34) = 3.35$, $p < .05$, $\eta_p^2 = .165$); Figure 4.7b). The absolute mean values for the lowest *ID*, *ID* 4, showed a θ_{max} smaller than 90° (77.40°), versus *ID* 5 (116.17°) and *ID* 6 (132.45°). These results

indicate that the movements at *ID* 4 were associated with limit cycle dynamics while those at *ID* 5 and 6 were associated with fixed point dynamics.

4.4.6 Difference probabilities

The movements' probability distributions in the state space (spanned by the horizontal position and its first derivative with respect to time, $(x(t), \mathrm{d}x(t)/\mathrm{d}t)$ show how long (i.e., how many samples) the participants spent in a given bin, that is, a small region in the state space. The probability to find a participant's movement in a certain state is specified by counting the samples in the corresponding bin in the state space. The difference probabilities in Figure 4.8 show the difference between the probability distributions in the small context condition and the big context condition (from the concatenated movements of all participants).

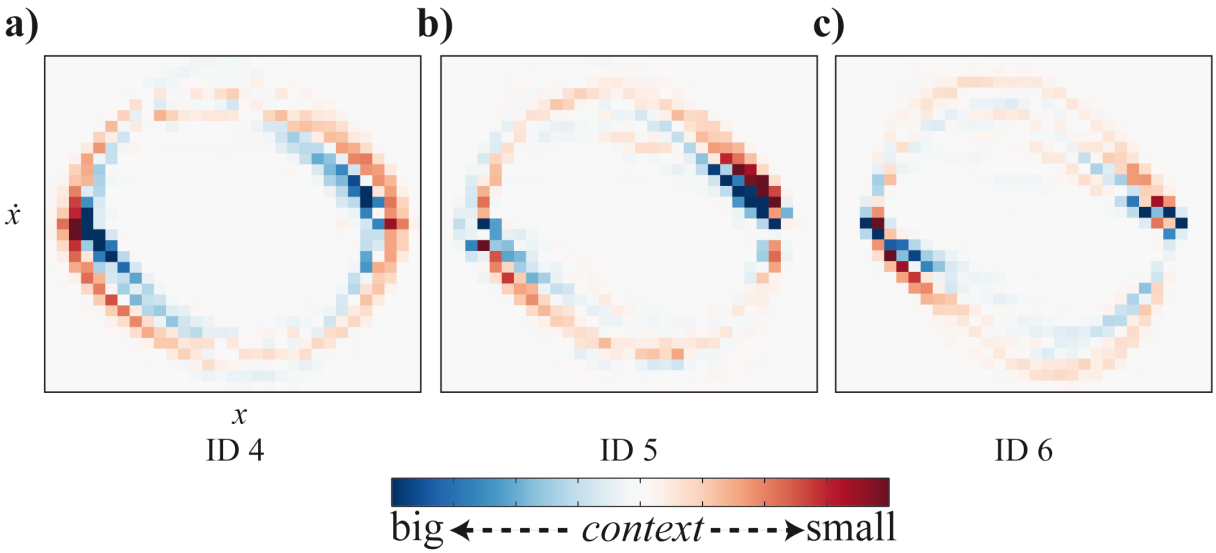

Figure 4.8 Difference probability distribution for **(A)** ID 4, **(B)** ID 5, and **(C)** ID 6. The red colouring marks a higher probability for the small context condition; the blue colouring signifies higher probabilities for the big context condition.

These difference probability distributions provide information about the movement kinematics and to some extent the underlying dynamical classes that have previously been identified for reciprocal aiming movements (Huys et al., 2010a). In probability distributions, limit cycle behaviour shows up as circular, more or less symmetrical orbits with probabilities that are fairly uniform (Huys et al., 2008). For single aiming

movements the symmetry is obtained by an acceleration and deceleration time of similar duration (Mottet and Bootsma, 1999). Fixed-point behaviour typically involves asymmetric velocity patterns with a deceleration (and dwell time) phase longer than the acceleration phase. The probability distributions typically show a peak close to the fixed point (Huys et al., 2008). Fixed-point behaviour is found for *ID* 5.6 and higher in a similar cyclic Fitts' task (Huys et al., 2015). Thus, hints as to which dynamics are adhered to may become apparent (among others) in a difference probability distribution. In Figure 4.8, a stronger deviation of a perfect circle, that is, asymmetry for the big context condition (in blue) becomes apparent for *ID* 4 and 5 (Figure 4.8a, 4.8b, respectively) compared to the symmetric, circular shaped probabilities for the small context condition (in red). For *ID* 6, an asymmetric pattern can be found for both the small and big context (red and blue, respectively). Thus, the big context condition prolonged the phase of movement deceleration as compared to the small context condition, and pushed the participant to perform a sequence of discrete movements rather than a smooth cyclic movement between the two targets.

4.4.7 Classified movement endpoints

The analysis of the classified movement endpoints (into misses, one-sided or two sided overshoots where the target is traversed once or twice, and the valid movements) showed that target size affected almost all the classes (except the misses). Bigger targets were associated with a larger amount of valid movements and less overshoots (i.e., one-sided and two-sided). No significant effects of context size, or context—target distance were found (see Supplementary Information for further details).

4.4.8 Endpoint distribution

The endpoint distribution (*EPD*; see Methods, equation 4.1) captures the density of the movements' endpoints. The first eigenvector was significantly affected by context size ($F(1,17) = 27.839$, $p<.001$, $\eta_p^2 = .621$): a small context increased the *EPD*, whereas a big context decreased the *EPD* relatively to the control condition (Figure 4.9). Thus, a small context size makes participants use more space in the target, while a big

context size makes the endpoints more focal. However, the correlation between the illusion magnitude (perception) and the *EPD* failed to reach significance (p = .22, r = .12).

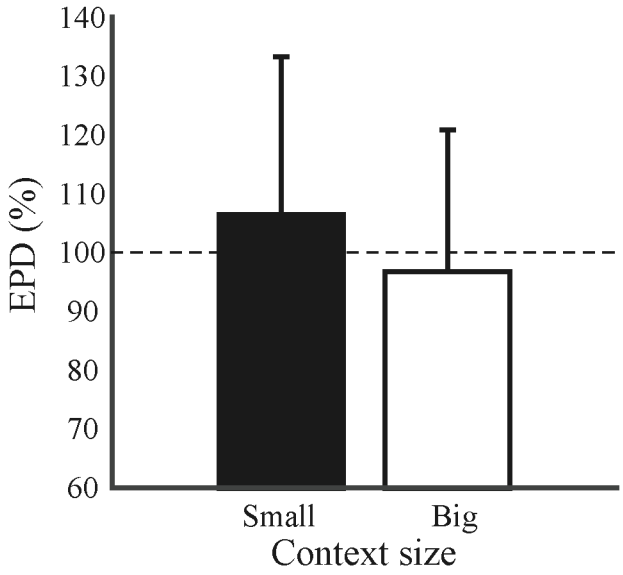

Figure 4.9 The endpoint distribution (*EPD*) in percentage for the small and big context, relative to the control condition. The error bars represent the standard deviation. The dotted line signifies the EPD of the control condition.

4.5 Discussion

The literature on (pointing) movements to size-contrast illusions (using, for example, the Ebbinghaus figure or the Müller-Lyer trapezoids) is filled with contradictory results. The experiment reported in this manuscript was especially designed to systematically examine the effect of various Ebbinghaus figure configurations on reciprocal, closed-loop aiming movements. We identified three hypotheses, each of which we discuss in the following with regard to the literature and reported experimental findings.

Hypothesis 1. The visual-stream is functionally dissociated, and hence a visual illusion does not affect movements.

If the anatomical dissociation between the ventral stream and the dorsal stream would indeed be associated with a dissociation of function as Milner and Goodale proposed (Goodale and Milner, 1992; Milner and Goodale, 1995) and provided evidence for (Aglioti et al., 1995; Haffenden and Goodale, 1998),

movements towards visual illusion figures would be insensitive to their illusionary (perceptual) effects. Our findings demonstrate that one of the Ebbinghaus figure parameters (but not the other two) influenced the movement's temporal and spatial (precision) features. They consequently speak against a strong and consistent functional dissociation of the visual system. These findings are the more surprising because dorsal stream activity is commonly related to the online control of movements (Milner and Goodale, 2008; Goodale, 2014), and especially to reciprocal aiming movements, which require continuous and direct visuomotor transformations (Skewes et al., 2011) as compared to discrete tapping/pointing. Thus, if in any context, the proposed insensitivity of movement to visual illusions should especially surface for reciprocal movements.

Little is known about the influence of size-contrast illusions on reciprocal, closed-loop aiming movements such as a Fitts' task, however. The few reported results on this subject are contradictory. For example, in the study of Skewes et al. (2011), the Müller-Lyer trapezoids affected the perception, the *MT*, and the movements' precision (Skewes et al., 2011). However, in another study, the combined Ebbinghaus-Müller Lyer figures did affect the perception but neither the *MT*, the amplitude nor the precision in reciprocal tapping (Alphonsa et al., 2014). In the latter study, however, the movement amplitude and the radial error of discrete tapping were susceptible to the perceived target size and perceived distance. Regardless the different protocols that were applied (i.e., the way authors implemented the visual illusions, quantified perception, and tested parameters), the common denominator for these reciprocal, closed-loop aiming studies is that they speak against a strict functional dissociation of the visual system.

In return, Skewes et al. (2011) pointed out that the illusion effects on movements that were reported by Franz (2001) and Van Donkelaar (1999) might have been due to the absence of visual feedback of the moving arm (Skewes et al., 2011; Milner and Goodale, 1995). That is, in the absence of this feedback, visual information is most likely processed in the ventral stream since the memory trace in the dorsal stream is short-lasting as compared to the trace in the ventral stream (i.e.,

visual memory)(Binsted et al., 2006). This was supported by empirical evidence showing that when visual feedback was introduced during the task, an effect of the illusion on pointing (Fischer, 2001) and grasping (Stöttinger et al., 2010) was not found. Our results, however, showed that the execution of the perceptual-motor task with visual feedback was consistently influenced by the visual illusion for one Ebbinghaus figure parameter (out of three). This finding is in accordance with Skewes et al. who conducted a closed-loop reciprocal tapping experiment with Müller-Lyer trapezoids, and found that both the *MT* and the precision were affected. Hence, it seems unlikely that differences in the ventral stream or the dorsal stream memory traces can account for the presence (or absence) of a 'motor' illusion.

Besides the studies that incorporated visual illusions, several studies have investigated the effect of visual feedback in Fitts' tasks by changing the mapping between the hand movement (effector space) and the cursor movement on the screen (task space)(Brenner and Smeets, 2011; Fernandez and Bootsma, 2008, 2004). These studies showed that visual feedback of the cursor movement in a particular nonlinear mapping with the hand movement were faster and more accurate than with a proportional mapping of cursor and hand movement. Although Fernandez and Bootsma (2004) argued that the visual feedback would be more effectively used because the cursor is moving slower when it is close to the target, Brenner and Smeets (2011) suggested that participants moved faster because they missed fewer targets (i.e., they traded off accuracy for speed). Following the latter line of reasoning, the participants might have moved slower when the target appeared smaller because they had more difficulties hitting the targets. However, the number of invalid movements (the total of misses, undershoots and overshoots; see supplementary information) remained unaffected by the illusion in our experiment. Thus, it seems more likely that velocity close to the target assured a successful hit of the target.

Hypothesis 2. A one-to-one mapping between vision for perception and vision for action exists; hence the (consciously) perceived target size determines the movement.

Franz and colleagues (Franz et al., 2000; Franz, 2001) proposed that the same visual representation underlies the illusion effect in perception and in action. That hypothesis finds support only if the factors that influence the perception are the same as the ones that influence the movement. The results presented in this work do not support this hypothesis: We showed that both *MT* and *DT* increased for 'looking smaller' targets surrounded by big context circles. This was not true for 'looking bigger' targets surrounded by small context circle. In accordance with this finding, context size has been found to affect the *MT* towards Ebbinghaus targets in pointing tasks (van Donkelaar, 1999; Handlovsky et al., 2004). In a previous study, we showed that the target size, the context size, as well as the distance between the context circles and the centre of the target may all contribute to the illusion magnitude (see Knol et al., 2015). Here, we show that only one parameter (context size) out of three that affected visual perception, consistently affected the movement (i.e., mainly context size that affected *MT*, *DT*, *EPD, max angle*). It should be noted, however, that a comparison between performances on tasks that are quantified via different measures, with in all likelihood unequal precision to pick up performance differences should be treated with care. At the same time, in Knol et al. all three parameters were found to effect perception whereas in the present study this was not the case. Given that it is unlikely that measurement precision is affected by how the Ebbinghaus figure is parameterized, we are quite confident in stating that our findings cannot be explained by the theory that perception and movement are governed by the same visual information (Franz, 2001; Franz et al., 2000; Franz and Gegenfurtner, 2008).

Regardless the factors that determine the effect of the illusion on movement and perception, the question remains whether the movement is scaled according to the perceived target size (as predicted by hypothesis 2 here above). Van Donkelaar (1999) suggested that the relative size of the targets determined the *MT* rather than the absolute size, by showing that movements towards perceptually smaller targets were significantly slower than to perceptually bigger targets. However, as said, in that study the perceptual illusion effect was unfortunately not quantified, that is, the *MT* was scaled with the (or: a supposedly) perceived target size (van Donkelaar,

1999; see also Lee et al., 2002). Handlovsky et al. (2004) also showed a decrease of *MT* when the target looked bigger, however, this effect was asymmetric; participants did not move slower when the target was surrounded with big context circles. This asymmetry might be explained by the lack of illusion effects for the big context size condition, because the experimental conditions failed to make a target appear smaller than it was. In the previous study in which we quantified the illusion magnitude of the Ebbinghaus figure on visual perception, we demonstrated that different experimental conditions could make a target look bigger and smaller. The results of the present reciprocal pointing task, however, demonstrated only an increase in *MT* when the target looked smaller, and therefore a unidirectional effect in the opposite direction as in the discrete aiming movements in Handlovsky et al. (2004).

The unidirectional effect might seem to contradict the correlation that we found between the perceptual illusion magnitude and the *MT* (for the given data range). This can be interpreted as if movements would be affected by the perceived target size, as Van Donkelaar (1999) suggested, and therefore support *Hypothesis 2*. However, the small correlation reported in our study was mainly explained by the big context condition. Although we found a small correlation with a relatively small sample size, the correlation that we found between perception and action is in accordance with similar (low) correlations in grasping (Kopiske et al., 2016). Taken together, our results partially confirm that the *MT* is scaled according to the perceived target size; the scaling was present (only) when the target looked smaller. Because the perceptual illusion effect was not quantified in Van Donkelaar (1999), and Handlovsky et al. (2004) failed to evoke a 'looking smaller' illusion, it cannot be excluded that these studies would confirm our findings under systematic parameter variations of a wider range of illusion evoking parameters. Whether or not movement adaptations scale in accordance with the perceived target size (when they do) remains an open question, however.

Hypothesis 3. Whether the movement is affected by visual illusions, depends on the movement type.

Continuous reciprocal aiming has been extensively analysed with regard to the underlying dynamics (Mottet and Bootsma, 1999; Bongers et al., 2009; Huys et al., 2010a; Buchanan et al., 2004). Under low accuracy constraints, movements have been shown to be continuous and governed by limit-cycle behaviour. Under high(er) accuracy constraints the movements are governed by fixed point behaviour (i.e., moving between to fixed points, which are (located at) the targets)(Huys et al., 2010a; Buchanan et al., 2006). Following previous studies (Huys et al., 2010a; Buchanan et al., 2006), we expected the transition to happen around *ID* 5, and hence we selected *ID* 4, 5, and 6 in our present experiment. If the perceived target size is driving the reciprocal movement, the underlying dynamics should correspond to those associated with the perceived target size instead of the real target size. The increase in both *DT* and *MT* together with a stronger pronounced presence of a fixed-point (i.e., bigger maximum angle between the vectors around the endpoint of the movement) hinted at changes in the underlying movement dynamics. These changes, however, were not indicative for a transition from limit cycle to fixed-point behaviour, and, moreover, were seen for each *ID*. That is, movement adjustments were not dependent on the motor class utilized. This leads us to conclude that if movements are affected by visual illusions, they are so irrespective of the dynamics that govern these movements. This conclusion stands in contrast to our expectation, namely that the Ebbinghaus figure would have less influence on fairly uniform cyclic movements as compared to a sequence of discrete movements. The expectation was based on a phylogenetic argument and the experimental finding showing that vision is of less importance in conditions demanding little accuracy than in stringent accuracy-constrained Fitts' conditions (Bootsma et al., 2002). We tentatively propose that our expectation was wrong because in the present task context, while the precision constraints were scaled by the task, in all conditions the movements had to be made relative to a precisely defined part of the workspace. That is, (spatial) drift is not compatible with successful task performance, the prevention of which requires visual monitoring (be it continual or intermittent).

Next to the three hypotheses discussed above, our findings bear on alternative views found in the literature that we will discuss here below. For instance, in the

planning-control model, proposed by Glover (2002), the planning of a movement is thought to be susceptible to the visual illusion, but its control is not (Glover, 2002). The planning, but not control component is small in reciprocal tapping movements, which therefore supposedly resist the visual illusion. However, this explanation cannot account for our findings of an affected *MT* and *DT*, maximal vector field angle, and endpoint distribution. Moreover, the effects of the illusion-based pointing movements were mainly present in the deceleration part of the movement (i.e., *DT*). *DT* is typically associated with online control (Elliott et al., 2001), and has been shown to be susceptible to visual illusions (Handlovsky et al., 2004). Therefore, the evidence presented here is at odds with the planning-control model.

In different studies, authors have considered the specificity of dependent variables to assess the effect of visual illusions on conscious perception and action. For example, it has been shown that grip aperture, that is, a measure widely used to highlight the effects of visual size illusions on action (Aglioti et al., 1995; Franz, 2001; Haffenden et al., 2001), is adjusted at the very beginning of movement onset based on the position of the grasp points on the object rather than the distance between them (Brenner and Smeets, 1996; Jackson and Shaw, 2000; Smeets and Brenner, 1999, 2008). Thus, the finding that some aspects of action are somewhat resistant to size illusions may reflect a dichotomy between the processing of visual information for different spatial attributes (e.g., size and position), rather than between perception and action (Brenner and Smeets, 1996; Jackson and Shaw, 2000; Smeets and Brenner, 2008). Our results show similarities with Smeets et al. (2002) who concluded that: "The illusions affect some aspects of spatial perception. Whether this affects execution of a task does not depend on whether the task is perceptual or motor, but on which spatial attributes are used in the task." Along similar lines we suggest that whether a task (perceptual or motoric) is sensitive to Ebbinghaus figures may well depend on the (type of) information that is being used for that given task. That is, whether and which task parameters result in an illusion (perceptual, motoric) depends on the information used for task accomplishment rather than whether the task is perceptual or motoric.

Several potential methodological pitfalls have been identified in previous studies on the effects of size-weight illusions on perception and/or action. As for example, the comparison between the perceptual illusion magnitude and the perceptual-motor illusion magnitude was previously not made due to the differences in measurement units (i.e., distance versus speed)(Skewes et al., 2011). Therefore, the data presented here are reported relative to within-participants' control conditions (in percentage), and the data for perception (retrieved from Knol et al. (2015)) and the Fitts' task were matched per participant. The comparison between studies needs to be handled with care, however. Clearly, the perception task, and its quantification, was not identical, and cannot be identical, to (that of) the perceptual-motor task. The perceptual staircase procedure that was used to quantify the perceptual illusion magnitude in Knol et al. (2015) consisted of a probe that was scaled according to the (binary) responses of the participant on one side, and an Ebbinghaus figure on the other side that was kept constant within one staircase (Knol et al., 2015). The Fitts' task was designed to be symmetric by presenting two identical Ebbinghaus figures (and not a participant-adjusted probe on one side and an Ebbinghaus figure on the other side) on the left and right side of the screen to avoid task-induced asymmetries between left-right and right-left movements, and to allow for inter-subject comparisons. Next to this procedural issue, and probably more important, it is clear that the quantification of the perception and the movements are different (with that of the movements arguably being far more precise than that of perception). One may therefore indeed question whether inferences based on the comparison between the Knol et al. (2015) and present study are valid. We believe they are for the following reason. The results of Knol et al.'s perceptual study indicated that the measurement precision sufficed to find effects for all three Ebbinghaus figure parameters. In the present movement study, we consistently found significant effects on movement for one parameter (context size) but not for the other two parameters (target size and target – context distance). As measurement precision cannot be assumed to depend on the parameter tested for, we may safely conclude that the movement measurement precision was sufficient to detect effects if present. Our failure to detect effects of the other two parameters must thus imply that these parameters did not influence the movements. Given that insufficient measurement precision in both

studies can be ruled to out to have impacted our pattern of results, we are confident that our inferences based on the comparison between the two studies hold.

Another issue that in potentially may have impacted our results is that of obstruction avoidance. Some authors have discussed whether the context circles of the Ebbinghaus figures might be identified as obstructions that should be avoided by the system (Goodale, 2011). By fixing the coverage of the circumference by the context circles to 75 %, and thus the open space to 25 %, we tried to keep the obstruction of the path towards a target equal over illusion conditions. If obstruction avoidance had been triggered by the size of the obstructers, in our case the size of the context circles, then the bigger context size would have obstructed more than the smaller context circles, and small context circles more than the control condition (i.e., no context circles). Furthermore, the distance between the target and context circles should have influenced the illusion effect on movement as was shown for grasping movements(Haffenden et al., 2001). We did not find evidence in that regard, and therefore assume that a different mechanism is responsible for the illusion effects on the perceptual-motor system. Note that our believe that obstruction avoidance has played a negligible role, if any, in our present study is supported by a large, multi-lab study of Kopiske et al. (2016) that examined the obstruction avoidance hypothesis in 144 participants. They found no evidence that the effects of visual illusions on grasping could be explained by obstruction avoidance. We therefore are confident that our reported effects cannot be traced back to obstacle avoidance.

In this work we developed a method to assess the movement on the plane (i.e., spanned by the horizontal x and vertical position y). This resulted in a detailed classification of targeting and movement. The reasoning for this assessment of movements on the plane is twofold. Firstly, the targets are of circular shape, which gives a restriction in all directions on the plane (e.g., compared to elongated target shapes such as bars). The target shape (e.g., squared, circular, diamond, and triangular) has shown to affect movement time in Fitts' tasks(Sheikh and Hoffmann, 1994). This experimental result may indicate not only a change in movement in horizontal direction (i.e., shortest path between the targets) but also an involvement

of the vertical direction. In other words, the length of the trajectory is longer than the shortest path depending on the target shape. This means that analysing the movement in horizontal direction (projection of the movement on the *xy*-plane onto the horizontal direction *x*) may not always be justified. Secondly, the effect of the Ebbinghaus figure on movements was expected to be quantitatively small. In a previous study we have shown that perception of the same Ebbinghaus figures resulted in small illusion magnitudes (rarely up to 10 % of the target size)(Knol et al., 2015). It was therefore unclear whether the effect of the Ebbinghaus figures could be measured from the displacement in horizontal direction, or that both directions were required. Because of these two points, the target shape effect on movement and the expected small effects that we aimed to quantify in the movement, we considered the actual trajectory on the plane. Thus, the here presented method allows for a detailed analysis of aiming movements, which especially suits experiments working with (visual or motor) perturbations.

We found unambiguous evidence that variations in one Ebbinghaus figure parameter (context size), similar to scaling the perceptual illusion effect, consistently affected the pointing movements. Therefore the hypothesis that the visual streams are functionally dissociated is not supported. Variations in the other figure's parameters that elicited perceptual illusions in the same group of participants did not (or hardly) affect the movement (target size affected the maximum angle in the vector fields). That is, we neither found evidence for the hypothesis that perception and action are guided by the same internal representation (nor for the hypothesis that the occurrence of 'motor illusions' depends on the motor class underlying the behaviour). Can these findings that lead to opposing interpretations as to the validity of the hypothesis that the visual steam if functionally dissociated be reconciled by acknowledging, as Milner and Goodale (Goodale and Milner, 1992) did, the existence of cross talk between the ventral and dorsal stream? One would expect that interactions between the streams could attenuate the effect of a functional segregation. To reconcile the present results via stream interaction requires that the (degree of) interaction depends on the parameters via which the (perceptual) illusion is brought about. This would imply that the visual system would be sensitive to

these at an early stage of the visual processing, which we deem unlikely. At least, we are not aware of research pointing into that direction. This issue, however, cannot be answered with purely behavioural studies but requires the utilization of high-resolution brain imaging techniques. Regardless, whether the geometry of a visual figure elicits a motor illusion appears to be independent of whether it elicits a perceptual illusion. These findings, which cast doubt on the assumption that visual illusions are an appropriate means to study the supposed functional dissociation of the visual system, can be explained by assuming that which informational variables are extracted from a geometrical outlook depends on the task, including whether it is perceptual or motoric. It remains to be discovered which anatomical regions are organized functionally in the execution of (visually perturbed) perception and action tasks using high resolution imaging techniques.

4.6 Supplementary information

Since the distribution of the classified movements (i.e., misses, two-sided and one-sided overshoots) is non-normally distributed, we performed a Friedman test instead of the parametric repeated measures ANOVA.

Misses

The number of misses neither showed significant differences for the left target and right target nor for any of the tested conditions.

Two-sided overshoot

On the left and right side, there was a significant influence of the experimental conditions on the number of 2-sided overshoots (left target: χ^2 (23)=87.62, p < .001; right target: χ^2 (23)=99.99, p < .001). Posthoc tests, using Wilcoxon signed-rank tests with the Bonferroni correction (α/number of comparisons), showed a significant difference between the small and medium (Z_{left} = 3.79, Z_{right} = 4.60, p<.001), medium and big target size (Z_{left} = 4.53, Z_{right}=5.48, p <.001), and small and big target size (Z_{left} = 6.01, Z_{right}=6.44, p <.001), for both the left and right target (see Figure S4.1). No significant effects were found for repetition, context size, and the distance between the target and context.

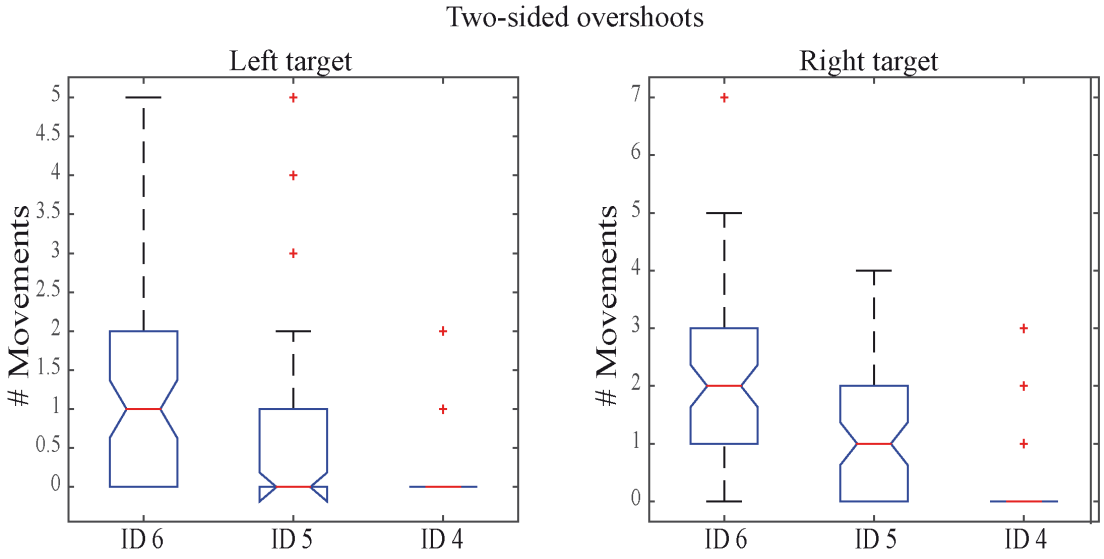

Figure S4.1 Box plots of the number of two-sided overshoots for ID 6, ID 5, and ID 4 for the left and right target.

One-sided overshoot

On the left and right side, there was a significant influence of the conditions on the number of 1-sided overshoots (left target: χ^2 (23)=43.65, p < .01; right target: χ^2 (23)=37.73, p < .05).

Posthoc tests showed a significant difference between the small and medium (Z_{left} = 3.96, p< .001, Z_{right} = 3.30, p= .001), and small and big target size (Z_{left} = 3.39, Z_{right}=3.89, p <.001), for both the left and right target (see Figure S4.2).

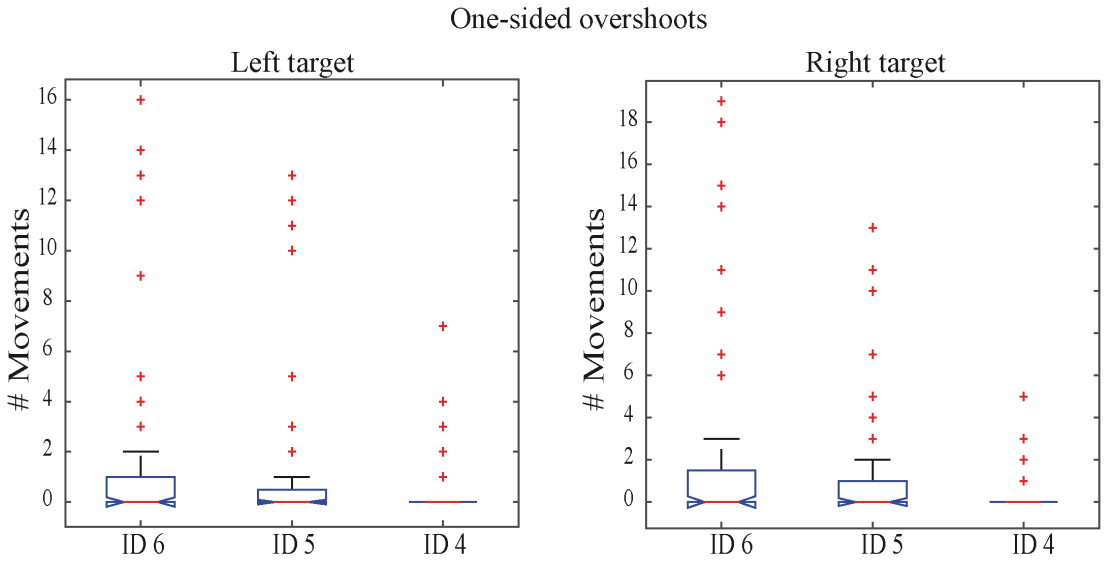

Figure S4.2 Box plots of the number of one-sided overshoots for ID 6, ID 5, and ID 4 for the left and right target.

Invalid movements

The sum of the misses, the one-sided and the two-sided overshoots represents the number of invalid movements for each experimental condition. On the left and right side, there was a significant influence of the conditions on the number of invalid movements (left target: χ^2 (23)=83.71, p < .001; right target: χ^2 (23)=112.17, p < .001). Posthoc tests showed a significant difference between the small and medium (Z_{left} = 4.51, Z_{right} = 4.38, p<.001), medium and big target size (Z_{left} = 4.20, Z_{right}=5.39, p <.001), and small and big target size (Z_{left} = 6.04, Z_{right}=6.61, p <.001), for both the left and right target (see Figure S4.3).

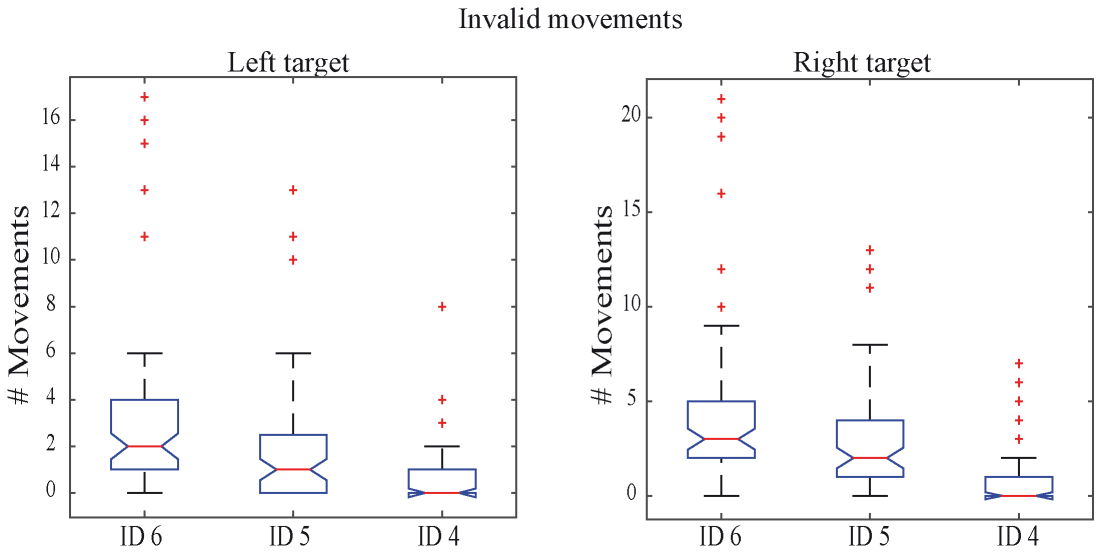

Figure S4.3 Box plots of invalid movements for ID 6, ID 5, and ID 4 for the left and right target.

Trajectory Length

The length of the trajectory l is obtained by calculating the Euclidean distance, that is, $l[n, n+1] = (x[n+1] - x[n])^2+(y[n+1] - y[n])^2)^{1/2}$ of pairs of successive samples $s[n]$ at time point n and n+1 on the plane ($x[n]$ and $y[n]$), and then calculating the sum $l = \sum_{n=1}^{N-1} l[n,n+1]$, where N is the total number of sampled points in the xy-plane. There was no difference between the trajectory length from left to right or right to left (from start to end) (t-test, p=.95). Furthermore, there was no significant effect of target size on the trajectory length in the control condition (χ^2 (26)=2.89, p = .24). Further analysis of factors context size, target—context distance, and trial number showed no effects on the trajectory length.

X-Y separation

To check whether the X-Y plane can be reduced to just the horizontal direction (X), we checked whether a scale separation occurred, with the criterion that the Y direction contributed more than 10% to the total trajectory length.

In 4.3% of all movements, the Y direction contributed more than 10% to the total movement length as compared to the X direction.

Linear Regressions

Linear regression analyses were performed on all data points at group level and individual level. The results of the linear regression analysis are shown in Table S4.1.

Table S4.1 Linear regressions' estimates for individual movement time data over the index of difficulty, with *a* representing the intercept, and *b* the slope for the control (C), small context (S), and big context condition (B).

Participant	R^2			$RMSE^2$			a			b		
	C	S	B	C	S	B	C	S	B	C	S	B
1	0.72	0.76	0.72	0.01	0.01	0.01	-0.25	-0.33	-0.14	0.21	0.24	0.20
2	0.57	0.60	0.60	0.02	0.02	0.02	0.02	-0.09	-0.04	0.19	0.21	0.21
3	0.81	0.83	0.78	0.01	0.01	0.01	-0.51	-0.60	-0.46	0.27	0.29	0.26
4	0.73	0.79	0.72	0.02	0.01	0.02	-0.48	-0.57	-0.49	0.27	0.28	0.27
5	0.72	0.79	0.75	0.06	0.05	0.03	-0.82	-1.16	-0.41	0.47	0.53	0.38
6	0.75	0.79	0.73	0.02	0.01	0.02	-0.49	-0.29	-0.25	0.30	0.26	0.25
7	0.76	0.74	0.77	0.01	0.01	0.02	-0.46	-0.43	-0.59	0.26	0.25	0.30
8	0.68	0.67	0.67	0.01	0.01	0.01	0.13	0.10	0.14	0.16	0.17	0.17
9	0.75	0.77	0.58	0.03	0.03	0.04	-0.67	-0.69	-0.25	0.36	0.36	0.30

Frequently the linear regression analysis is performed over mean movement time data, leading to higher R^2 values and a smaller $RMSE^2$. For completeness the results of the linear regression analyses for the control condition (C), the small context (S), and the big context (B) are reported in Table S4.2.

Table S4.2 Linear regressions' estimates for group mean movement time data over the index of difficulty, with *a* representing the intercept, and *b* the slope for the control (C), small context (S), and big context condition (B).

R^2			$RMSE^2$			a			b		
C	S	B	C	S	B	C	S	B	C	S	B
0.9974	0.9939	0.9997	<.0001	0.001	<.0001	-0.39	-0.45	-0.28	0.28	0.29	0.26

Chapter 5 | *Perception and Action Mechanisms*

"Order parameters in biological systems are just as real as our thoughts."

- Hermann Haken

5.1 Introduction

The discussion around perception and its coupling to action is age-old. This long history of vision, perception, and perception-action research has led to numerous theories and hypotheses. One theory that has been applied to complex behaviour, also perceptual and motoric behaviour, is the dynamical systems theory (DST). The dynamical systems theory has emerged as an applicable framework for modelling biological systems by means of (nonlinear) differential equations (among others).

In the previous chapters, mainly *Chapter 3* and *Chapter 4* we[5] sought to identify the dynamics that are underlying pointing movements in Fitts' tasks. With the mathematical descriptions that allow for predicting behaviour given a current state, like vector fields and probability distributions as described in *Chapter 3* and *Chapter 4*, we found indications for changes in the behavioural dynamics. In this chapter we want to explore whether the changes in dynamics that we have observed experimentally due to the Ebbinghaus figure, can be explained by structural changes in the parameters of a non-linear dynamical model. Thus, we aim to combine perception and action in a dynamical systems framework. This type of comparison of

[5] 'we' is a synonym for the collaborators of this work: A. Spiegler, R. Huys, and V.K. Jirsa.

experimental data and (dynamical) models can provide a deeper knowledge of the coupling of perception and action.

5.2 Background

5.2.1 DST - Motor control

Bernstein rejected the idea that integrated movements can be best described as a chain of interlocking reflexes. Bernstein postulated a few key questions about motor control and the coordination thereof. He identified a problem that is called the degrees-of-freedom problem (Bernstein, 1967). The degrees-of-freedom problem poses the question of how the human body coordinates the redundant anatomical, neurophysiological, and kinematic degrees of freedom. It states that there are multiple ways to execute a task with the same outcome, and that there is no unique map between task execution and the result thereof. He suggested that synergies (i.e., functional units spanning multiple muscles and joints) were temporarily organized to minimize the degrees of freedom. This revolutionary conceptualization of motor control was the fundament for approaching motor control in terms of (non-linear) dynamical structures. From that perspective, the human neuro-musculo-skeletal system is a dynamical system that can transiently organize (and disorganize) its components into functional units and into regimes to meet different task demands (Kelso, 1995; Haken et al., 1985). Or, as Kelso (1995) said: "I envisage it as a constantly shifting dynamic system; more like the flow of a river in which patterns emerge and disappear, than a static landscape."

This view on motor control gained much attention, mainly because the human body and brain were not considered to be a mere computer-like device, with static and timeless entities that are unaffected by the past. In stead, motor control was seen as a dynamic coming and going of (stable) patterns that were thus not timeless and independent, and could therefore be constantly changing. As a result of this dynamic concept of motor control, pattern formation was studied at a behaviour and muscular level, including for example in reciprocal aiming movements (e.g., Mottet and Bootsma, 1999; Huys et al., 2010b; Sleimen-Malkoun et al., 2012; Vernooij et al., 2016; Guiard, 1993).

Voluntary reaching movements require precision to reach the target in order to be able to manipulate it (e.g., grasping a pen, or pointing at a black board). As described in *Chapter 1*, time and space relate in a systematic fashion with regard to pointing movements (e.g., Woodworth, 1899; Fitts, 1954). As summarized and discussed in *Chapter 3*, the speed-accuracy trade-off imply that any (experimental) increase in relative precision requirements will lead to a systematic drop in average speed, accompanied by systematic changes in movement kinematics (e.g., longer deceleration phase for small targets). To describe the dynamics of goal directed reaching movements, a mathematical model needs to be able to describe how time and space relate. Mottet and Bootsma (1999) proposed a minimal dynamical model to account for the main features of a reciprocal aiming movement under various accuracy constraints that were identified experimentally. The model contains a self-sustaining, velocity-driven Rayleigh oscillator and a nonlinear stiffness being the softening spring Duffing term (the RD-model),

$$\ddot{x} + d_{10}x - d_{30}x^3 - d_{01}\dot{x} + d_{03}\dot{x}^3 = 0 \qquad (5.1)$$

for which x represents the horizontal position, $\dot{x}$ the first derivative of x, $\ddot{x}$ the second derivative of x, and d_{ij} are the model coefficients.

According to the bifurcation analysis (see supplementary information in Huys et al., 2010a), the Duffing term is related to the temporal constraints (i.e., frequency), and the Rayleigh oscillator to the spatial constraints (i.e., amplitude). The model has some limitations, but by and large it reproduced the kinematic patterns that were observed experimentally and captured most of the variance (Mottet and Bootsma, 1999). The coefficients d_{ij} changed in a systematic fashion as a function of the index of difficulty (see Figure 5.1).

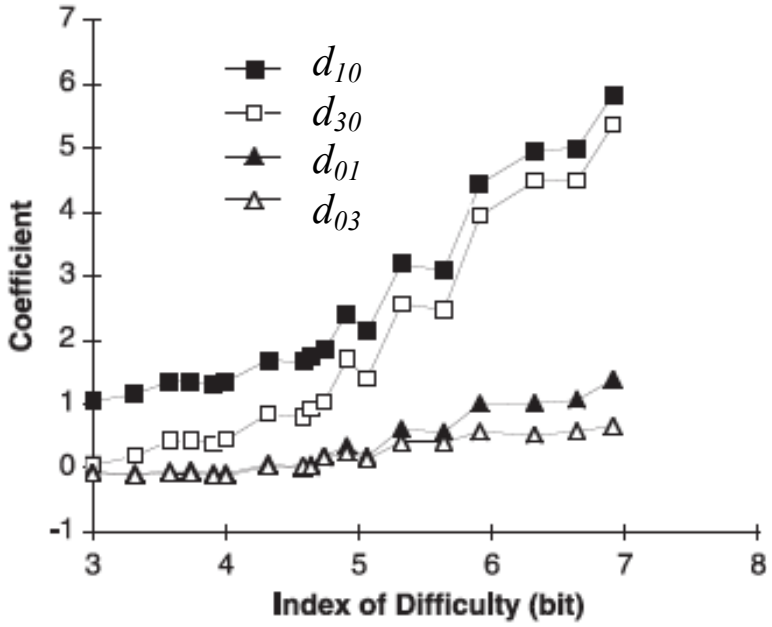

Figure 5.1 Coefficients of the RD model (normalized time and space) as a function of task difficulty. Increasing *ID* shows a parallel increase of the damping (*triangles*) and stiffness (*squares*) coefficients, denoting an increasing contribution of the nonlinear terms. Adapted from "*The dynamics of goal-directed rhythmic aiming*" by D. Mottet and R.J. Bootsma, 1999, *80*(4), 235-245.

5.2.2. DST – perception

Visual percepts are almost invariably monostable (Hock and Schöner, 2010). The same percept occurs each time an object is presented. However, exceptions exist when ambiguous percepts occur evoked by visual illusions. That is, bistability of perception occurs when two different percepts are possible for one stimulus. Have a look at the Necker cube (Figure 5.2). While looking at cube A you can either perceive the cube as in panel B or C. This percept can change from B to C while you are looking at A.

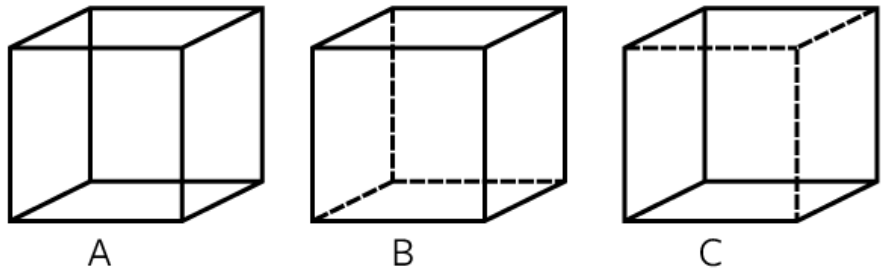

Figure 5.2 Necker's cube.

The ambiguous perception of the figures that allow for a continuous fluctuation between two possible percepts (i.e., non stationarity) has been successfully captured by a nonlinear dynamical model of human perception (Ditzinger and Haken, 1989, 1990). It models the switches between ambiguous patterns by humans by a set of coupled differential equations, which describe the formation of percepts by means of order parameters. The degree to which a participant recognizes an individual pattern k is described by the order parameters ξ_k, which in turn is determined by the saturation of the corresponding attention parameters λ_k. This model relies on the hypothesis to explain the bistable percepts by means of saturation of perception (Köhler, 1940). The oscillation between percept B and percept C (from Figure 5.2) is due to neural fatigue, inhibition or saturation. This model also can account for hysteresis in perception, in which the place of the transition from one percept to another percept depends on the direction of view (e.g., see Figure 5.3).

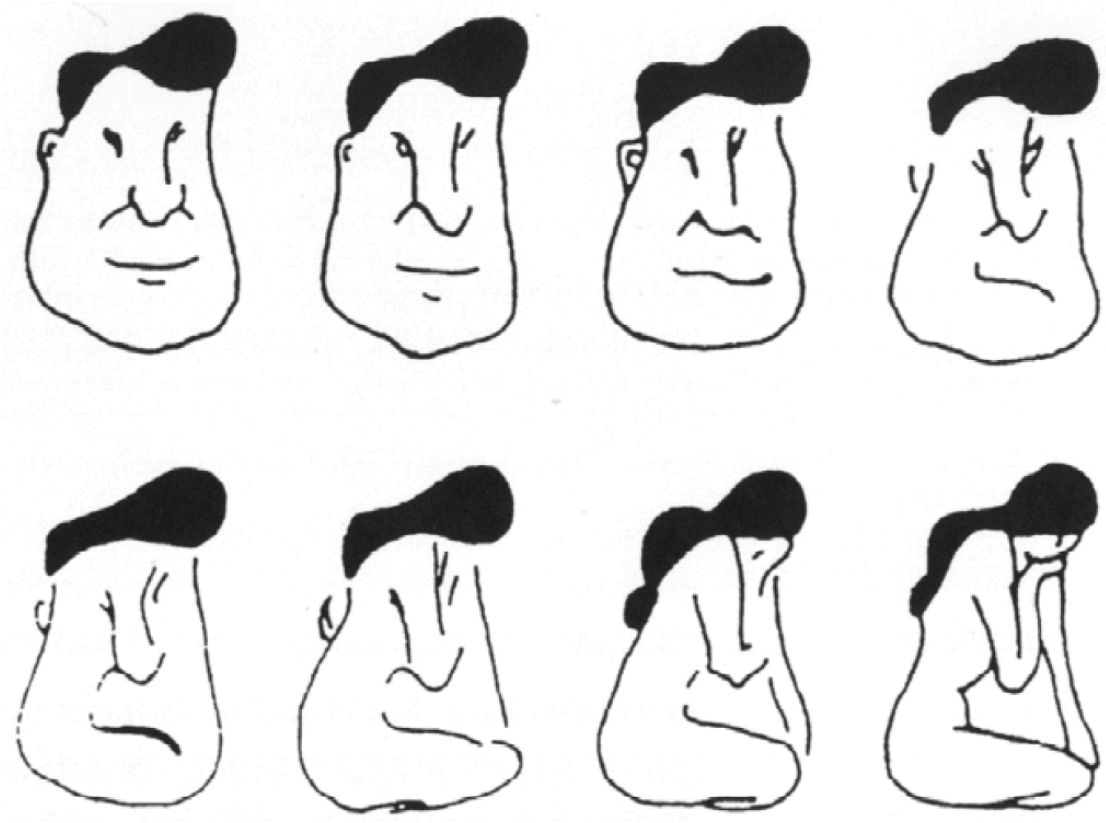

Figure 5.3 The bistable Reagan-Nude woman illusion. Hysteresis occurs since the percept depends on the direction of view. Adapted from Ditzinger, T (2010). Optical illusions: examples for nonlinear dynamics in perception. In Huys R. and Jirsa V.K. (Eds.). *Nonlinear Dynamics in Human Behavior* (p. 182).

However, this conceptualization works with figures that evoke either one percept, or the other (i.e., bistability). Unless the target size is categorized in a binary category (e.g., *bigger*, or *smaller*) there is no bistability. Thus, for the perception of size illusions (see *Chapter 1*) there is no clear bistability (or multistability: see Figure 5.4), since the size of a target can be perceived and estimated on a continuous scale. However, as we have hypothesized in *Chapter 2*, there are some indications of hysteresis in the perception of the Ebbinghaus figure. Modelling this relation requires more experimental data, and is beyond the scope of this thesis. Regardless, in the next section the relation between the percepts of Ebbinghaus figures and the movements towards these figures will be analysed based on a dynamical model of voluntary reaching movements.

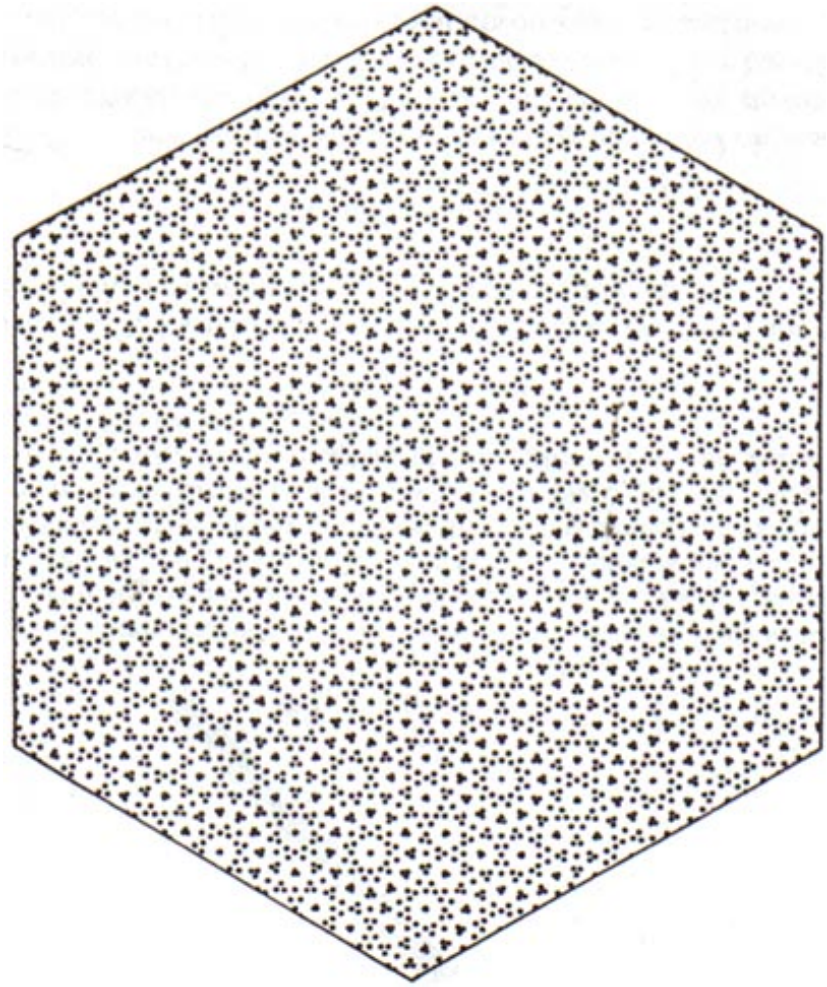

Figure 5.4 An example of multistability in perception.[6]

5.2.3 DST – perception-action coupling

RD-model influenced by Ebbinghaus figure

While having seen an increase in deceleration time and movement time as a function of context size (and perceived target size), and some indications for changes in the dynamics of the pointing movements (see Figure 4.5 and 4.8), we were wondering if these RD-model coefficients would change in a systematic fashion as a function of the Ebbinghaus figure conditions. In other words, does the percept influence movement?

[6] The name of this figure, and the author are unknown.

Therefore we wanted to match our experimental data to the model (Equation 5.1) of Mottet and Bootsma (1999). The model parameters d_{ij} are scaled to find the best fit with the experimental data.

Hypotheses

In order to formulate a hypothesis in equations, we will reformulate the findings of the previous chapters. Recall that we quantified the perceived target size for a set of Ebbinghaus figures with different target sizes, context sizes and target—context distances. A probe (i.e., a circle without context circles) was scaled following a staircase procedure. The main finding of *Chapter 2* was that all factors of the Ebbinghaus figure (target size, context size, target—context distance) influenced the normalized perceived target size (i.e., normalized with respect to the control condition). In addition, interactions between target size and target—context distance, and between target and context size further influenced the perceived target size. The experimental results of the perception study (*Chapter 2*) can be reformulated as follows:

I. Percept P_v relative to the control condition:

In both experiments (*Chapter 2* and *4*), the parameters were separately adjusted. The parameters are the target size *a*, the target-context distance *b*, the context size *c*, and the scaled probe size *r* (see Figure 2.1). In the perception task, the participants were asked to relate the centre circle of the Ebbinghaus figure, which is parameterized by *a*, with respect to the probe circle, parameterized by *r*. The percept P_v may be formulated as a function *f* of the set of Ebbinghaus parameters {*a*, *b*, *c*} given a probe of size *r*:

$$P_v = f\left\{ \; a,\, b,\, c \;\middle|\, r \;\right\}. \qquad (5.2)$$

Note that the Ebbinghaus figure is geometrically described (see *Chapter 2*). Although the three geometrical parameters are independently controlled during the experiments, changes of the parameters may have similar effects on the participants' perception. Indeed, the statistical analysis of the perceptual task (presented in *Chapter 2*) suggests an interaction between the context size *c* and the target size *a*; and

an interaction between the target-context distance b and the target size a. As a consequence of the perceptual task to judge the target size a given the probe of size r, that is, $(a \mid r)$, the relation between the Ebbinghaus parameters $\{a, b, c\}$ in equation (5.2) can be specified as follows:

$$P_v = f\left\{ \begin{array}{c} a \mid r \\ b\left(a \mid r\right) \\ c\left(a \mid r\right) \end{array} \right\}, \tag{5.3}$$

where the target-context distance b is a function of the target size a given the probe r, and the context size c is expressed as a function of the target size a given the probe r. This indicates that the percept P_v mainly relates the target size a to the probe r, and thus equation (5.3) can be written so that the target-context distance b and the context size c are separate modulators:

$$P_v = f\left\{ \begin{array}{c} b \\ c \end{array} \right\}\left(a \mid r\right). \tag{5.4}$$

Next, the potential role of the percept P_v in the movement is discussed.

II. Perception-action:

We want to study three (extreme) hypotheses that we have previously seen in *Chapter 4* for the movement task. Because the movement task displayed two identical (i.e., symmetrical) Ebbinghaus figures, and there was no scalable probe r, r is taken out of equation 5.4 and the *vision for perception* P_v reads:

$$P_v = f\left\{b, c\right\}(a) \tag{5.5}$$

The question is however, how the perceptual information for movements is influencing the action. Therefore, we formulate the *vision for action* P_a (or vision for action) as a function k of the effective (or perceived) target size W, the distance between the two targets D, and the movement x in time t:

$$P_a = k\left(W, D, x, t\right). \tag{5.6}$$

Furthermore, the question is whether perception for vision P_v (equation 5.5) is different from vision for action P_a (equation 5.6). The movement x itself is a function h of time t, perceived target size W, and the distance between the targets D. This can be expressed as

$$x = h(t,\ W,\ D) \tag{5.7}$$

Possibilities to test these hypotheses with the Mottet and Bootsma (1999) model (Equation 5.1) are to test the relationship of d_{10} to the experimental parameters and fix d_{30}, d_{01}, d_{03} to the parameters identified by Mottet and Bootsma (1999; see figure 5.1). The conservative linear stiffness coefficient d_{10} can make the system run slower, and thus might correspond to the increase in MT, through an increase in DT that we have observed in *Chapter 4*. Because we are interested in the changes of the RD-model coefficients, we want to study the movements x over time t as a function of the set δ of the RD-model coefficients d_{ij}:

$$x = g(t,\ \delta), \tag{5.8}$$

where δ is the set of model coefficients $\delta = (d_{01}, d_{10}, d_{03}, d_{30})$. The model configuration δ is then a function l of the target size W and the distance between the two targets D:

$$\delta = l(W, D), \tag{5.9}$$

where every coefficient depends on target size and target distance d_{ij} (W, D). As identified in *Chapter 4*, three different hypotheses will be presented in the following paragraph.

Hypothesis 1 — *The visual-stream is functionally dissociated, hence a visual illusion does not affect movements.*

If the visual streams are functionally dissociated, and the visual illusions do not affect movements, then the perceived target size W equals the physical size a of the target circle:

$$W \equiv a \tag{5.10}$$

Thus, P_m is independent of P_v. This leads to

$$\begin{cases} P_a = k\left(a, D, x, t\right) \\ P_v = f\left\{b,\ c\right\}(a) \end{cases} \tag{5.11}$$

Note that the vision for perception P_v is unchanged compared to equation (5.5). Whereas the percept P_v is influenced by the set of Ebbinghaus parameters {*a*, *b*, *c*}, the vision for action P_a is not influenced by the context circles in the Ebbinghaus figure, which are parameterized by {*b*, *c*}, but only by the target size *a*. The movement described in equations (5.7 to 5.9) is hence a function of the physical target size $W \equiv a$, and the target distance *D*. This simply obeys Fitts' law (see *Chapters 3* and *4*). Note that this is in line with the modelling study by Mottet and Bootsma (1999).

Hypothesis 2 — *A one-to-one mapping between vision for perception and vision for action exists; hence the (consciously) perceived target size determines the movement.*

If a one-to-one mapping exists, then the perceived target size *W* during the vision for action P_a, is related to the vision for perception P_v:

$$W = \tilde{P}_v, \tag{5.12}$$

where P_v is given by equation (5.5), and the tilde refers to a possibly altered function *f* with respect to the perceived target size *W*

$$W = \tilde{f}\left\{b,\ c\right\}(a). \tag{5.13}$$

Considering a relation of the vision for perception P_v in the perceived target size *W*, the vision for action P_a reads:

$$\begin{cases} P_a = \tilde{k}\left(P_v,\ D,\ x,\ t\right) \\ P_v = f\left\{b,\ c\right\}(a) \end{cases}, \tag{5.14}$$

where the tilde again indicates a possibly altered function *k*. Note that the vision for perception P_v is unchanged compared to equation (5.5). Both, the vision for perception P_v and the vision for action P_a are influenced by the set of Ebbinghaus parameters {*a*, *b*, *c*}. As a consequence, the movement described in equations (5.7 to

5.9) is a function of the perceived target size $W = \tilde{P}_v$ given by equation (5.11), and the target distance D. Hence, the movement may not obey Fitts' law (see *Chapters 3* and *4*), indicating that Fitts' law can be adapted into a perception-action framework considering vision for perception and vision for action. The coefficients d_{ij} (a, b, c, D) of the RD-model in equations (5.1), (5.8) and (5.9), are then modulated by the set of all three parameters of the Ebbinghaus figure, {a, b, c}, which specifies the perceived target size W (see equation 5.12), and the distance D. This is extending the modelling work by Mottet and Bootsma (1999) by including perception.

Hypothesis 3 — *Perception is influenced by all Ebbinghaus factors, but only one Ebbinghaus factor influences movement*

In case that the vision for action is sensitive to specific Ebbinghaus parameters, then the vision for perception in equation (5.5) can be divided into two parts so that the perception of the target is either modulated by the target-context distance b or the context size c (given a target of size a):

$$W \subseteq P_v, \tag{5.15}$$

where the sign $\subseteq$ indicates that W is a proper subset of P_v which is $b(a)$ or $c(a)$:

$$W = \begin{cases} b(a) \\ c(a) \end{cases}. \tag{5.16}$$

As a consequence, vision for perception and vision for action are differently related to the set of Ebbinghaus parameters {a, b, c}, and thus the vision for perception relates differently to the vision for action in contrast to the hypotheses 1 and 2. Considering the partial relation of the vision for perception P_v in the perceived target size W, the vision for action P_a reads:

$$\begin{cases} P_a = \tilde{k}\left(\subseteq P_v,\, D,\, x,\, t\right) \\ P_v = f\left\{b,\, c\right\}(a) \end{cases}, \tag{5.17}$$

where the tilde indicates a possibly altered function k in equation (5.6).

Note that the vision for perception P_v is unchanged compared to equation (5.5). Both, the vision for perception P_v and the vision for action P_a are influenced by the set of Ebbinghaus parameters {*a*, *b*, *c*}. Whereas the vision for perception P_v is modulated by the target-context distance *b* and the context size *c* given a target of size *a,* the vision for action P_a is either sensitive to the target-context distance *b* or the context size *c* (given a target of size *a*). As a consequence, the movement described in equations (5.7 to 5.9) is a function of the perceived target size, given by equation (5.16), modulated by the target-context distance *b* or the context size *c*, and the target distance *D*. Hence, again, the movement may not obey Fitts' law (see *Chapters 3* and *4*), indicating that Fitts' law can be adapted into a perception-action framework considering vision for perception and vision for action. The coefficients $\delta = \left(d_{01}, d_{10}, d_{03}, d_{30}\right)$ of the RD-model in equations (5.1), (5.8) and (5.9), are then function of the target distance *D*, the target size *a* and one of the modulators *b*(*a*) or *c*(*a*) of the perceived target size *W* (see equation 5.16). This is an alternative extension of the modelling work by Mottet and Bootsma (1999).

Assessment of the hypotheses — *based on the results from Chapter 4.*

In *Chapter 4* we found that context size was the only factor influencing the movement resulting from Fitts' task. This suggests that hypothesis 3 will hold, whereas hypothesis 1 and 2 will fail.

Possibilities to test these hypotheses with the Mottet and Bootsma (1999) model (Equation 5.1) are to test the relationship of d_{10} to the experimental parameters and fix d_{30}, d_{01}, d_{03} to the parameters identified by Mottet and Bootsma (1999; see figure 5.1). The conservative linear stiffness coefficient d_{10} can make the system run slower, and thus might correspond to the increase in MT, through an increase in DT that we have observed in *Chapter 4*.

Then it can be identified whether the experimental parameters influence d_{10} is a function of the set of Ebbinghaus parameters {a, b, c}. One possibility is that the coefficient d_{10} is a linear superposition of weighted d_{10} with respect to the Ebbinghaus parameters {a, b, c}. The weighted coefficient d_{10} is indicated with the superscripts in

$$d_{10} = d_{10}(a,\ b,\ c) = d_{10}{}^{1}a + d_{10}{}^{2}b + d_{10}{}^{3}c. \qquad (5.18)$$

If only c plays a significant role on movements (as was identified in *Chapter 4*), we expect d_{10} to be a function of context size c only.

This chapter reflects on-going work and will show some preliminary results. Many additional analysis and simulations need to be performed in order to draw conclusions and to verify the hypotheses. Therefore, this chapter serves as a brief discussion about the dynamics of perception, action and its interaction.

5.3 Methods

To compare the RD-model (Equation 5.1) to the experimental data from *Chapter 4*, we applied Bayesian statistical modelling techniques. Bayesian statistics is frequently applied to experimental data to find the statistically optimal way to combine multiple information sources for maximally accurate estimation (e.g., Brayanov and Smith, 2010). Bayesian statistics has also been used as a model comparison tool in order to find the model with the maximally accurate estimation. Instead of comparing models, we wanted to get the best fit for the RD-model to the experimental movement data. The RD-model parameter d_{10} can be estimated using an automated approach. Such estimates of the parameters of the RD-model can be obtained by using the RD-model and a reduced data set for the fitting (i.e., the horizontal position data $x(t)$).

To infer the parameters, prior probabilities are formulated for the unknown parameters, $\pi(\theta \mid I)$ with π representing the probability, θ the parameters, and I any other external information, or the assumed model. The generative model predicts observations from parameters, $\pi(D \mid \theta, I)$ with D being data, also called the likelihood.

The posterior probability of parameters, given data, $\pi(\theta|D,I) \propto \pi(D|\theta,I)\,\pi(\theta|I)$ which is thus *posterior α likelihood* x *prior*.

We selected the RD-model, and were mainly interested in model coefficient d_{10}. Therefore, the model parameters d_{30}, d_{01}, d_{03} were fixed to the values as reported in Mottet and Bootsma (1999) (see Figure 5.1). The model coefficient d_{10} was bound and sampled between 0 and 10. To infer posterior estimates for unknown variables in the model, in this case for d_{10}, the Hamiltonian Monte Carlo inference algorithm was applied. The model is implemented using PyMC3, an open-source probabilistic programming framework for Bayesian inference, which finds the maximum a posteriori point using the Broyden-Fletcher-Goldfarb-Shanno optimization algorithm. Subsequently, it implements both Hamiltonian Monte-Carlo and automatic variation inference algorithms for generic differential probability models (Salvatier et al., 2016).

Experimental data

The horizontal position time series of the reciprocal aiming task performed in *Chapter 4* (for more details on the methods, see *Chapter 4*) were low-pass filtered using a fourth order Butterworth filter, with a cut-off frequency of 10 Hz. The time series were normalized and down-sampled.

Statistics

The mean posterior value for the unknown model parameter d_{10} is subjected to a repeated measures ANOVA, with the within subjects factors target size, target—context distance, and context size, i.e. *a, b, c* in equation 5.2 respectively.

5.4 Preliminary results

The absolute model parameter d_{10} was significantly affected by the target size ($F(2,34)=2974.346$, $p=.000$, $\eta_p^2=.994$; Figure 5.4A) and context size ($F(1,17)=18.775$, $p=.000$, $\eta_p^2=.525$; Figure 5.4B). The factors target—context distance did not significantly influence d_{10}.

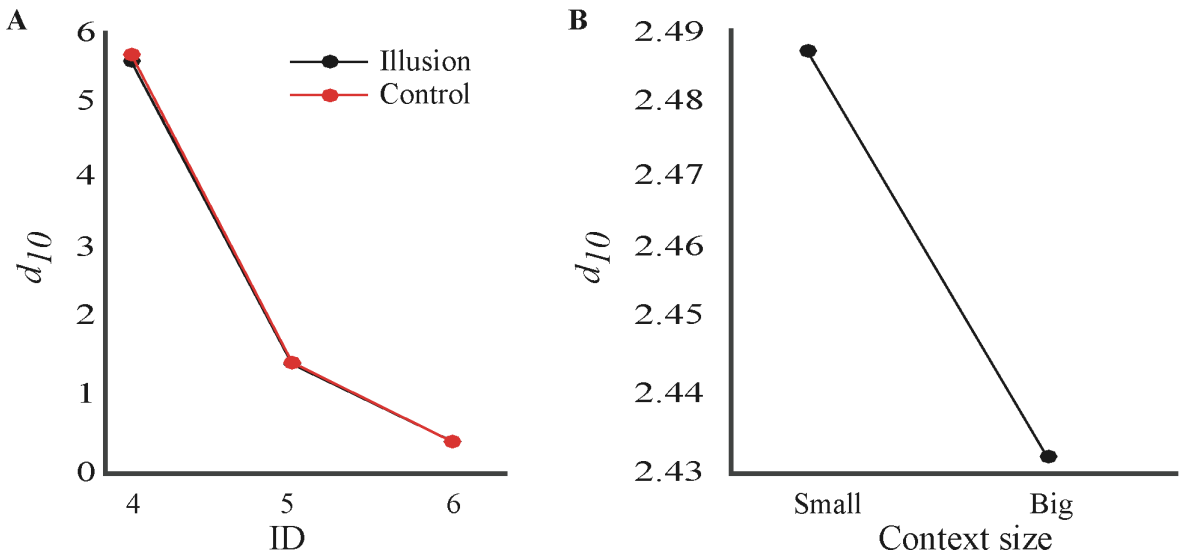

Figure 5.5 Coefficient d_{10} of the RD-model as a function of (**A**) *ID* and (**B**) context size.

To distinguish the effects of the Ebbinghaus figure from the Fitts' task effects due to the changes of the target size, we calculated the effects of the Ebbinghaus figure on d_{10} relative to the control condition, in percentage. Context size significantly influenced the d_{10} parameter ($F(1,17)=19.477$, $p=.000$, $\eta_p^2=.534$; Figure 5.5). The target size and target—context distance did not significantly influence d_{10}.

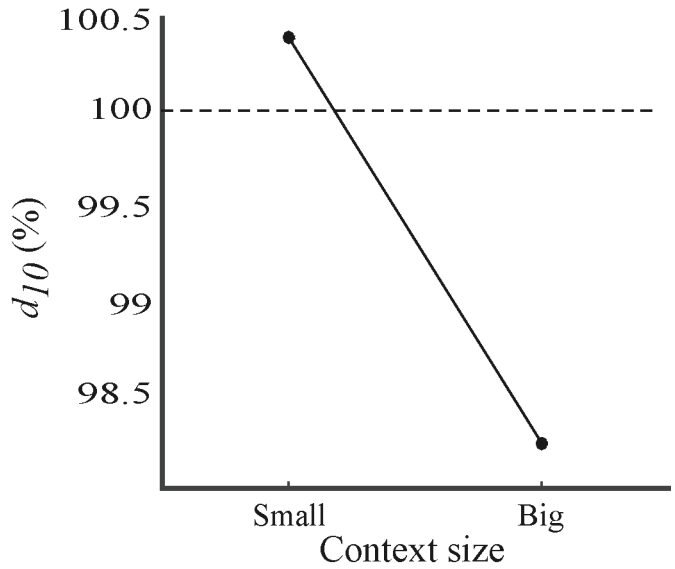

Figure 5.6 Coefficient d_{10} of the RD-model relative to the control condition as a function of context size.

5.5 Discussion

In this chapter we presented a first attempt to fit the RD-model to our experimentally obtained data to investigate the effect of Ebbinghaus figures on the behavioural dynamics by using a Bayesian statistical framework.

In Mottet and Bootsma (1999), the authors showed d_{10} to increase with target width, and decrease with distance. The increase of *MT* in their Fitts' task denotes a global slowing of the motion, which is mainly due to the decrease in the linear stiffness d_{10}. In *Chapter 4* we reported an increase in *MT* when a target was surrounded with big context circles (Figure 4.5), and looked smaller. In line with these findings, the model parameter d_{10} decreased when a target was surrounded with big context circles. These results indicate a slowing down due to the big context circles.

However, the experimentally observed increase of *DT* (Figure 4.5c) that indicates a slowing down towards the target might not be explained by d_{10} only. The interplay of the softening spring coefficient d_{30} and the linear stiffness d_{10} are able to explain an increased dwell time at the targets, and thus possibly also an increase in *DT*. To date, however, the model coefficient d_{30} and the interplay of d_{10} and d_{30} remain to be investigated.

The results of this study are preliminary, and therefore should be handled with caution. Regardless, these results seem in accordance with *Hypothesis 3* and the results of *Chapter 4*. The results, therefore, suggest that there are indeed changes in behavioural dynamics, and that these changes are only due to the introduction of context circles around targets (i.e., the Ebbinghaus illusion). These preliminary findings speak against a strict functional dissociation of the visual system (*Hypothesis 1*), as well as a one-to-one mapping between vision for perception and action (*Hypothesis 2*).

These results might seem obvious since they are fitted to the experimental data, the data that was showing exactly the same factor as influencing movements.

The benefit of the Bayesian statistical methods that we have applied is the minimal processing, the relatively little filtering, and the long time series that can be fitted. If we compare this method to the *MT* (and *DT*) analysis of *Chapter 4*, we can conclude that the Bayesian statistical approach can give information about the type of movements resulting from the model that is under study. In *Chapter 4* we got and showed some hints of the slowing down, and enhanced fixed point dynamics. However, vector fields and probability distributions (see *Chapter 4*) that show topological changes of the movements, require quite some pre-processing and criteria to be set. Therefore, instead of replacing these insightful techniques to study the movement topology, we believe that the Bayesian framework to study (non linear) dynamical models as compared to data can give new insights regarding the qualitative changes of movement dynamics.

Figure 5.1 shows the values for the RD-coefficients as reported in Mottet and Bootsma (1999). The coefficient d_{10} increases almost in parallel with d_{30} over *ID* in normalized time and space. Our results demonstrate the inverse: d_{10} is decreasing with *ID* (see Figure 5.4A). Since the distance between the targets remained constant (160 mm), and the target width was varied, the increase of *ID* was synonymous with a decrease of target width. In absolute physical metrics d_{10} was demonstrated to increase with target width, which corresponds to our finding (see Figure 5.1). The increase of d_{10} over *ID* seems to contrast the increase over target width (i.e., an increase in target width *W* equals a decrease of *ID* under a constant distance *D*). Whether our finding would be inverted when distance would be manipulated remains unknown for this data set. However, since in *Chapter 3* we have demonstrated that the distance and width manipulations in a Fitts' task leading to a same *ID* result in qualitative different movement dynamics (Figure 3.2 and Table 3.1), we deem it possible that the parameters d_{10} and d_{30} vary differently under a *D* and *W* manipulation. As discussed in *Chapter 3*, there are doubts whether the notion of task difficulty as quantified through target distance and divided by its width is appropriate. Future investigations should thus explore whether distance and width manipulations lead to systematic, different changes in the RD-model coefficients.

The findings presented in Figure 5.1 and 5.2 allow for a discussion of the changes in the behavioural dynamics due to the introduction of context circles around targets. To give a mechanistic explanation, we will reflect on the merit of fixed points and of limit cycles. Fixed points are locally well defined in state space. Limit cycles emerge in nonlinear systems and describe a cyclic movement, whose flow is in particular not governed by fixed points and therefore constant. Having said that, inside any closed trajectory is at least one fixed point. Thus, there is at least one fixed point within a limit cycle (if the vector field is defined everywhere inside) (see, e.g., Hirsch and Smale, 1974).

With respect to the reciprocal aiming movements between targets, targets can be interpreted as fixed points because they are local and well defined in space. The fairly uniform cyclic movements are perhaps spatially restricted by the targets but in fact orbiting a fixed point. Limit cycle behaviour is fundamentally different from discrete fixed-point behaviour. The fixed-point behaviour around the target is attractive, when the participant is aiming at it, and repelling, when the participant is departing from it to aim at another target. This fixed-point behaviour is called a saddle. The movement between two targets is due to the link of the repelling force from one target with the attraction of the other target, and vice versa. This is called a heteroclinic orbit (which can be a heteroclinic cycle; Rabinovich et al., 2008). Within this heteroclinic orbit a limit cycle emerges in virtue of another fixed point (i.e., an unstable spiral) between the two targets such as described in the work authored by Mottet and Bootsma (1999). Note that by definition, there are no fixed points in the course of movements on limit cycles, in contrast to the heteroclinic orbit. This means that the two fixed points representing the targets are simply framing the movement where the third fixed point that is enclosed by the limit cycle shows repelling behaviour of spiral forms, supporting cyclic and uniform movements.

Under both circumstances, for discrete and for cyclic aiming, movements do not reach or traverse any fixed points with finite speed. This suggests revisiting the fixed-point concept for the targets. Considering a saddle-fixed point at the centre of each of the two targets implies that at least one half of the target face (facing outside)

is not reachable. To work around this issue, the fixed points could be placed with maximum distance between each other on the contour of both targets. By all means, this still does not account for overshoots as addressed in Mottet and Botosma (1999), but it can account for undershoots. Also note that the model is globally repelling (i.e., unstable) especially in the parameter ranges used by Mottet and Bootsma (1999) for describing movements in reciprocal aiming tasks. Globally repelling means that the movement is sensitive to its initial starting position. If this position is in the range where a system is instable, oscillations will not take place. Starting between the two saddles (i.e., targets) gives a movement towards a target, starting otherwise result in a faster and faster movement away from all (both targets). However, using a different parameterization, the same model can be globally stable and show similar behaviour (see Chen and Zou, 2016). Finally, the discrete movements as well as the fairly uniform cyclic movements depend on the fixed-points and their attractions and repulsions. The fact that discrete movements are essentially linked fixed points, whereas uniform cyclic movements are distant from any fixed points, suggests that the latter is less sensitive to local perturbations than the former.

The question thus arises what quantitative and qualitative changes in behaviour are the result of adding the context circles around targets. There are three possibilities how context sizes of Ebbinghaus figures could change the behaviour. With respect to the targets and its modifications reported in this manuscript, the underlying assumption was that the target width and its context (i.e., Ebbinghaus figure) directly affect the (saddle) fixed point at each target, its location and its stability. Given the mechanistic framework, the second explanation is that the Ebbinghaus figure adjusts the stability of the third (focus) fixed point (i.e., the unstable spiral) and its location throughout the interplay of the fixed points at both targets. For instance, changing the distance between the target's fixed points (and the third fixed-point in between the target's fixed points) can interrupt an established limit cycle and induce fixed-point behaviour, or link attracting and repelling forces of the fixed-points so that a limit cycle can emerge. The third possibility is associated with an increase in complexity due to the Ebbinghaus figure. In this spirit, the fixed points locally remain the same but their interaction changes in virtue of at least one

additional fixed point. In this way, the context circles of the Ebbinghaus figure enrich and hence alter the landscape of attractors (e.g., fixed points limit cycles). All the three mentioned considerations can cause quantitative changes (e.g., MT) but also qualitative changes (called bifurcations such as the transition from discrete fixed-point behaviour to cyclic limit cycle behaviour).

The fact that the Ebbinghaus figure is associated with perceptual size illusions of the centre circle (which is here used as target for the movements) implies a direct effect of the context circles on the targets and consequently a change of its fixed point in location and in attraction/repulsion. In contrast to altered target fixed points due to an illusion, the context circles of the Ebbinghaus figure may be interpreted as additional elements in the workspace, and therefore simply increase the complexity. Because the performed statistics provide only evidence for the context size to affect the behaviour (in addition to Fitts' *ID*), we conclude that the fixed point at each target is changed directly or indirectly by the size of the context circles.

We can now open up the discussion to the integration of perception and action. How are (visual) perception and action coupled? How does this coupling change the flow, and can this change in the flow drive the system through a bifurcation involving for example a switch from rhythmic to discrete movements? The coupling-induced deformation of the phase flow due to a reduced spatio-temporal variability is often present at particular regions of the phase space (generally around the movement endpoints), which is referred to as anchoring (Beek, 1989; Byblow et al., 1994; Jirsa et al., 2000; Roerdink et al., 2005, 2008). Around anchor points, critical task-specific information is available for the organization of behaviour (Beek, 1989). In the study of visual information on cyclic arm movements it was found that fixating the gaze at movement endpoints actively created anchor points (Roerdink et al., 2005). Anchor points may also be imposed through constraining gaze to particular regions (Roerdink et al., 2008). Although auditory anchoring in bimanual coordination is studied, the theoretical work of Jirsa et al. (2000) showed anchoring and the influence on coordination patterns with external information. The effect of external driving directly affected the system's state variables, that is,

multiplicative coupling. Thus, potentially the introduction of Ebbinghaus figures can create anchor points, or change its strength. More specifically, the context circles can serve as anchor points for the visual gaze for which visual perception and action are linked through multiplicative coupling terms. This hypothesis, however, remains to be tested.

Many studies have investigated the behavioural coordination pattern between perception and action. For example the stability of multimodal coordination in flexion-extension movements with auditory and tactile stimulation (Lagarde and Kelso, 2006). The latter study showed that both the action as the stimulus modality (touch and sound) influenced multimodal coordination. In a rhythmic presentation of visual and auditory stimuli, three perceptual states were found (asynchrony, synchrony, and non-phase locked or also called drift), that were based on how the dynamical states of coupled and hence interacting oscillations were described (Dhamala et al., 2007). Although the perception of the Ebbinghaus figure can most likely not be identified as synchronous, asynchronous, or drift, the influence of sensory information (in our case mainly touch and vision) on the cyclic aiming movements might be multimodal coordinated. How the multimodal integration influences motor behaviour, and how continuous sensory stimulation can be used to enhance motor performance, remains unknown. Future studies could explore the possible benefits of controlled, multimodal integration on enhanced sensorimotor behaviour.

In conclusion, quantitative and qualitative changes in the behavioural dynamics have been attributed to the effect of the Ebbinghaus figure's context circles. The linear stiffness of the RD-model decreased due to the big context size, inducing a global slowing down of the system. This finding confirms the influence of the Ebbinghaus figure on movements, and therefore refutes the functional dissociation of the visual system.

Chapter 6 | *General discussion*

"The whole is greater than the sum of its parts."
- Aristotle

6.1 Summary

How do you perceive the world? And how do you interact with it? Have you ever thought about all the interactions you had with your surrounding in a minute, an hour, or a day? How do we coordinate our movements towards (consciously) perceived objects in our environment? These pivotal questions lie at the heart of this thesis—but at the same time this question will not be answered in this thesis. To clarify a piece of this complex jigsaw puzzle, we systematically studied the *perception* of size-weight illusions (*Chapter 2*), the *movements* towards targets (*Chapter 3*), the *movements and perception* by studying movements towards visual illusions (*Chapter 4*), and the *mechanisms of perception and action* (*Chapter 5*). The experimental proof allows for an evidence-based re-evaluation of hypotheses on the human perception-action system. Based on the findings, a piece of the complex jigsaw puzzle can be unravelled.

As stated in *Chapter 1*, the visual system has been hypothesized to be functionally dissociated in a ventral and a dorsal stream, also called the two visual streams hypothesis (Goodale and Milner, 1992). This hypothesis results from clinical studies with patients that suffered from ventral or dorsal stream lesions. Patient

based research, however, is complicated due to a high variability of lesions, symptoms, and adaptations to the pathology. Furthermore, the patient population to study is limited. Therefore, the challenge is to design experiments for healthy subjects. Goodale's group therefore tested the TVSH in healthy participants by using visual illusions in grasping tasks (Aglioti et al., 1995). But, as summarized in *Chapter 1*, this landmark study and the studies that followed, resulted in contradictory results. Therefore, the study presented in *Chapter 4* aimed to resolve the conflicting results by exploring the unknown relation between the presence of illusion effects and motor classes (motor classes as in Huys et al., 2010a). In order to be able to evaluate the illusion in a movement task, we first quantified the illusion effect for a set of Ebbinghaus figures since it was unknown if and how different parameters of the size illusion affected the perception of the figure. The main result was that 33% of the tested Ebbinghaus figures did not result in significant illusion effects. If there was an illusion effect, this effect was determined by all three parameters of the Ebbinghaus figure, that is: target size, context size and target—context distance. Then the movement part needed to be quantified and qualified (*Chapter 3*). The Fitts' task was analyzed for both reciprocal as discrete pointing movements, with the aim to identify the dynamics, and further characterize the movements' kinematics, when changing the Fitts' parameters *W* and *D* independently. The main finding was that Fitts' law held under all conditions (i.e., *MT* was predicted by the *ID*), however, the prediction of movement organization for discrete and reciprocal aiming given an *ID* (i.e. qualitative and quantitative dynamics as well as kinematics) was limited. With a quantification of perception and action at hand, the influence of visual illusions on reciprocal aiming was analyzed (*Chapter 4*). The results of the latter study were interpreted as evidence that the ventral and dorsal streams are not completely functionally distinct, nor do they rely on the same informational variables. The presence of illusion effects on movement appeared independent of the underlying motor class of movements. These findings invalidate the main hypotheses claiming i) a functional dissociation of the visual system, ii) claiming no dissociation, as well as our hypothesis iii) that the illusion effect is movement type dependent. Having refuted these hypotheses thus leaves us to speculate on the possible interactions of perception and movements. Therefore, possible mechanisms for the interaction of

perception and action have been proposed in *Chapter 5*. Taken together, we conclude that the Ebbinghaus illusion affects *perception* as well as *action* directed towards it, but not analogously.

The triptych that is presented in the *Chapters 2, 4,* and *5* led us to conclude that the TVSH, as well as the inverse hypothesis claiming one internal representation underlying perception and action, did not correspond to the results. In the following section our conclusions will be discussed with respect to alternative perspectives that are making a distinction between conscious and unconscious perception (*Section 5.2.1*), between perceptual and conceptual knowledge (*Section 5.2.2*), and between discrete and rhythmic movements (*Section 5.2.3*). In *Section 5.3* we will explore the possibilities of integrating the findings in a constructivist and ecological framework. In *Section 5.4* the methodological contributions and limitations are highlighted and reflected upon. And before concluding the discussion, directions for future research are developed.

6.2 Dichotomies in perception and action

6.2.1 Dichotomy between conscious and unconscious perception

Several dichotomies have been proposed with regard to vision and perception. Next to the distinction of the visual system in a ventral and dorsal stream (see *Chapter 1*), the function has been parted into attentive and pre-attentive vision (Wolfe and Bennett, 1997; Treisman and Gelade, 1980), and into conscious and unconscious visual processing. For the latter dichotomy between conscious and unconscious perception, a distinction can be made between conscious perception as we mostly experience it, and the stimuli that bypass visual awareness. The stimuli that bypass visual awareness can still be acted upon by patients with blindsight (Stoerig and Cowey, 1997), but also by humans without any known deficiencies (Milner and Goodale, 1995). This dissociation has been linked to the ventral stream for conscious perception, and the dorsal stream for visually guided action without conscious perception (Milner and Goodale, 1995; Milner, 1995). The results from several studies suggest that conscious perception and visually guided action can be dissociated. For example, in tasks where the target of a grasping or aiming movement is

unpredictably moved during the movement (i.e., a double-step reaching task; Castiello et al., 1991; Johnson et al., 2002). As a result, corrections of the trajectory can be observed within 100-150 ms (Carlton, 1981; Day and Lyon, 2000; Paulignan et al., 1990, 1991; Prablanc and Martin, 1992; Soechting and Lacquaniti, 1983; Zelaznik et al., 1983). Interestingly, these visuomotor adjustments can occur while a shift of target location remains unnoticed (Goodale et al., 1986), or when visual feedback is distorted but remains unnoticed (Fourneret and Jeannerod, 1998). The latency between conscious experience of target shifts and the movement adjustments was found to be about 300 ms (Castiello et al., 1991). Based on these findings, the ventral stream for conscious perception and the dorsal stream for visuomotor actions have been claimed to be functionally distinct and associated with different time constants.

These studies distinguished motor performance, and visual awareness. In contrast, other studies investigated the relation between visuomotor pointing or grasping and visual consciousness induced by a visual illusion. Skewes et al. (2011) present an experiment in which they claim that a change in visual consciousness induced by a perceptual illusion affects the speed and accuracy of goal-directed movements, suggesting that perceptual and visuomotor processes do interact in the speed/accuracy trade-off. They remain silent, however, on the meaning and the level of consciousness and therefore the use of 'visual consciousness' seems otiose. Interestingly, Hu and Goodale (2000) have shown that online grasping movements (here the size of the aperture at the initiation of the grasping movement) remained unaffected by visual illusions, whereas the same grasping movements were sensitive to the illusions when the movement was initiated after a time delay of 5 seconds. A similar size-contrast effect was also observed when participants gave manual estimates of the perceived size of the target object. The authors suggested that real-time visuomotor control relies on absolute metrics, whereas delayed grasping operates the relative metrics associated with conscious perception. Thus, with respect to the metrics and frame of reference that each system uses and with respect to the time-scale over which each system operates, there is strong evidence that whether action and conscious perception are congruent with each other appears to depend on the presence of a delay. But, why does the introduction of a time delay increase the

congruence between movement and reportable subjective experience (Sarrazin, Cleeremans & Haggard, 2008), so that movements (e.g., pointing or grasping) are influenced by conscious representations? Is it possible that participants were not, or less, conscious in tasks without time-delays?

If we consider conscious experience as a dynamic process, instead of a static 'all-or-none' process, this dynamic process allows for many degrees and components (see Cleeremans and Jiménez, 2002). In neural terms, considering the differences between the various types of connections in the visual cortex (e.g., Lamme et al., 1998), as soon as feed forward connections have transmitted information from lower to higher cortical areas, horizontal connections start to connect distant cells within that area, and feedback connections start sending information from higher-level areas back to lower levels. Together, these connections provide what is called recurrent processing (Lamme and Roelfsema, 2000). Relating the distinction between connection types to functional dichotomy in visual processing, several studies have demonstrated that recurrent connections are crucially necessary for conscious perception (e.g., Tononi and Edelman, 1998; Lamme and Roelfsema, 2000; Dehaene et al., 2003; Lamme, 2004). But is recurrent processing not equally necessary for visuomotor behaviour? And, can visuomotor processing not lead to consciousness? Possibly, visuomotor processing eventually can lead to consciousness, but due to the difference in latency, this conscious experience comes only after the visuomotor act.

Thus, the question is whether the degree of conscious perception be an explanatory factor in the presence or absence of illusion effects in movement tasks? With the experiment presented in *Chapter 4* we cannot distinguish to what degree, if at all, targets were perceived consciously, and we did not control the delay between stimulus presentation and movement onset. However, under the assumption that illusion effects only occur when perception is conscious, the fact that we found illusion effects on pointing movements suggests the involvement of conscious perception. This involvement of conscious perception might come about by the recurrent processes of information, as a continuous process of top-down and bottom-up information stream. Therefore, this might speak against the hypothesis of Milner and Goodale (1995) who claimed that what we know about our own movements may

be a filtered and delayed version of the rapid operation of the action circuits embodied by the dorsal stream (Milner and Goodale, 1995). Or, possibly the anatomical connections between ventral and dorsal stream allow for a more direct interaction between the two streams, in which a degree of consciousness emerges out of the continuous interaction of the visual network. The latter might suggest that the interaction between the streams hinders the experimenters to capture a possible functionally distinction.

We cannot distinguish the degree of conscious perception in the studies presented in this dissertation, and thus we have to remain inconclusive with regard to the debate about conscious perception and its impact on visuomotor action. Future studies working with controlled presentation time, around the point of visual awareness, and with time delays should give more clarity on the role of consciousness in perception and sensorimotor transformations.

6.2.2 Dichotomy between conceptual and perceptual knowledge

Gregory (1997) proposes another dichotomy, namely between conceptual and perceptual knowledge. He wrote:

> *It is significant that many illusions are experienced perceptually though the observer knows conceptually that they are illusory--- even to the point of appreciating the causes of the phenomena. This does not, however, show that knowledge has no part to play in vision. Rather, it shows that conceptual and perceptual knowledge are largely separate. This is not altogether surprising because perception must work extremely fast (in a fraction of a second) to be useful for survival, though conceptual decisions may take minutes, or even years. Further perceptions are of particulars, rather than the generalities of conceptions. (We perceive a triangle, but only conceptually can we appreciate triangularity.) Also, if knowledge or belief determined perception we would be blind to the unusual, or the seemingly impossible, which would be dangerous in unusual situations, and would limit perceptual learning.*

Then can the development of conceptual knowledge about visual illusions influence the illusion effect? Jacobs et al. (2011) have shown that illusion effects can be unlearned when participants receive feedback about their judgments. This could indicate that the conceptual knowledge was developed in a way that would be guiding the perceptual knowledge. Whether this could also be the case for the perception of Ebbinghaus figures remains to be explored. The potential influence of a conceptually learned Ebbinghaus figure on movements, that is, perceiving the figure without an illusion effect, would be an interesting next study.

6.2.3 Dichotomy between discrete and rhythmic movements

In *Chapter 3* we have investigated the discrete and reciprocal Fitts' task. In *Chapter 4,* we have, however, studied the effect of the Ebbinghaus figure on reciprocal movements only. Would we expect to see the same results for discrete (aiming) movements, as the results we have observed in *Chapter 4*?

Recall that we chose reciprocal aiming movements because they were expected to be less susceptible to visual illusions. This hypothesis was based on three arguments. The first argument is a phylogenetic argument: the evolutionary older rhythmic movements owe their functional integrity to a large part to body-related information (in particular kinaesthesia and proprioception), whereas the evolutionary younger discrete movements are associated in particular with the visual system (Bernstein, 1996). A second argument is given by Glover et al. (2002) that motor planning is susceptible to illusions, but not the online motor control. A series of discrete movements need to be planned and initialised before each individual movement initiation, whereas rhythmic movements need to be planned only once because from movement initiation the movements are under online control. A third argument was found in the aiming literature in describing larger effects of reducing the availability of visual information on tasks of high level difficulty (typically associated with fixed-point behaviour) compared to low levels of task difficulty (typically associated with limit cycle behaviour)(Bootsma et al., 2002). If the movements in the fixed point regime would be (more) susceptible to visual illusions, then discrete movements would be susceptible to visual illusions for each *ID* that was tested in *Chapter 3* and *4*.

To our surprise, the conclusion of *Chapter 4* was that the effect of the Ebbinghaus figure was not limited to a specific target size, and thus discrete movements (high *ID*) and limit cycle governed movements (low *ID*) were both influenced by the Ebbinghaus figure. Discrete movements were thus equally susceptible to visual illusions in the range of conditions that we tested. Based on these findings there is thus no reason to expect that discrete pointing movements would be more or less susceptible to visual illusion. However, if the goal is to evoke transitions from limit cycle behaviour to fixed point behaviour, then reciprocal aiming movements are the only candidates.

Why reciprocal aiming movements under low accuracy constraints are susceptible to visual illusions remains, however, unexplained. Bootsma et al. (2002) showed that manipulating vision at low *ID* hardly changed the movements, as compared to high *ID*. Furthermore, when *ID* was high, vision of the hand was necessary when approaching the target, even at the price of no vision in between. At low *ID* decreasing the amount of vision was less damaging. Could this mechanism have an opposite effect as what we expected? Thus, could it be that because the hand was followed more during high *ID* conditions, the participants observed the target (and thus the illusion) relatively less than in the low *ID* condition? Indeed, saccades are made to the targets for low *ID* conditions as compared to high *ID* conditions (Lazzari et al., 2009). Without tracking eye-movements during our tasks, we cannot rule out the possible confounding factor of net time spent looking at the target. Studies that track eye movements during a similar task can answer the question whether visual behaviour, and thus the time spent looking at an Ebbinghaus figure, plays a role in the presence (or not) of illusion effects on visuomotor behaviour.

6.3 Illusions from a constructivist end ecological perspective

In a review entitled *Visual illusions and neurobiology,* Eagleman (2001) wrote:

> "The complex structure of the visual system is sometimes exposed by its illusions. The historical study of **systematic misperceptions**, combined with a recent explosion of techniques to measure and stimulate neural activity, has

provided a rich source for guiding neurobiological frameworks and experiments."

The description of visual illusions as systematic misperceptions is commonplace. That is, if you perceive an object that is surrounded with small round objects around it (e.g., the Ebbinghaus figure) as being 2 cm, but the ruler shows that the object is 2.3 cm, than we could say that the subjective experience of the target size was incorrect. This line of reasoning requires an indirect way of perception, in which the visual system actively constructs a percept of the environment by inferring the cause of the stimulus information. The stimulus information is enriched with expectations, knowledge, and assumptions that are all based on previous experience of the perceiver. Thus, a mental representation of the environment is constructed and consolidated by the brain. The argument that subjective experience can thus be incorrect has often been forwarded to refute Gibson's (1966, 1979/1986) theory of direct perception.

Ecological psychologists do not think of perception as being indirect. In the theory of *direct perception* animals (including humans) have direct access to the environment. In the work of Gibson (1979/1986), he described a lawful one-to-one relation between optical variables in the ambient energy array (i.e., the pattern of light that is reflected by the environment) and the properties of the environment or the "organism-environment relation" (see: Gibson, 1979; Reed, 1996). Typically, optical variables become available as a result of movement of the organism or of the environment. As an example of optical variables present in static ambient energy arrays, texture gradients specify the relative size of objects (Gibson, 1966). Thus, unlike the stimulus information available from the retinal image, optical variables do not relate ambiguously to the environment; instead, they specify the environment.

So how do ecological psychologists think about illusions? Gibson (1979/1986) wrote: "Is information always valid and illusion simply a failure to pick it up? Or is the information picked up sometimes impoverished, masked, ambiguous, equivocal, contradictory, even false?" Gibson accounted for the illusion not in terms of inference

but in terms of informational patterns in the ambient array. He asserted that the information that is normally used by observers to perceive line length is "inadequate" in the context of the Müller-Lyer illusion (Gibson, 1966). That is, it does not specify line length in that picture but instead relates ambiguously to it. Furthermore, he suggested that a picture can have several informational variables, and that the occurrence of the illusion depends on the particular information that is used by the observer. The latter argumentation is supported by evidence that there is considerable variability between and within humans in the extent to which they are susceptible to visual illusions. This variability is related to culture (de Fockert et al., 2007; van der Kamp et al., 2013), learning (Jacobs et al., 2011; van der Kamp et al., 2013), experience (e.g., Doherty et al., 2010; Káldy and Kovács, 2003; Weintraub, 1979), task, and anatomical differences (Schwarzkopf and Rees, 2013; Schwarzkopf et al., 2011).

De Wit et al. (2015) elaborated on the link of visual illusions and direct perception, and concluded: "…susceptibility to illusions is not (always) necessarily a consequence of "inadequate" or unavailable information (cf., for example, Turvey et al., 1981), but rather that the optical variable that is specific to the property of interest to the observer is not always detected or exploited."

Or as Jacobs et al. (2011) formulated concerning their study with the Müller-Lyer illusion:

> "Reliance on the variable x = .12 in our space can lead to judgments that are correct if being correct is measured with regard to actual shaft length. Likewise, judgments based on variables other than x = .12 can be said to be erroneous or illusory if they are evaluated with regard to shaft length. Perception and action, however, should typically not be evaluated with regard to standard physical quantities such as shaft length. If a scientist measures performance on the basis of a standard physical property and claims that the perceiver is in error, then, rather than the perceiver, it might be that "*the scientist is in error – that is, he or she is measuring the wrong thing* (Michaels and Carello, 1981; Turvey et al., 1981)". In sum, although in the following we do

refer to a discrepancy between judgments and shaft length as error, we are aware that this terminology is questionable."

This leaves us with mainly three statements that we can relate to the research that was presented in *Chapter 2* and *4*. First of all, in *Chapter 1* we encountered the problem that the terminology around 'perception', 'visual illusions' and 'action' is far from clear. This confusion as a result of the unclear terminology seems to be tightly linked to the different theories scientists have followed. In this thesis we refer to Illusion Magnitude (IM) instead of 'error'. Regardless, we acknowledge that terms like *misperception*, *error*, *misjudgment*, *action,* and also *illusions* are questionable and are only appropriate for certain theories, as well is either *direct* or *indirect perception.*
The second point concerns the measurement standard. It is common to relate the outcome measures to its physical measure. In our case the physical measure is size. However, instead of relating the outcome measures to its physical size, we related the outcome measures to the individuals' control condition. By relating the measures to its control counterparts, we aimed to look at individual changes due to experimental conditions.

The main discussion, however, is around the information variables that are being picked up by the observer. Thus, rather than speaking of illusion effects and misperceptions, the picked up information variables might not have been detected, by the observer and/or by the experimenter. With our systematic approach we aimed to identify which geometrical parameters played a role in the object's size perception, and the movements directed towards it. However, how these parameters constrained the informational variables available, and which variables the participants used, remains unanswered.

6.4 Methodological contribution and limits

The use of visual illusions to test hypotheses about the visual system and its interaction with the action-system has gained a lot of attention in the last 20 years. This resulted in many publications, and many contradictions (see *Chapter 1*). In *Chapter 2* and *4* we argue that these differences might be partly explained by the

differences in methods. To make a valuable contribution to the field of perception and action, a refined methodology was required. Therefore, the illusion effect of the Ebbinghaus figure on perception was quantified by using an adapted staircase procedure. This is a well-developed (psychophysical) method that was hardly used in the study on the visual stream hypothesis. For the evaluation of movements towards targets surrounded by the Ebbinghaus figure, a detailed description and classification of the movements was developed. These methodological developments allowed for a controlled and detailed analysis of perception and action. The application of these methods is not limited to studies with visual illusions.

The question can be raised, however, whether visual illusions are a good 'tool' to explore perception, action and perception-action coupling. In most of the experiments, the judgment of visual illusions is considered stationary. Once a certain image is perceived as such, it will remain like it is. Is this indeed the case? For example, as we have seen in the section on the conceptual and perceptual knowledge, it was shown that illusion effects of the Müller-Lyer illusion could be 'unlearned' when feedback was given about the shaft length (Jacobs et al., 2011). Does the illusion magnitude as we quantified it in *Chapter 2* change over time in longer trials as in *Chapter 4*? This answer should be addressed in future studies.

In this thesis we have tried to study the qualitative features of aiming trajectories, and whether these aiming movements are influenced by the perception of size illusions. The methods used to capture these qualitative features (i.e., phase flow analyses) allowed for a description of the movement trajectory. Phase transitions have previously been identified as a function of *ID*. Traditional measures applied to analyse Fitts' tasks have mainly studied the changes in *MT* as a function of *ID*. Movement time analyses would not have captured phase transitions. Phase flow analysis techniques have allowed to identify distinct control mechanisms in reciprocal aiming (Huys et al., 2010a).

However, these methods also know limitations. For example, the phase flow analyses for reciprocal aiming movements have considered the horizontal displacement (x) and the velocity (dx/dt). Movement fluctuations in the orthogonal

direction are thus not accounted for. Incorporating the anterior-posterior direction (*y*) and its velocity (*dy/dt*) would add two more dimensions, which complicates the analyses, visualisation, and interpretation. To date, statistical measures are hardly available to quantify changes in phase flows. Therefore, investigating the qualitative features of trajectories as compared to a model, can add weight to the understanding of the qualitative behaviour. As we have shown in *Chapter 5,* a non-linear model (RD-model) could be compared to the data from *Chapter 4* by using Bayesian statistics. This method showed systematic changes in the model coefficient under study. The model coefficients give information about the qualitative features of the aiming movements. While this is on-going work, we think that the comparison of models (which is not restricted to the RD-model) to experimental data using Bayesian statistics can be a valuable addition to the phase flow analyses and beyond. Regardless its limitations, to our knowledge, this is the first time that phase flow analyses have been used to study the possible phase transitions due to size-illusions. The model comparison methods might uncover hidden, but crucial variables for the interplay of perception and action. These types of analyses can give complementary insights about the how, and when perception influences movements.

Systematic studies allow for reproducibility, which is the path that scientists should pursue. The methods that we developed or applied in *Chapter 2, 3, 4,* and *5* allow for a detailed analysis of perception and action. Though numerous unanswered questions remain, we hope to have answered a part of the questions about perception and its interaction with action due to our systematic approach. Multi-laboratory studies like Kopiske et al. (2016) that reproduced previous landmark studies with a large number of participants (N = 144) can test the validity of the contradictory results (*see Chapter 1, 4*). Regardless the smaller number of participants that we included in our studies, we reported similar findings as in Kopiske et al. Their findings support our conclusions. This gives confidence in the work presented in this thesis, and confirms that systematic (small) studies, with a detailed analysis of the sensorimotor system can unravel parts of the puzzle.

The methods applied in the experiments that are presented in this thesis know limitations. We have tried to study the functional dissociation of the visual system. With behavioural tasks, the conclusions about the presence (or absence) of a functional dissociation between the ventral and dorsal stream remains suggestive.

6.5 Future directions

The research presented in this thesis lead to multiple questions that we were unable to pursue. One of these questions concerns the implication of the ventral stream during reciprocal aiming movements. We were unable to answer whether, and when, the ventral and dorsal streams are recruited during our perception task (*Chapter 2*) and the Fitts' task (*Chapter 4*). With the availability and the vast improvement of neuroimaging techniques, questions about the activity of brain regions and functional brain networks could be simulated, stimulated, and imaged. With the availability of magnetoencephalography (MEG) the brain activity could be recorded while performing an easy motor task towards visual stimuli (e.g., visual illusions). MEG recordings allow for a relatively high spatio-temporal resolution, and seem therefore the most suitable imaging technique at hand. We expect that these high-resolution imaging techniques can answer the question whether, and when, the ventral stream is recruited in motor control tasks (like reciprocal pointing). And thus, these techniques might resolve the debate whether, when, and how the ventral and dorsal streams are functionally distinct.

The application of transcranial magnetic stimulation (TMS) allows for a transient functional disruption of a given cortical target. The pulse can be applied in space and time, and with the desired frequency and intensity. The stimulation can exist of a single pulse, or a sequence of pulses (repetitive TMS). To get a clearer picture of the visual system, and the (task-related) functional networks, the dorsal stream and ventral stream could be temporarily disrupted with (bilateral) repetitive TMS (rTMS). So far, few studies have applied TMS in combination with visual illusions (e.g., Mancini et al., 2011; Lee et al., 2002). These studies, however, worked mainly with a unilateral single pulse (Lee et al., 2002), or unilateral rTMS. Therefore, simultaneous bilateral rTMS could temporarily interrupt either the ventral or dorsal

stream. Such a study can give new insights in the activity of functional ventral and dorsal networks.

The experimental work in this thesis has not incorporated time delays between stimulus presentation and response (i.e., movement onset, or judgment). Discrete pointing movements allow nicely for time delays between stimulus presentation and movement onset. Especially for answering questions regarding the influence of conscious perception on movements, time delays can be used as a tool to distinguish between conscious perception and unconscious perception. Delayed movements and judgments are more likely based on conscious perception than on visuomotor information. Delayed, memory-based movements lead to stronger illusion effects. Since we could not rule out the presence of conscious perception (and possible ventral stream activity) during our pointing task, a discrete Fitts' task with visual illusions that are introduced at, or after, movement onset could answer the question whether conscious perception modulates action.

In *Section 6.3* we suggested that rather than speaking of illusion effects or misperception, the picked up information variables by both the participants, as also the experimenter, might have remained undetected. Extra information can be gained by following the gaze of the participant by making use of eye-tracking techniques. This technique allows verifying how the participant sampled the visual information. This can answer questions about whether the participant focused on the targets only, and if that changes when context circles are introduced, and if this changes differently for big than for small context sizes. Getting a clearer picture of the visual behaviour of participants in perception-action tasks as presented in *Chapter 2* and *4* can potentially uncover relations between vision, attention, perception and action that are related to the displayed visual information (e.g., the Ebbinghaus figure), but are no illusions (e.g., the Ebbinghaus illusion). If participants focus more on the target in one condition than in another, this might explain why an illusion effect is found in only one condition (as was the case for the illusion effect for mainly big target sizes in *Chapter 2*).

An opportunity for the field of (conscious) perception and action lies in the integration of disciplines. By combining philosophers, psychologists, movement scientists, computational neuroscientists, and physicists, the theories on perception, movement and its coupling can be validated, developed, and improved.

6.6 Conclusions

In conclusion, we wish to emphasize the systematic classification approach we have introduced in the field of perception, action and perception-action coupling. This approach allowed us to shed light on the influence (and its absence) of visual illusions on the organization of movement types in simple reciprocal aiming tasks. The results showed Ebbinghaus illusion effects on movements and perception. This finding takes edge of the famous theory that the ventral and dorsal visual streams are functionally dissociated. By showing that these effects on perception are not induced by the same factors as action, we conclude that the ventral and dorsal stream do not rely on the same type of information. Finally, illusion effects were not movement type dependent. The mechanism(s) behind the interaction between perception and action remains to be uncovered.

Bibliography

Aglioti, S., DeSouza, J. F., and Goodale, M. A. (1995). Size-contrast illusions deceive the eye but not the hand. *Curr. Biol.* 5, 679–685. doi:10.1016/S0960-9822(95)00133-3.

Alphonsa, S., Dai, B., Benham-Deal, T., and Zhu, Q. (2014). Combined visual illusion effects on the perceived index of difficulty and movement outcomes in discrete and continuous fitts' tapping. *Psychol. Res.* doi:10.1007/s00426-014-0641-x.

Beek, P. J. (1989). Timing and Phase Locking in Cascade Juggling. *Ecol. Psychol.* 1, 55–96. doi:10.1207/s15326969eco0101_4.

Bernstein, N. A. (1996). *Dexterity and Its Development.* , eds. M. L. Latash and M. T. Turvey Mahwah, New Jersey: Lawrence Erlbaum Associates doi:10.1007/s13398-014-0173-7.2.

Bernstein, N. A. (1967). The co-ordination and regulation of movements: Conclusions towards the Study of Motor Co-ordination. *Biodyn. Locomot.*, 104–113. doi:10.1097/00005072-196804000-00011.

Binkofski, F., and Buxbaum, L. J. (2013). Two action systems in the human brain. *Brain Lang.* 127, 222–229. doi:10.1016/j.bandl.2012.07.007.

Binsted, G., Rolheiser, T. M., and Chua, R. (2006). Decay in visuomotor representations during manual aiming. *J. Mot. Behav.* 38, 82–87. doi:10.3200/JMBR.38.2.82-87.

Bongers, R. M., Fernandez, L., and Bootsma, R. J. (2009). Linear and logarithmic speed-accuracy trade-offs in reciprocal aiming result from task-specific parameterization of an invariant underlying dynamics. *J. Exp. Psychol. Hum. Percept. Perform.* 35, 1443–1457. doi:10.1037/a0015783.

Bootsma, R. J., Boulard, M., Fernandez, L., and Mottet, D. (2002). Informational constraints in human precision aiming. *Neurosci. Lett.* 333, 141–145. doi:10.1016/S0304-3940(02)01003-0.

Brainard, D. H. (1997). The Psychophysics Toolbox. *Spat. Vis.* 10, 433–436. doi:10.1163/156856897X00357.

Brayanov, J. B., and Smith, M. a (2010). Bayesian and "Anti-Bayesian" Biases in Sensory Integration for Action and Perception in the Size-Weight Illusion. *J. Neurophysiol.* 103, 1518–1531. doi:10.1152/jn.00814.2009.

Brenner, E., and Smeets, J. B. J. (2011). Quickly "learning" to move optimally. *Exp. Brain Res.* 213, 153–161. doi:10.1007/s00221-011-2786-9.

Brenner, E., and Smeets, J. J. (1996). Size illusion influences how we lift but not how we grasp an object. *Exp. Brain Res.* 111, 473–476. doi:10.1007/BF00228737.

Bressan, P., and Kramer, P. (2013). The relation between cognitive-perceptual schizotypal traits and the Ebbinghaus size-illusion is mediated by judgment time. *Front. Psychol.* 4, 1–8. doi:10.3389/fpsyg.2013.00343.

Bruno, N., Bernardis, P., and Gentilucci, M. (2008). Visually guided pointing, the Müller-Lyer illusion, and the functional interpretation of the dorsal-ventral split: conclusions from 33 independent studies. *Neurosci. Biobehav. Rev.* 32, 423–437. doi:10.1016/j.neubiorev.2007.08.006.

Bruno, N., and Franz, V. H. (2009). When is grasping affected by the Muller-Lyer illusion? A quantitative review. *Neuropsychologia* 47, 1421–1433. doi:10.1016/j.neuropsychologia.2008.10.031.

Buchanan, J. J., Park, J.-H., and Shea, C. H. (2004). Systematic scaling of target width: Dynamics, planning, and feedback. *Neurosci. Lett.* 367, 317–322. doi:10.1016/j.neulet.2004.06.028.

Buchanan, J. J., Park, J.-H., and Shea, C. H. (2006). Target width scaling in a repetitive aiming task: Switching between cyclical and discrete units of action. *Exp. Brain Res.* 175, 710–725. doi:10.1007/s00221-006-0589-1.

Byblow, W. D., Carson, R. G., and Goodman, D. (1994). Expressions of asymmetries and anchoring in bimanual coordination. *Hum. Mov. Sci.* 13, 3–28.

Carey, D. P. (2001). Do action systems resist visual illusions? *Trends Cogn. Sci.* 5, 109–113. doi:10.1016/S1364-6613(00)01592-8.

Carlton, L. G. (1981). Processing visual feedback information for movement control. *J. Exp. Psychol. Hum. Percept. Perform.* 7, 1019–30. doi:10.1037/0096-1523.7.5.1019.

Castiello, U., Paulignan, Y., and Jeannerod, M. (1991). Temporal dissociation of motor responses and subjective awareness. *Brain* 114, 2639–2655. doi:10.1093/brain/114.6.2639.

Chen, H., and Zou, L. (2016). Global study of Rayleigh–Duffing oscillators. *J. Phys. A Math. Theor.* 49, 165202. Available at: http://stacks.iop.org/1751-8121/49/i=16/a=165202.

Cleeremans, A., and Jiménez, L. (2002). "Implicit learning and concsciousness: A graded, dynamic perspective.," in *Implicit learning and concsciousness. An empirical, philosophical and computational consensus in the making*, eds. R. M. French and A. Cleeremans (Hove, UK: Psychology Press), 1–40.

Conti, P., and Beaubaton, D. (1980). Role of structured visual field and visual reafference in accuracy of pointing movements. *Percept. Mot. Skills* 50, 239–244. doi:10.2466/pms.1980.50.1.239.

Coren, S., Girgus, J. S., Erlichman, H., and Hakstian, A. R. (1976). An empirical taxonomy of visual illusions. *Percept. Psychophys.* 20, 129–137.

Crossman, E. R., and Goodeve, P. J. (1963). Feedback control of hand-movement and Fitts' Law. *J. Exp. Psychol. A, Hum. Exp. Psychol.* 35, 407–425. doi:10.1080/14640748308402133.

Daffertshofer, A., Van Veen, B., Ton, R., and Huys, R. (2014). Discrete and rhythmic movements - Just a bifurcation apart? in *Conference Proceedings - IEEE International Conference on Systems, Man and Cybernetics*, 778–783. doi:10.1109/SMC.2014.6974005.

Daprati, E., and Gentilucci, M. (1997). Grasping an illusion. *Neuropsychologia* 35, 1577–1582. doi:10.1016/S0028-3932(97)00061-4.

Day, B. L., and Lyon, I. N. (2000). Voluntary modification of automatic arm movements evoked by motion of a visual target. *Exp. Brain Res.* 130, 159–168. doi:10.1007/s002219900218.

Dehaene, S., Sergent, C., and Changeux, J.-P. (2003). A neuronal network model linking subjective reports and objective physiological data during conscious perception. *Proc. Natl. Acad. Sci.* 100, 8520–8525. doi:10.1073/pnas.1332574100.

Dhamala, M., Assisi, C. G., Jirsa, V. K., Steinberg, F. L., and Scott Kelso, J. A. (2007). Multisensory integration for timing engages different brain networks. *Neuroimage* 34, 764–773. doi:10.1016/j.neuroimage.2006.07.044.

Ditzinger, T., and Haken, H. (1989). Oscillations in the perception of ambiguous patterns a model based on synergetics. *Biol. Cybern.* 61, 279–287.

doi:10.1007/BF00203175.

Ditzinger, T., and Haken, H. (1990). The impact of fluctuations on the recognition of ambiguous patterns. *Biol. Cybern.* 63, 453–456. doi:10.1007/BF00199577.

Doherty, M. J., Campbell, N. M., Tsuji, H., and Phillips, W. A. (2010). The Ebbinghaus illusion deceives adults but not young children. *Dev. Sci.* 13, 714–721. doi:10.1111/j.1467-7687.2009.00931.x.

van Donkelaar, P. (1999). Pointing movements are affected by size-contrast illusions. *Exp. Brain Res.* 125, 517–520. Available at: http://eutils.ncbi.nlm.nih.gov/entrez/eutils/elink.fcgi?dbfrom=pubmed&id=10323299&retmode=ref&cmd=prlinks.

van Doorn, H., van der Kamp, J., de Wit, M., and Savelsbergh, G. J. P. (2009). Another look at the Müller-Lyer illusion: Different gaze patterns in vision for action and perception. *Neuropsychologia* 47, 804–812. doi:10.1016/j.neuropsychologia.2008.12.003.

Ebbinghaus, H., and Dürr, E. (1902). *Grundzüge der Psychologie*. Leipzig: Veit & Comp.

Ellenbürger, T., Krüger, M., Shea, C. H., and Panzer, S. (2012). Sind motorische Handlungen auf eine präzise Wahrnehmung angewiesen? *Z Sportpsychol* 19, 135–144. doi:10.1026/1612-5010/a000079.

Elliott, D., Helsen, W. F., and Chua, R. (2001). A century later: Woodworth's (1899) two-component model of goal-directed aiming. *Psychol. Bull.* 127, 342–357. doi:10.1037//0033-2909.127.3.342.

Feldman, a G. (1986). Once more on the equilibrium-point hypothesis (lambda model) for motor control. *J. Mot. Behav.* 18, 17–54. doi:15136283.

Fernandez, L., and Bootsma, R. J. (2004). Effects of biomechanical and task constraints on the organization of movement in precision aiming. *Exp. Brain Res.* 159, 458–466. doi:10.1007/s00221-004-1964-4.

Fernandez, L., and Bootsma, R. J. (2008). Non-linear gaining in precision aiming: making Fitts' task a bit easier. *Acta Psychol. (Amst).* 129, 217–27. doi:10.1016/j.actpsy.2008.06.001.

Fischer, M. H. (2001). How sensitive is hand transport to illusory context effects? *Exp. Brain Res.* 136, 224–230. doi:10.1007/s002210000571.

Fitts, P. M. (1964). "Perceptual-motor skill learning.," in *Categories of Human Learning*, ed. A. W. Melton (New York, New York, USA: Academic Press), 244–283.

Fitts, P. M. (1954). The information capacity of the human motor system in controlling the amplitude of movement. *J. Exp. Psychol.* 47, 381–391. doi:10.1037/h0055392.

Fitts, P. M., and Peterson, J. R. (1964). Information capacity of discrete motor responses. *J. Exp. Psychol.* 67, 103–112. doi:10.1037/h0045689.

de Fockert, J., Davidoff, J., Fagot, J., Parron, C., and Goldstein, J. (2007). More accurate size contrast judgments in the Ebbinghaus Illusion by a remote culture. *J. Exp. Psychol. Hum. Percept. Perform.* 33, 738–742. doi:10.1037/0096-1523.33.3.738.

Foley, J. M. (1975). Error in visually directed manual pointing. *Percept. Psychophys.* 17, 69–74. doi:10.3758/BF03204000.

Fourneret, P., and Jeannerod, M. (1998). Limited conscious monitoring of motor performance in normal subjects. *Neuropsychologia* 36, 1133–1140. doi:10.1016/S0028-3932(98)00006-2.

Franz, V. H. (2001). Action does not resist visual illusions. *Trends Cogn. Sci.* 5, 457–459. doi:10.1016/S1364-6613(00)01772-1.

Franz, V. H., Fahle, M., Bülthoff, H. H., and Gegenfurtner, K. R. (2001). Effects of visual illusions on grasping. *J. Exp. Psychol. Hum. Percept. Perform.* 27, 1124–1144. doi:10.1037/0096-1523.27.5.1124.

Franz, V. H., and Gegenfurtner, K. R. (2008). Grasping visual illusions: Consistent data and no dissociation. *Cogn. Neuropsychol.* 25, 920–50. doi:10.1080/02643290701862449.

Franz, V. H., Gegenfurtner, K. R., Bülthoff, H. H., and Fahle, M. (2000). Grasping visual illusions: no evidence for a dissociation between perception and action. *Psychol. Sci.* 11, 20–25. doi:10.1111/1467-9280.00209.

Ganel, T., Tanzer, M., and Goodale, M. A. (2008). A double dissociation between action and perception in the context of visual illusions: opposite effects of real and illusory size. 19, 221–225. doi:10.1111/j.1467-9280.2008.02071.x.

García-Pérez, M. a. (1998). Forced-choice staircases with fixed step sizes: Asymptotic and small-sample properties. *Vision Res.* 38, 1861–1881. doi:10.1016/S0042-

6989(97)00340-4.

van Gelder, T. (1998). The dynamical hypothesis in cognitive science. *Behav. Brain Sci.* 21, 615-628-665. doi:10.1017/S0140525X98001733.

Gentilucci, M., Chieffi, S., Daprati, E., Saetti, M. C., Toni, I., and Deprati, E. (1996). Visual illusion and action. *Neuropsychologia* 34, 369–376.

Gentilucci, M., Daprati, E., Gangitano, M., and Toni, I. (1997). Eye position tunes the contribution of allocentric and egocentric information to target localization in human goal-directed arm movements. *Neurosci. Lett.* 222, 123–126. doi:10.1016/S0304-3940(97)13366-3.

Gentilucci, M., and Negrotti, A. (1996). Mechanisms for distance reproduction in perceptual and motor tasks. *Exp. brain Res.* 108, 140–146. doi:10.1007/BF00242911.

Gibson, J. J. (1979). *The ecological approach to visual perception*. Psychology Press.

Gibson, J. J. (1966). *The Senses Considered as Perceptual Systems*. Boston, MA: Houghton Mifflin Company.

Girgus, J. S., Coren, S., and Agdern, M. (1972). The interrelationship between the Ebbinghaus and Delboeuf illusions. *J. Exp. Psychol.* 95, 453–455. doi:10.1037/h0033606.

Glover, S. (2002). Visual illusions affect planning but not control. *Trends Cogn. Sci.* 6, 288–292. Available at: http://linkinghub.elsevier.com/retrieve/pii/S1364661302019204.

Goodale, M. a (2011). Transforming vision into action. *Vision Res.* 51, 1567–87. doi:10.1016/j.visres.2010.07.027.

Goodale, M. A. (2014). How (and why) the visual control of action differs from visual perception. *Proc. R. Soc. B Biol. Sci.* 281, 20140337. doi:10.1098/rspb.2014.0337.

Goodale, M. A., and Milner, A. D. (1992). Separate visual pathways for perception and action. *Trends Neurosci.* 15, 20–25. doi:10.1016/0166-2236(92)90344-8.

Goodale, M. a, Pelisson, D., and Prablanc, C. (1986). Large adjustments in visually guided reaching do not depend on vision of the hand or perception of target displacement. *Nature* 320, 748–750. doi:10.1038/320748a0.

Guiard, Y. (1997). Fitts' law in the discrete vs. cyclical paradigm. *Hum. Mov. Sci.* 16, 97–131. doi:10.1016/S0167-9457(96)00045-0.

Guiard, Y. (1993). On Fitts's and Hooke's laws: Simple harmonic movement in upper-limb cyclical aiming. *Acta Psychol. (Amst).* 82, 139–159. doi:10.1016/0001-6918(93)90009-G.

Guiard, Y. (2009). The problem of consistency in the design of Fitts' law experiments: Consider either target distance and width or movement form and scale. *Proc. 27th Int. Conf. …*, 1809–1818. doi:http://doi.acm.org/10.1145/1518701.1518980.

Guiard, Y., Olafsdottir, H. B., and Perrault, S. T. (2011). Fitts' law as an explicit time/error trade-off. *Proc. 2011 Annu. Conf. Hum. factors Comput. Syst. - CHI '11*, 1619. doi:10.1145/1978942.1979179.

Haffenden, A. M., and Goodale, M. A. (1998). The Effect of Pictorial Illusion on Prehension and Perception. *J. Cogn. Neurosci.* 10, 122–136. doi:10.1162/089892998563824.

Haffenden, A. M., Schiff, K. C., and Goodale, M. A. (2001). The dissociation between perception and action in the Ebbinghaus illusion. *Curr. Biol.* 11, 177–181. doi:10.1016/S0960-9822(01)00023-9.

Haken, H., Kelso, J. A. S., and Bunz, H. (1985). A theoretical model of phase transitions in human hand movements. *Biol. Cybern.* 51, 347–356. doi:10.1007/BF00336922.

Handlovsky, I., Hansen, S., Lee, T. D., and Elliott, D. (2004). The Ebbinghaus illusion affects on-line movement control. *Neurosci. Lett.* 366, 308–311. doi:10.1016/j.neulet.2004.05.056.

Harris, C. M., and Wolpert, D. M. (1998). Signal-dependent noise determines motor planning. *Nature* 394, 780–4. doi:10.1038/29528.

Hirsch, M. W., and Smale, S. (1974). *Differential Equations, Dynamical Systems and Linear Algebra*. New York, New York, USA: Academic Press.

Hock, H. S., and Schöner, G. (2010). "A neural basis for perceptual dynamics," in *Nonlinear Dynamics in Human Behavior*, eds. R. Huys and V. K. Jirsa (Springer Berlin Heidelberg), 151–177. doi:10.1007/978-3-642-16262-6_7.

Hu, Y., and Goodale, M. A. (2000). Grasping after a delay shifts size-scaling from absolute to relative metrics. *J. Cogn. Neurosci.* 12, 856–868. doi:10.1162/089892900562462.

Huys, R., Fernandez, L., Bootsma, R. J., and Jirsa, V. K. (2010a). Fitts' law is not

continuous in reciprocal aiming. *Proc. Biol. Sci.* 277, 1179–1184. doi:10.1098/rspb.2009.1954.

Huys, R., Knol, H., Sleimen-Malkoun, R., Temprado, J.-J., and Jirsa, V. K. (2015). Does changing Fitts' index of difficulty evoke transitions in movement dynamics? *EPJ Nonlinear Biomed. Phys.* 3, 8. doi:10.1140/epjnbp/s40366-015-0022-4.

Huys, R., Perdikis, D., and Jirsa, V. K. (2014). Functional architectures and structured flows on manifolds: A dynamical framework for motor behavior. *Psychol. Rev.* 121, 302–36. doi:10.1037/a0037014.

Huys, R., Studenka, B. E., Rheaume, N. L., Zelaznik, H. N., and Jirsa, V. K. (2008). Distinct timing mechanisms produce discrete and continuous movements. *PLoS Comput. Biol.* 4. doi:10.1371/journal.pcbi.1000061.

Huys, R., Studenka, B. E., Zelaznik, H. N., and Jirsa, V. K. (2010b). Distinct timing mechanisms are implicated in distinct circle drawing tasks. *Neurosci. Lett.* 472, 24–8. doi:10.1016/j.neulet.2010.01.047.

Im, H. Y., and Chong, S. C. (2009). Computation of mean size is based on perceived size. *Atten. Percept. Psychophys.* 71, 375–384. doi:10.3758/APP.71.2.375.

Jackson, S. R., and Shaw, A. (2000). The Ponzo illusion affects grip-force but not grip-aperture scaling during prehension movements. *J. Exp. Psychol. Hum. Percept. Perform.* 26, 418–423. doi:10.1037/0096-1523.26.1.418.

Jacobs, D. M., Ibáñez-Gijón, J., Díaz, A., and Travieso, D. (2011). On Potential-Based and Direct Movements in Information Spaces. *Ecol. Psychol.* 23, 123–145. doi:10.1080/10407413.2011.566046.

Jirsa, V. K., Fink, P., Foo, P., and Kelso, J. A. S. (2000). Parametric stabilization of biological coordination: A theoretical model. *J. Biol. Phys.* 26, 85–112. doi:10.1023/A:1005208122449.

Jirsa, V. K., and Kelso, J. A. S. (2005). The excitator as a minimal model for the coordination dynamics of discrete and rhythmic movement generation. *J. Mot. Behav.* 37, 35–51. doi:10.3200/JMBR.37.1.35-51.

Johnson, H., van Beers, R. J., and Haggard, P. (2002). Action and awareness in pointing tasks. *Exp. Brain Res.* 146, 451–459. doi:10.1007/s00221-002-1200-z.

Káldy, Z., and Kovács, I. (2003). Visual context integration is not fully developed in 4-year-old children. *Perception* 32, 657–666. doi:10.1068/p3473.

van der Kamp, J., Withagen, R., and de Wit, M. M. M. (2013). Cultural and learning differences in the Judd illusion. *Attention, Perception, Psychophys.* 75, 1027–1038. doi:10.3758/s13414-013-0458-5.

Kay, B. A. (1988). The dimensionality of movement trajectories and the degrees of freedom problem: A tutorial. *Hum. Mov. Sci.* 7, 343–364. doi:10.1016/0167-9457(88)90016-4.

Kay, B. A., Kelso, J. A. S., Saltzman, E. L., Schoner, G., Kelso, J. A. S., and Sch6ner, G. (1987). Space-time behavior of single and bimanual rhythmical movements: data and limit cycle model [published erratum appears in J Exp Psychol [Hum Percept] 1987 Aug;13(3):334]. *J Exp Psychol Hum Percept Perform* 13, 178–192. doi:10.1037//0096-1523.13.2.178.

Kelso, J. A. S. (1995). *Dynamic Patterns : The Self-Organization of Brain and Behavior.* Cambridge, Massachusetts: The MIT Press.

Kleiner, M., Brainard, D., Pelli, D., Ingling, A., Murray, R., and Broussard, C. (2007). What's new in Psychtoolbox-3? *Percept. 36 ECVP Abstr. Suppl.*, 14. doi:10.1068/v070821.

Knol, H., Huys, R., Sarrazin, J.-C., and Jirsa, V. K. (2015). Quantifying the Ebbinghaus figure effect: target size, context size, and target-context distance determine the presence and direction of the illusion. *Front. Psychol.* 6, 1–11. doi:10.3389/fpsyg.2015.01679.

Köhler, W. (1940). *Dynamics in Psychology*. New York, New York, USA: Liveright Publishing Corporation Available at: https://books.google.fr/books?id=YdHlxD2zDV8C.

Kopiske, K. K., Bruno, N., Hesse, C., Schenk, T., and Franz, V. H. (2016). The functional subdivision of the visual brain: Is there a real illusion effect on action? A multi-lab replication study. *Cortex* 79, 130–152. doi:10.1016/j.cortex.2016.03.020.

Kostrubiec, V., Zanone, P.-G., Fuchs, A., and Kelso, J. A. S. (2012). Beyond the blank slate: routes to learning new coordination patterns depend on the intrinsic dynamics of the learner-experimental evidence and theoretical model. *Front. Hum. Neurosci.* 6, 222. doi:10.3389/fnhum.2012.00222.

Kugler, P. N., Scott Kelso, J. A., and Turvey, M. T. (1980). On the Concept of

Coordinative Structures as Dissipative Structures: I. Theoretical Lines of Convergence. *Adv. Psychol.* 1, 3–47. doi:10.1016/S0166-4115(08)61936-6.

Lagarde, J., and Kelso, J. A. S. (2006). Binding of movement, sound and touch: multimodal coordination dynamics. *Exp. Brain Res.* 173, 673–688. doi:10.1007/s00221-006-0410-1.

Lamme, V. A. F. (2004). Separate neural definitions of visual consciousness and visual attention; a case for phenomenal awareness. *Neural Netw.* 17, 861–72. doi:10.1016/j.neunet.2004.02.005.

Lamme, V. A. F., and Roelfsema, P. R. (2000). The distinct modes of vision offered by feedforward and recurrent processing. *Trends Neurosci.* 23, 571–579. doi:10.1016/S0166-2236(00)01657-X.

Lamme, V. A., Supèr, H., and Spekreijse, H. (1998). Feedforward, horizontal, and feedback processing in the visual cortex. *Curr. Opin. Neurobiol.* 8, 529–535. doi:10.1016/S0959-4388(98)80042-1.

Lazzari, S., Mottet, D., and Vercher, J.-L. (2009). Eye-Hand Coordination in Rhythmical Pointing. *J. Mot. Behav.* 41, 294–304. doi:10.3200/JMBR.41.4.294-304.

Lee, J.-H., van Donkelaar, P., and Donkelaar, P. (2002). Dorsal and ventral visual stream contributions to perception-action interactions during pointing. *Exp. brain Res.* 143, 440–446. doi:10.1007/s00221-002-1011-2.

MacKenzie, I. S. (1992). Fitts' law as a research and design tool in human-computer interaction. *Human-computer Interact.* 7, 91–139. Available at: papers3://publication/uuid/61EAFCDC-559A-41E5-901C-8BFDAD57DDE3.

Mancini, F., Bolognini, N., Bricolo, E., and Vallar, G. (2011). Cross-modal processing in the occipito-temporal cortex: a TMS study of the Müller-Lyer illusion. *J. Cogn. Neurosci.* 23, 1987–1997. doi:10.1162/jocn.2010.21561.

Marzi, C. A., Mancini, F., Metitieri, T., and Savazzi, S. (2006). Retinal eccentricity effects on reaction time to imagined stimuli. *Neuropsychologia* 44, 1489–1495. doi:10.1016/j.neuropsychologia.2005.11.012.

Massaro, D. W., and Anderson, N. H. (1971). Judgmental model of the Ebbinghaus illusion. *J. Exp. Psychol.* 89, 147–151. Available at: papers3://publication/uuid/1A0538AC-92CA-456E-B563-948FDAF917EA.

McCarthy, J. D., Kupitz, C., and Caplovitz, G. P. (2013). The Binding Ring Illusion:

assimilation affects the perceived size of a circular array. *F1000Research* 2, 58. doi:10.12688/f1000research.2-58.v2.

Meyer, D. E., Abrams, R. a, Kornblum, S., Wright, C. E., and Smith, J. E. (1988). Optimality in human motor performance: ideal control of rapid aimed movements. *Psychol. Rev.* 95, 340–370. doi:10.1037/0033-295X.95.3.340.

Michaels, C. F., and Carello, C. (1981). *Direct perception*. Englewood Cliffs, NJ: Prentice-Hall doi:10.1037/a0023510.

Milner, A. D. (1995). Cerebral correlates of visual awareness. *Neuropsychologia* 33, 1117–1130. doi:10.1016/0028-3932(95)00052-5.

Milner, A. D., and Goodale, M. A. (2008). Two visual systems re-viewed. *Neuropsychologia* 46, 774–785. doi:10.1016/j.neuropsychologia.2007.10.005.

Milner, D., and Goodale, M. (1995). *The visual brain in action*. Oxford University Press.

Mottet, D., and Bootsma, R. J. (1999). The dynamics of goal-directed rhythmical aiming. *Biol. Cybern.* 80, 235–245. doi:10.1007/s004220050521.

van Mourik, A. M., Daffertshofer, A., and Beek, P. J. (2008). Extracting global and local dynamics from the stochastics of rhythmic forearm movements. *J. Mot. Behav.* 40, 214–231. doi:10.3200/JMBR.40.3.214-231.

Murphy, K. J., Carey, D. P., and Goodale, M. A. (1998). The perception of spatial relations in a patient with visual form agnosia. *Cogn. Neuropsychol.* 15, 705–722. doi:10.1080/026432998381069.

Nemati, F. (2009). Size and direction of distortion in geometric-optical illusions: Conciliation between the M??Ller-Lyer and Titchener configurations. *Perception* 38, 1585–1600. doi:10.1068/p6450.

Obonai, T. (1954). Induction effects in estimates of extent. *J. Exp. Psychol.* 47, 57–60. doi:10.1037/h0057223.

Osaka, N. (1976). Reaction time as a function of peripheral retinal locus around fovea: effect of stimulus size. *Percept. Mot. Skills* 42, 603–606. doi:10.2466/pms.1976.43.2.603.

Oyama, T. (1960). Japanese studies on the so-called geometrical-optical illusions. *Psychologia* 3, 7–20.

Paulignan, Y., MacKenzie, C., Marteniuk, R., and Jeannerod, M. (1991). Selective perturbation of visual input during prehension movements - 1. The effects of

changing object position. *Exp. Brain Res.* 83, 502–512. doi:10.1007/BF00229827.

Paulignan, Y., MacKenzie, C., Marteniuk, R., and Jeannerod, M. (1990). The coupling of arm and finger movements during prehension. *Exp. Brain Res.* 79, 431–435.

Pavani, F., Boscagli, I., Benvenuti, F., Rabuffetti, M., and Farnè, A. (1999). Are perception and action affected differently by the Titchener circles illusion? *Exp. Brain Res.* 127, 95–101. doi:10.1007/s002210050777.

Payne, W. H. (1967). Visual reaction times on a circle about the fovea. *Science* 155, 481–482. doi:10.1126/science.155.3761.481.

Pelli, D. G., and Farell, B. (1999). Why use noise? *J. Opt. Soc. Am. A* 16, 647. doi:10.1364/JOSAA.16.000647.

Perdikis, D., Huys, R., and Jirsa, V. (2011). Complex processes from dynamical architectures with time-scale hierarchy. *PLoS One* 6. doi:10.1371/journal.pone.0016589.

Perenin, M. T., and Vighetto, A. (1988). Optic ataxia: A specific disruption in visuomotor mechanisms: I. Different aspects of the deficit in reaching for objects. *Brain* 111, 643–674. doi:10.1093/brain/111.3.643.

Plamondon, R., and Alimi, A. M. (1997). Speed/accuracy trade-offs in target-directed movements. *Behav. Brain Sci.* 20, 279–349. doi:10.1017/S0140525X97001441.

Plewan, T., Weidner, R., and Fink, G. R. (2012). The influence of stimulus duration on visual illusions and simple reaction time. *Exp. Brain Res.* 223, 367–375. doi:10.1007/s00221-012-3265-7.

Prablanc, C., and Martin, O. (1992). Automatic control during hand reaching at undetected two-dimensional target displacements. *J. Neurophysiol.* 67, 455–69. Available at: http://jn.physiology.org/content/jn/67/2/455.full.pdf\nhttp://www.ncbi.nlm.nih.gov/pubmed/1569469.

Rabinovich, M. I., Huerta, R., Varona, P., and Afraimovich, V. S. (2008). Transient cognitive dynamics, metastability, and decision making. *PLoS Comput. Biol.* 4, 25–30. doi:10.1371/journal.pcbi.1000072.

Reed, E. S. (1996). *Encountering the World: Toward an Ecological Psychology*. New York, New York, USA: Oxford University Press doi:10.1093/acprof:oso/9780195073010.001.0001.

Roberts, B., Harris, M. G., and Yates, T. A. (2005). The roles of inducer size and distance in the Ebbinghaus illusion (Titchener circles). *Perception* 34, 847–856. doi:10.1068/p5273.

Robertson, S. D., Zelaznik, H. N., Lantero, D. a, Bojczyk, K. G., Spencer, R. M., Doffin, J. G., and Schneidt, T. (1999). Correlations for timing consistency among tapping and drawing tasks: evidence against a single timing process for motor control. *J. Exp. Psychol. Hum. Percept. Perform.* 25, 1316–30. doi:10.1037/0096-1523.25.5.1316.

Robinson, J. O. (1998). *The psychology of visual illusion*. London: Hutchinson & Co. Ltd.

Roerdink, M., Ophoff, E. D., (Lieke) E. Peper, C., and Beek, P. J. (2008). Visual and musculoskeletal underpinnings of anchoring in rhythmic visuo-motor tracking. *Exp. Brain Res.* 184, 143–156. doi:10.1007/s00221-007-1085-y.

Roerdink, M., Peper, C. E., and Beek, P. J. (2005). Effects of correct and transformed visual feedback on rhythmic visuo-motor tracking: Tracking performance and visual search behavior. *Hum. Mov. Sci.* 24, 379–402. doi:10.1016/j.humov.2005.06.007.

Saltzman, E., and Kelso, J. a (1987). Skilled actions: A task-dynamic approach. *Psychol. Rev.* 94, 84–106. doi:10.1037/0033-295X.94.1.84.

Saltzman, E. L., and Munhall, K. G. (1992). Skill acquisition and development: the roles of state-, parameter, and graph dynamics. *J. Mot. Behav.* 24, 49–57.

Salvatier, J., Wiecki, T. V., and Fonnesbeck, C. (2016). Probabilistic programming in Python using PyMC3. *PeerJ Comput. Sci.* 2, e55. doi:10.7717/peerj-cs.55.

Sarris, V. (2010). Relational psychophysics - major messages from Hermann Ebbinghaus' and Max Wertheimer's work. *Philos. Psychol.* 23, 207–216.

Schmidt, R. a, Zelaznik, H., Hawkins, B., Frank, J. S., and Quinn, J. T. (1979). Motor-output variability: a theory for the accuracy of rapid motor acts. *Psychol. Rev.* 47, 415–451. doi:10.1037/0033-295X.86.5.415.

Schöner, G. (1990). A dynamic theory of coordination of discrete movement. *Biol. Cybern.* 63, 257–270. doi:10.1007/BF00203449.

Schwarzkopf, D. S., and Rees, G. (2013). Subjective Size Perception Depends on Central Visual Cortical Magnification in Human V1. *PLoS One* 8. doi:10.1371/journal.pone.0060550.

Schwarzkopf, D. S., Song, C., and Rees, G. (2011). The surface area of human V1

predicts the subjective experience of object size. *Nat. Neurosci.* 14, 28–30. doi:10.1038/nn.2706.

Shannon, C. E., and Weaver, W. (1949). The Mathematical Theory of Communication. *Math. theory Commun.* 27, 117. doi:10.2307/3611062.

Sheikh, I. H., and Hoffmann, E. R. (1994). Effect of target shape on movement time in a Fitts task. *Ergonomics* 37, 1533–1547. doi:10.1080/00140139408964932.

Skewes, J. C., Roepstorff, A., and Frith, C. D. (2011). How do illusions constrain goal-directed movement: perceptual and visuomotor influences on speed/accuracy trade-off. *Exp. brain Res.* 209, 247–255. doi:10.1007/s00221-011-2542-1.

Sleimen-Malkoun, R., Temprado, J.-J., and Berton, E. (2013). Age-related changes of movement patterns in discrete Fitts' task. *BMC Neurosci.* 14, 145. doi:10.1186/1471-2202-14-145.

Sleimen-Malkoun, R., Temprado, J.-J. J., Huys, R., Jirsa, V., and Berton, E. (2012). Is Fitts' law continuous in discrete aiming? *PLoS One* 7, e41190. doi:10.1371/journal.pone.0041190.

Smeets, J. B., and Brenner, E. (1999). A new view on grasping. *Motor Control* 3, 237–271.

Smeets, J. B. J., and Brenner, E. (2006). 10 years of illusions. *J. Exp. Psychol. Hum. Percept. Perform.* 32, 1501–1504. doi:10.1037/0096-1523.32.6.1501.

Smeets, J. B. J., and Brenner, E. (2008). Grasping Weber's law. *Curr. Biol.* 18, R1089-90–1. doi:10.1016/j.cub.2008.10.008.

Smeets, J. B. J., and Brenner, E. (1995). Perception and action are based on the same visual information: distinction between position and velocity. *J. Exp. Psychol. Hum. Percept. Perform.* 21, 19–31. doi:10.1037/0096-1523.21.1.19.

Smeets, J. B. J., Brenner, E., De Grave, D. D. J., and Cuijpers, R. H. (2002). Illusions in action: Consequences of inconsistent processing of spatial attributes. *Exp. Brain Res.* 147, 135–144. doi:10.1007/s00221-002-1185-7.

Smits-Engelsman, B. C. M., Swinnen, S. P., and Duysens, J. (2006). The advantage of cyclic over discrete movements remains evident following changes in load and amplitude. *Neurosci. Lett.* 396, 28–32. doi:10.1016/j.neulet.2005.11.001.

Soechting, J. F., and Flanders, M. (1989). Errors in pointing are due to approximations in sensorimotor transformations. *J. Neurophysiol.* 62, 595–608.

doi:10.1017/S0140525X00068849.

Soechting, J. F., and Lacquaniti, F. (1983). Modification of trajectory of a pointing movement in response to a change in target location. *J Neurophysiol* 49, 548–564. Available at: http://jn.physiology.org/content/49/2/548 [Accessed November 1, 2016].

Sperandio, I., Savazzi, S., and Marzi, C. a. (2010). Is simple reaction time affected by visual illusions? *Exp. Brain Res.* 201, 345–350. doi:10.1007/s00221-009-2023-y.

Stoerig, P., and Cowey, A. (1997). Blindsight in man and monkey. *Brain* 120 (Pt 3, 535–59. doi:10.1093/brain/120.3.535.

Stöttinger, E., Pfusterschmied, J., Wagner, H., Danckert, J., Anderson, B., and Perner, J. (2012). Getting a grip on illusions: replicating Stöttinger et al [Exp Brain Res (2010) 202:79–88] results with 3-D objects. *Exp. Brain Res.* 216, 155–157. doi:10.1007/s00221-011-2912-8.

Stöttinger, E., Soder, K., Pfusterschmied, J., Wagner, H., and Perner, J. (2010). Division of labour within the visual system: Fact or fiction? Which kind of evidence is appropriate to clarify this debate? *Exp. Brain Res.* 202, 79–88. doi:10.1007/s00221-009-2114-9.

Strogatz, S. H. (1994). *Nonlinear Dynamics And Chaos: With Applications To Physics, Biology, Chemistry And Engineering*. Cambridge, Massachusetts: Perseus Books Publishing doi:10.1063/1.2807947.

Thompson, S. G., McConnell, D. S., Slocum, J. S., and Bohan, M. (2007). Kinematic analysis of multiple constraints on a pointing task. *Hum. Mov. Sci.* 26, 11–26. doi:10.1016/j.humov.2006.09.001.

Toni, I., Gentilucci, M., Jeannerod, M., and Decety, J. (1996). Differential influence of the visual framework on end point accuracy and trajectory specification of arm movements. *Exp. Brain Res.* 111, 447–454. Available at: http://www.ncbi.nlm.nih.gov/pubmed/8911939.

Tononi, G., and Edelman, G. M. (1998). Consciousness and Complexity. *Science (80-.).* 282, 1846–1851. doi:10.1126/science.282.5395.1846.

Treisman, A. M., and Gelade, G. (1980). A feature-integration theory of attention. *Cogn. Psychol.* 12, 97–136. doi:10.1016/0010-0285(80)90005-5.

Trevarthen, C. B. (1968). Two mechanisms of vision in primates. *Psychol. Forsch.* 31,

299–337. doi:10.1007/BF00422717.

Tuller, B., Case, P., Ding, M., and Kelso, J. a. S. (1994). The nonlinear dynamics of speech categorization. *J. Exp. Psychol. Hum. Percept. Perform.* 20, 3–16. doi:10.1037//0096-1523.20.1.3.

Turvey, M. T., Shaw, R. E., Reed, E. S., and Mace, W. M. (1981). Ecological laws of perceiving and acting: In reply to Fodor and Pylyshyn (1981). *Cognition* 9, 237–304. doi:10.1016/0010-0277(81)90002-0.

Ungerleider, L. G., and Mishkin, M. (1982). "Two cortical visual systems," in *Analysis of Visual Behavior*, eds. D. J. Ingle, M. A. Goodale, and R. J. W. Mansfield (The MIT Press), 549–586.

Vernooij, C. A., Rao, G., Perdikis, D., Huys, R., Jirsa, V. K., and Temprado, J.-J. (2016). Functional coordination of muscles underlying changes in behavioural dynamics. *Sci. Rep.* 6, 27759. doi:10.1038/srep27759.

Vishton, P. M., Rea, J. G., Cutting, J. E., and Nuñez, L. N. (1999). Comparing the Effects of the Horizontal-Vertical Illusion on Grip Scaling and Judgment. Relative Versus Absolute, Not Perception Versus Action. *J. Exp. Psychol. Hum. Percept. Perform.* 25, 1659–1672.

Weintraub, D. J. (1979). Ebbinghaus illusion: context, contour, and age influence the judged size of a circle amidst circles. *J. Exp. Psychol. Hum. Percept. Perform.* 5, 353–364. doi:10.1037/0096-1523.5.2.353.

Welford, A. T. (1968). *Fundamentals of Skill.* doi:10.2307/1421343.

Welford, A. T., Norris, A. H., and Schock, N. W. (1969). Speed and accuracy of movement and their changes with age. *Acta Psychol*, 3–15.

Westwood, D. a., Heath, M., and Roy, E. a. (2000). The effect of a pictorial illusion on closed-loop and open-loop prehension. *Exp. Brain Res.* 134, 456–463. doi:10.1007/s002210000489.

Wolfe, J. M., and Bennett, S. C. (1997). Preattentive Object Files: Shapeless Bundles of Basic Features. *Vision Res.* 37, 25–43. doi:10.1016/S0042-6989(96)00111-3.

Woodworth, R. S. (1899). Accuracy of voluntary movement. *Psychol. Rev. Monogr. Suppl.* 3, i-114. doi:10.1037/h0092992.

Zelaznik, H. N., Hawkins, B., and Kisselburgh, L. (1983). Rapid Visual Feedback Processing in Single-Aiming Movements. *J. Mot. Behav.* 15, 217–236.

doi:10.1080/00222895.1983.10735298.